

## **ABSTRACT**

Title of Document: INVESTIGATION OF REFRIGERANT DISTRIBUTION IN  
A HOUSEHOLD REFRIGERATOR WITH A FOCUS ON  
THE ROLE OF THE ACCUMULATOR

Cara Sanderson Martin, M.S. Mechanical Engineering, 2007

Directed By: Professor Reinhard Radermacher, Ph.D.  
Department of Mechanical Engineering

In order to maximize household refrigerator performance, it is important to understand the basic relationship between each component as well as the relationship between refrigerant and lubricant used in the system.

This study examines the particular role of the accumulator in a household refrigeration system as well as the oil and refrigerant distribution within the compressor and accumulator. Data and video images were collected to understand the fluid motion throughout the system, particularly in the compressor shell, accumulator, accumulator outlet, and suction and discharge lines. General trends and relationships between the oil and refrigerant were established and the beneficial use of the accumulator for compressor protection was verified.

Testing was also conducted without the accumulator. Removal of the accumulator caused changes in oil and refrigerant flow patterns and presented a danger for the compressor at low ambient temperatures during cycling and defrost periods.

INVESTIGATION OF REFRIGERANT DISTRIBUTION IN HOUSEHOLD  
REFRIGERATORS WITH A FOCUS ON THE ROLE OF THE ACCUMULATOR

By

Cara Sanderson Martin

Thesis submitted to the Faculty of the Graduate School of the  
University of Maryland, College Park, in partial fulfillment  
of the requirements for the degree of  
Masters of Science  
2007

Advisory Committee:  
Professor Dr. Reinhard Radermacher, Chair  
Associate Professor Dr. Linda Schmidt  
Assistant Professor Dr. Bao Yang

© Copyright by

Cara Martin

2007

# **Dedication**

Dedicated to my father, Robert W. Sanderson

October 13, 1944 – January 21, 2000

I know you'd be proud.

## Acknowledgements

I would like to thank Dr. Reinhard Radermacher and the Center for Environmental Energy Engineering (CEEE) for giving me the opportunity to research in an academic setting and interact with a variety of peers, colleagues, and business professionals. The experiences that I have gained from my work here are invaluable and will forever impact the way that I think, act, and learn. Dr. Radermacher's support, critical thinking, and positive attitude have continuously provided a constructive atmosphere for developing new ideas, solving problems, and exercising engineering principles. For his leadership in research, I'd also like to thank Dr. Yunho Hwang. Dr. Hwang awarded me my first opportunity within CEEE as an undergraduate research assistant and I am deeply thankful for the chance to experience research at such an early point in my college career. His persistence and breadth of knowledge have also taught me to examine problems at multiple angles and to never be completely satisfied with results; there will always be something else to learn and explore.

For their friendship, advice, conversation, laughs, support, and dedication, I'd like to thank all the guys of CEEE. Magnus Eisele, Ethan Lust, and Jon Schonfeld, thank you for your willingness to pursue the energy project of the summer of 2007 and for your moral support through tough research moments. Nick Fernandez, Kyle Gluessenkamp and all of the software folks, thanks for your camaraderie and all of our Friday lunches. Mr. Jin (now Dr. Jin) and Xudong Wang (soon to be Dr. Xudong Wang), thank you for showing me the ropes around the CEEE labs and for answering all of my questions at any time. Ahmet Ors, thank you for getting me started with this project and providing so much support in its early stages. And last, but certainly not least, many, many thanks to

Jan Muehlbauer. Without your skills, talent, brute force, and determined thinking, much of my project would have gone undone. You have made my experience here at CEEE all the more worthwhile and I thank you for all of the many lessons you've taught me along the way.

Finally, thank you to all of my friends and family, especially my mother and my husband. Without your love, support, willingness to listen, and kind words I never would have made it through. To "Helpful Corn" and the players of Maryland Ultimate, thank you for your constant smiles and jokes about running refrigerators. Matt, thank you for your patience and understanding at all times. Mom, thank you for your constant support and continued encouragement to follow my dreams.

# Table of Contents

Dedication.....	ii
Acknowledgements.....	iii
Table of Contents.....	v
List of Tables.....	x
List of Figures.....	xv
List of Figures.....	xv
Nomenclature.....	xxiii
1 Introduction.....	1
2 Background.....	3
2.1 The Working Principle of Vapor Compression Cycles.....	3
2.2 Literature Review.....	6
2.2.1 Effects and Characteristics of Oil and Refrigerant Migration and Distribution.....	6
2.2.2 Measurement of Oil and Refrigerant Mixture Concentrations.....	9
2.2.3 Accumulator Studies.....	16
3 Motivation and Objectives.....	20
3.1 Motivation.....	20
3.2 Objectives.....	20
4 Experimentation with the Accumulator.....	21
4.1 Experimental Set-up.....	21
4.1.1 Refrigerator/Freezer.....	21
4.1.2 Compressor.....	22

4.1.3	Evaporator and Accumulator .....	25
4.1.4	System Sight Glasses .....	27
4.1.5	Refrigerant and Oil Flow Visualization.....	28
4.1.5.1	Compressor Visualization.....	28
4.1.5.2	Accumulator Visualization .....	29
4.1.5.3	Accumulator Outlet Visualization .....	31
4.1.5.4	Suction and Discharge Line Visualization.....	31
4.1.6	Experimental Measurements.....	32
4.1.6.1	Pressure Measurements.....	32
4.1.6.2	Temperature Measurements.....	35
4.1.6.3	Power Measurement.....	38
4.1.6.4	Humidity Measurement .....	39
4.1.7	Environmental Chamber .....	40
4.1.8	Data Acquisition System.....	41
4.1.9	Power Supply .....	41
4.1.10	Cabinet Door Sealing.....	42
4.1.11	Refrigerant .....	43
4.2	Experimental Method.....	43
4.2.1	Experimental Procedures .....	43
4.2.2	Experimental Analysis .....	44
4.2.2.1	Calculation of the Cycle Properties .....	44
4.2.2.2	Uncertainty Analysis.....	54
4.2.2.3	Sample Collection.....	57

4.3	Experimental Results .....	66
4.3.1	Data Results and Trends .....	67
4.3.1.1	Pressure Results .....	67
4.3.1.2	Temperature Results .....	70
4.3.1.3	Power Results.....	74
4.3.1.4	Specific Capacity Results .....	76
4.3.1.5	Total Superheat Results .....	79
4.3.1.6	Solubility Results .....	80
4.3.1.7	Mixture Density and Correction Factor Results .....	82
4.3.2	Visualization Results and Trends with the Accumulator.....	86
4.3.2.1	Compressor Visualization Results .....	86
4.3.2.2	Accumulator Visualization Results.....	89
4.3.2.3	Accumulator Outlet Visualization Results.....	93
4.3.2.4	Suction and Discharge Line Visualization Results.....	95
4.3.3	Refrigerant and Oil Mass Analysis Results .....	96
4.3.3.1	Mass Balance Trends during Pull-down .....	96
4.3.3.2	Mass Balance Trends during Cycling .....	101
4.3.3.3	Mass Balance Trends during Defrost.....	104
4.3.3.4	Issues with mass balance calculations .....	107
4.4	Summary of Oil and Refrigerant Flow with the Accumulator .....	108
4.5	Conclusions.....	110
5	Experimentation without the Accumulator .....	112
5.1	Experimental Set-up.....	112

5.1.1	Compressor .....	112
5.1.2	Evaporator .....	113
5.1.3	System Sight Glasses .....	114
5.1.4	Refrigerant and Oil Flow Visualization .....	115
5.1.5	Experimental Measurements .....	115
5.2	Experimental Methods .....	115
5.2.1	Experimental Procedures .....	115
5.2.2	Experimental Analysis .....	116
5.3	Experimental Results .....	116
5.3.1	Data Results and Trends .....	119
5.3.1.1	Pressure Results .....	119
5.3.1.2	Temperature Results .....	124
5.3.1.3	Power Results.....	128
5.3.1.4	Specific Capacity Results .....	130
5.3.1.5	Total Superheat Results .....	133
5.3.1.6	Solubility Results .....	135
5.3.2	Visualization Results and Trends without the Accumulator.....	136
5.3.2.1	Compressor Visualization Results .....	136
5.3.2.2	Evaporator Outlet Visualization Results.....	139
5.3.2.3	Suction and Discharge Line Visualization Results.....	141
5.3.3	Refrigerant and Oil Mass Analysis Results .....	143
5.3.3.1	Mass Balance Trends during Pull-down.....	143
5.3.3.2	Mass Balance Trends during Cycling.....	146

5.3.3.3	Mass Balance Trends during Defrost.....	148
5.4	Summary of Oil and Refrigerant Flow without the Accumulator .....	149
5.5	Advantages and Disadvantages of Removing the Accumulator.....	151
5.6	Conclusions.....	152
6	Recommendations and Future Work .....	154
7	Appendices.....	157
7.1	Mass Balance Data for Results with the Accumulator .....	157
7.1.1	Pull-down Data .....	157
7.1.2	Cycling Data .....	160
7.1.3	Defrost Data.....	164
7.2	Mass Balance Data for Results without the Accumulator .....	169
7.2.1	Pull-down Data .....	169
7.2.2	Cycling Data .....	171
7.2.3	Defrost Data.....	177
8	References.....	180

## List of Tables

Table 1: Refrigerator-Freezer Specifications [16] .....	22
Table 2: Compressor Specifications [16].....	22
Table 3: Visualization Pipe Liquid Line Levels .....	24
Table 4: Compressor Oil Specifications [17].....	24
Table 5: Properties of the UView Dye [18] .....	25
Table 6: Liquid Level Lines with Corresponding Total Volume for the Accumulator ....	26
Table 7: Pressure Transducer Specifications [19] .....	33
Table 8: Thermocouple Specifications [20].....	35
Table 9: Watt Meter Specifications [21].....	39
Table 10: Specifications for the Relative Humidity Sensor [22] .....	40
Table 11: R600a Refrigerant Properties [23].....	43
Table 12: Experimental Matrix .....	44
Table 13: Average Cycle Properties for 5°C Ambient Condition .....	55
Table 14: Average Cycle Properties for 32°C Ambient Condition .....	56
Table 15: Error Analysis for 5°C Ambient Condition .....	56
Table 16: Error Analysis for 32°C Ambient Condition .....	56
Table 17: Specifications for the Ohaus Explorer High Accuracy Scale [27] .....	62
Table 18: Test Results Summary .....	67
Table 19: Pressure Ratios for Each Ambient Condition with the Accumulator .....	70
Table 20: Compressor Liquid Level Results for Each Ambient Condition for Testing with the Accumulator .....	89

Table 21: Accumulator Liquid Level Results for Each Ambient Condition for Testing with the Accumulator.....	92
Table 22: Compressor Data Points for Mass Balance for Pull-down at the 5°C Ambient Condition for Testing with the Accumulator .....	97
Table 23: Accumulator Data Points for Mass Balance for Pull-down at the 5°C Ambient Condition for Testing with the Accumulator .....	97
Table 24: Liquid Level Scale for New Compressor .....	113
Table 25: Extended Experimental Matrix.....	116
Table 26: Comparison of Test Results for Tests completed with and without the Accumulator at the 5°C Ambient Condition.....	117
Table 27: Comparison of Test Results for Tests completed with and without the Accumulator at the 32°C Ambient Condition.....	118
Table 28: Average Comparison of Test Results for Tests completed with and without the Accumulator at 5°C .....	118
Table 29: Average Comparison of Test Results for Tests completed with and without the Accumulator at 32°C .....	119
Table 30: Pressure Ratios for Conditions without the Accumulator .....	121
Table 31: Data Comparison with and without Accumulator for Compressor On-Time during Cycling at the 5°C Ambient Condition .....	123
Table 32: Data Comparison with and without Accumulator for Compressor On-Time during Cycling at the 32°C Ambient Condition .....	124
Table 33: Compressor Liquid Level Results for Each Ambient Condition for Testing without the Accumulator.....	139

Table 34: Compressor Data Points for Mass Balance for Pull-down at 5°C, 44g Charge, for Testing without the Accumulator .....	144
Table 35: Compressor Mass Balance Data for Pull-down for 32°C, I .....	157
Table 36: Compressor Mass Balance Data for Pull-down for 32°C, II .....	157
Table 37: Accumulator Mass Balance Data for Pull-down for 32°C, I.....	158
Table 38: Accumulator Mass Balance Data for Pull-down for 32°C, II.....	158
Table 39: Compressor Mass Balance Data for Pull-down for 43°C, I .....	159
Table 40: Compressor Mass Balance Data for Pull-down for 43°C, II .....	159
Table 41: Accumulator Mass Balance Data for Pull-down for 43°C, I.....	159
Table 42: Accumulator Mass Balance Data for Pull-down for 43°C, II.....	160
Table 43: Compressor Mass Balance Data for Cycling for 5°C, I .....	160
Table 44: Compressor Mass Balance Data for Cycling for 5°C, II .....	161
Table 45: Accumulator Mass Balance Data for Cycling for 5°C, I.....	161
Table 46: Accumulator Mass Balance Data for Cycling for 5°C, II.....	162
Table 47: Compressor Mass Balance Data for Cycling for 32°C, I .....	162
Table 48: Compressor Mass Balance Data for Cycling for 32°C, II .....	162
Table 49: Accumulator Mass Balance Data for Cycling for 32°C, I.....	163
Table 50: Accumulator Mass Balance Data for Cycling for 32°C, II.....	163
Table 51: Compressor Mass Balance Data for Defrost for 5°C, I .....	164
Table 52: Compressor Mass Balance Data for Defrost for 5°C, II.....	164
Table 53: Accumulator Mass Balance Data for Defrost for 5°C, I.....	165
Table 54: Accumulator Mass Balance Data for Defrost for 5°C, II .....	165
Table 55: Compressor Mass Balance Data for Defrost for 32°C, I .....	166

Table 56: Compressor Mass Balance Data for Defrost for 32°C, II.....	166
Table 57: Accumulator Mass Balance Data for Defrost for 32°C, I.....	166
Table 58: Accumulator Mass Balance Data for Defrost for 32°C, II .....	167
Table 59: Compressor Mass Balance Data for Defrost for 43°C, I.....	167
Table 60: Compressor Mass Balance Data for Defrost for 43°C, II.....	167
Table 61: Accumulator Mass Balance Data for Defrost for 43°C, I.....	168
Table 62: Accumulator Mass Balance Data for Defrost for 43°C, II .....	168
Table 63: Compressor Mass Balance Data for Pull-down for 32°C, 44g Charge, I.....	169
Table 64: Compressor Mass Balance Data for Pull-down for 32°C, 44g Charge, II.....	169
Table 65: Compressor Mass Balance Data for Pull-down for 32°C, 48g Charge, I.....	170
Table 66: Compressor Mass Balance Data for Pull-down for 32°C, 48g Charge, II.....	170
Table 67: Compressor Mass Balance Data for Cycling for 5°C, 44g Charge, I.....	171
Table 68: Compressor Mass Balance Data for Cycling for 5°C, 44g Charge, II.....	172
Table 69: Compressor Mass Balance Data for Cycling for 5°C, 48g Charge, I.....	172
Table 70: Compressor Mass Balance Data for Cycling for 5°C, 48g Charge, II.....	172
Table 71: Compressor Mass Balance Data for Cycling for 5°C, 52g Charge, I.....	173
Table 72: Compressor Mass Balance Data for Cycling for 5°C, 52g Charge, II.....	174
Table 73: Compressor Mass Balance Data for Cycling for 32°C, 44g Charge, I.....	175
Table 74: Compressor Mass Balance Data for Cycling for 32°C, 44g Charge, II.....	175
Table 75: Compressor Mass Balance Data for Cycling for 32°C, 50g Charge, I.....	175
Table 76: Compressor Mass Balance Data for Cycling for 32°C, 50g Charge, II.....	176
Table 77: Compressor Mass Balance Data for Defrost for 5°C, 44g Charge, I.....	177
Table 78: Compressor Mass Balance Data for Defrost for 5°C, 44g Charge, II .....	177

Table 79: Compressor Mass Balance Data for Defrost for 32°C, 44g Charge, I.....	178
Table 80: Compressor Mass Balance Data for Defrost for 32°C, 44g Charge, II .....	178
Table 81: Compressor Mass Balance Data for Defrost for 32°C, 48g Charge, I.....	178
Table 82: Compressor Mass Balance Data for Defrost for 32°C, 48g Charge, II .....	179

## List of Figures

Figure 1: Schematic of a Vapor Compressor System .....	3
Figure 2: Sample P-h Diagram for an Ideal Refrigeration Cycle [1].....	4
Figure 3: Sample Schematic with SLHX, Accumulator, and Filter Dryer .....	5
Figure 4: Measurement Principle for Fukuta et al. Experimentation [9].....	11
Figure 5: Changing Vapor Pressure with Time for Different Temperature Conditions [12] .....	14
Figure 6: Concentration Dependence on Vapor Pressure for R600a/Mineral Oil Solution [12].....	15
Figure 7: Concentration Dependence on Density for R600a/Oil Solution [12].....	15
Figure 8: Accumulator and Saturated Temperatures Showing Refrigerant Trapped in the Accumulator after Start-up [3].....	17
Figure 9: Accumulator View during Compressor Start-up [6] .....	19
Figure 10: Commercial Frost Free Bottom Freezer Refrigerator-Freezer [16] .....	21
Figure 11: Unmodified Commercial Compressor.....	22
Figure 12: Compressor with Visualization Tube and UV Dye.....	23
Figure 13: System Evaporator with Installed Clear Accumulator .....	25
Figure 14: Clear Accumulator Installed with Calibration Lines.....	26
Figure 15: Suction (solid circle) and Discharge (dotted circle) Sight Glasses .....	27
Figure 16: Accumulator Outlet Sight Glass.....	28
Figure 17: Camera View of Compressor .....	29
Figure 18: Unmodified Evaporator Panels in front of the Accumulator within the Freezer Compartment.....	29

Figure 19: Heater Removed from the Rear of the Fan Panel.....	30
Figure 20: Modified Evaporator Panels for Accumulator Visualization.....	30
Figure 21: Camera View of Accumulator with LED Lights.....	30
Figure 22: Camera View of the Accumulator Outlet with LED Lights.....	31
Figure 23: Camera View of the Suction and Discharge Lines.....	31
Figure 24: Pressure Transducer and Thermocouple Placement.....	32
Figure 26: Setra Pressure Transducer [19].....	33
Figure 26: Pressure Transducers Outside of the Unit.....	33
Figure 27: Evaporator Inlet Pressure Transducer Connection.....	34
Figure 28: T-type Thermocouple [20] .....	35
Figure 29: Air Side Evaporator Thermocouples.....	36
Figure 30: Food Compartment Thermocouples.....	37
Figure 31: Freezer Compartment Thermocouples.....	37
Figure 32: Environmental Chamber Temperature Measurements.....	38
Figure 34: Watt Meter.....	39
Figure 34: Vaisala Humidity Sensor.....	40
Figure 35: Environmental Chamber and Computer Controls.....	40
Figure 36: Hewlett Packard Data Acquisition Unit (HP 3497A) .....	41
Figure 37: Voltage and Frequency Inverters (Manufactured by LeMarche).....	42
Figure 38: Silicon Sealant for Refrigerator and Freezer Doors .....	42
Figure 39: System Schematic with State Points .....	46
Figure 40: State Points of the Refrigeration Cycle on a P-h Diagram.....	46

Figure 41: Original Solubility Data for Freol S-10 Mineral Oil and R600a (Provided by the Manufacturer).....	48
Figure 42: Solubility Curve Developed in TableCurve® 3D .....	50
Figure 43: Original Mixture Density Data Provided by the Manufacturer for Freol S-10 Oil and R600a .....	51
Figure 45: Mixture Density Correlation Developed by TableCurve® 3D .....	52
Figure 45: Cycles Used for Random Error Calculations from a 5°C Ambient Test .....	55
Figure 46: Cycles Used for Random Error Calculations from a 32°C Ambient Test .....	55
Figure 47: Sample Collection Pipe through the Sight Tube at the bottom of the Compressor .....	58
Figure 48: Sample Pipe in the Accumulator (front view).....	58
Figure 49: Sample Pipe in Accumulator (rear view) .....	59
Figure 50: Oil/Refrigerant Collection Vessel .....	60
Figure 51: Valve System for Sample Collection .....	60
Figure 52: Oil Charging "U" Tube.....	61
Figure 53: Oil Port U-tube Assembly in the Suction Line.....	61
Figure 54: Valve System for the Oil Port U-tube Assembly .....	61
Figure 56: Ohaus Explorer High Accuracy Scale.....	62
Figure 56: Suction Pressure for Each Ambient Condition for Testing with the Accumulator.....	68
Figure 57: Discharge Pressure for Each Ambient Condition for Testing with the Accumulator.....	69

Figure 58: P-h Diagram for Each Ambient Condition at Averaged Values for Compressor-On Time Periods for Testing with the Accumulator .....	70
Figure 59: Inside Oil Temperature at the Base of the Compressor for Each Ambient Condition for Testing with the Accumulator .....	71
Figure 60: Average Accumulator Temperature for the 5°C and 32°C Conditions for Testing with the Accumulator.....	72
Figure 61: Accumulator Inlet and Outlet Temperatures for the 5°C Ambient Condition for Testing with the Accumulator .....	73
Figure 62: Evaporator Inlet and Outlet Temperatures for the 5°C Ambient Condition for Testing with the Accumulator.....	74
Figure 63: System Power for Each Ambient Condition for Testing with the Accumulator .....	75
Figure 64: Pull-down, Cycling, and Defrost Periods for the 32°C Condition for Testing with the Accumulator.....	76
Figure 65: Evaporator Specific Capacity vs. Time for 5°C and 32°C Conditions for Testing with the Accumulator.....	78
Figure 66: Condenser Specific Capacity vs. Time for 5°C and 32°C Conditions for Testing with the Accumulator.....	78
Figure 67: Degrees of Superheat for Each Ambient Condition for Testing with the Accumulator.....	79
Figure 68: Compressor Solubility for Each Ambient Condition for Testing with the Accumulator.....	81

Figure 69: Accumulator Solubility for Each Ambient Condition for Testing with the Accumulator.....	82
Figure 70: Compressor Mixture Density for Each Ambient Condition.....	83
Figure 71: Accumulator Mixture Density for Each Ambient Condition .....	84
Figure 72: Ideal and Actual Mixture Density for the 5°C Condition for Testing with the Accumulator.....	85
Figure 73: Correction Factors for R600a and Freol S-10 Mineral Oil Based on Calculated Ideal and Mixture Densities .....	85
Figure 74: Start-up Trends in the Compressor for a) 5°C, b) 32°C and c) 43°C Ambient Conditions for Testing with the Accumulator .....	87
Figure 75: Cycling Trends for the Compressor at the 32°C Condition while a) Compressor is on and b) Compressor is off for Testing with the Accumulator .....	88
Figure 76: Accumulator Start-up Trends at the 32°C Condition at a) initial start-up and b) just prior to defrost.....	90
Figure 77: Mass Balance for the Pull-down Period for the 5°C Ambient Condition for Testing with the Accumulator.....	98
Figure 78: Mass Balance for the Pull-down Period for the 32°C Ambient Condition for Testing with the Accumulator.....	100
Figure 79: Mass Balance for the Pull-down Period for the 43°C Ambient Condition for Testing with the Accumulator.....	101
Figure 80: Mass Balance for the Cycling Period at the 5°C Ambient Condition for Testing with the Accumulator.....	103

Figure 81: Mass Balance for the Cycling Period at the 32°C Ambient Condition for Testing with the Accumulator.....	103
Figure 82: Mass Balance for the Defrost Period at the 5°C Ambient Condition for Testing with the Accumulator.....	105
Figure 83: Mass Balance for the Defrost Period at the 32°C Ambient Condition for Testing with the Accumulator.....	106
Figure 84: Mass Balance for the Defrost Period for the 43°C Ambient Condition for Testing with the Accumulator.....	106
Figure 85: New Compressor with Modified Sight Glass Liquid Level Scale .....	113
Figure 86: Accumulator Removal and Pipe Replacement.....	114
Figure 87: System Schematic for Testing without the Accumulator .....	114
Figure 88: Suction and Discharge Pressures for Tests with and without the Accumulator at Various Charges at the 5°C Ambient Condition.....	120
Figure 89: Suction and Discharge Pressures for Tests with and without the Accumulator at Various Charges at the 32°C Ambient Condition.....	121
Figure 90: P-h Diagram for Tests with and without the Accumulator at Various Charges at the 5°C Ambient Condition .....	122
Figure 91: P-h Diagram for Tests with and without the Accumulator at Various Charges at the 32°C Ambient Condition .....	123
Figure 92: Suction and Inside Compressor Temperatures for Tests with and without the Accumulator at Various Charges at the 5°C Ambient Condition.....	125
Figure 93: Suction and Inside Compressor Temperatures for Tests with and without the Accumulator at Various Charges at the 32°C Ambient Condition.....	126

Figure 94: Evaporator Temperatures for Tests with and without the Accumulator at Various Charges at the 5°C Ambient condition.....	127
Figure 96: Evaporator Temperatures for Tests with and without the Accumulator at Various Charges at the 32°C Ambient condition.....	128
Figure 96: Power Results for Tests with and without the Accumulator at Various Charges at the 5°C Ambient Condition .....	129
Figure 97: Power Results for Tests with and without the Accumulator at Various Charges at the 32°C Ambient Condition .....	129
Figure 98: Evaporator Capacity for Tests with and without the Accumulator at Various Charges at the 5°C Ambient Condition .....	131
Figure 99: Evaporator Capacity for Tests with and without the Accumulator at Various Charges at the 32°C Ambient Condition .....	131
Figure 100: Condenser Capacity for Tests with and without Accumulator at Various Charges at the 5°C Ambient Condition .....	132
Figure 101: Condenser Capacity for Tests with and without Accumulator at Various Charges at the 32°C Ambient Condition .....	132
Figure 102: Superheat Results for Tests with and without the Accumulator for Various Charges at the 5°C Ambient Condition .....	134
Figure 103: Superheat Results for Tests with and without the Accumulator for Various Charges at the 32°C Ambient Condition .....	134
Figure 104: Compressor Solubility for Tests with and without the Accumulator for Various Charges at the 5°C Ambient Condition.....	135

Figure 105: Compressor Solubility for Tests with and without the Accumulator for Various Charges at the 32°C Ambient Condition.....	136
Figure 106: Mass Balance for Pull-down Period for 5°C Ambient Condition, 44g Charge, for Testing without the Accumulator.....	144
Figure 107: Mass Balance for Pull-down Period for 32°C Ambient Condition, 44g Charge, for Testing without the Accumulator.....	145
Figure 108: Mass Balance for Cycling Period at 5°C Ambient Condition, 44g Charge, for Testing without the Accumulator.....	147
Figure 109: Mass Balance for Cycling Period at 32°C Ambient Condition, 44g Charge, for Testing without the Accumulator.....	147
Figure 110: Mass Balance for Defrost Period at 32°C Ambient Condition, 44g Charge, for Testing without the Accumulator.....	149
Figure 112: Mass Balance for Pull-down Period at 32°C Ambient Condition, 48g Charge, for Testing without the Accumulator.....	171
Figure 113: Mass Balance for Cycling Period at 5°C Ambient Condition, 48g Charge, for Testing without the Accumulator.....	173
Figure 114: Mass Balance for Cycling Period at 5°C Ambient Condition, 52g Charge, for Testing without the Accumulator.....	174
Figure 115: Mass Balance for Cycling Period at 32°C Ambient Condition, 50g Charge, for Testing without the Accumulator.....	176
Figure 116: Mass Balance for Defrost Period at 32°C Ambient Condition, 48g Charge, for Testing without the Accumulator.....	179

## Nomenclature

A	Correction Factor
ACC	Accumulator
ASHRAE	American Society of Heating, Refrigeration, and Air-Conditioning Engineers
DAS	Data Acquisition System
$h$	Enthalpy
HFC	Hydrofluorocarbon
HVAC	Heating, ventilation, and air-conditioning
L	Length
LED	Light-Emitting Diode
$m$	Mass
P	Pressure
POE	Polyolester (oil)
PT	Pressure Transducer
PVE	Polyvinylether (oil)
$q$	Capacity
RH	Relative Humidity
SLHX	Suction Line Heat Exchanger
T	Temperature
TC	Thermocouple
UV	Ultraviolet
V	Volume

$w$  Mass Fraction of Refrigerant in Solution

$z$  Solubility

### **Greek Symbols**

$\rho$  Density

### **Subscripts**

cond Condenser

dis Discharge

dis,i Discharge, instream

evap Evaporator

evap,s Evaporator, surface

id Ideal

m Mixture

o Oil

r Refrigerant

sat,Pi Saturated at pressure  $i$

subcooling Subcooling

suc Suction

superheat Superheat

t Total

# 1 Introduction

In industry and business, it is always necessary to continue to search for improvements in a product in order to maximize profit and customer satisfaction. In refrigeration, most testing revolves around improving efficiency and reducing harmful effects on the environment with the use of improved refrigerants. In addition to this work, however, it is also very important to understand the basic relationship between each component and how their interaction affects the overall performance of the entire system. Because refrigerators include compressors, it is important to examine the type and amount of lubricant and refrigerant used. Lubricant, typically a mineral or POE oil, is necessary to keep the compressor operating properly so that components do not create excessive friction that could cause damage to the mechanical components or motor. Refrigerant in the system provides the means for cooling and flows freely throughout the system changing from gas to liquid and liquid to gas, depending on the stage of the cycle. When in the compressor, however, the refrigerant and lubricant must co-exist and consequently have important effects on one another. It is often possible for the refrigerant to dissolve in the oil, reducing the volume of pure refrigerant available to the system. It is also possible for the oil to migrate throughout the system. This phenomenon is not well understood as the likelihood for migration depends greatly on the lubricant, refrigerant, and the system itself. It is unknown if oil is ever trapped in certain components and if so, what effects it may have on overall performance.

In addition to the compressor, the accumulator is an important component for a refrigeration system. While this component is not an active feature in the refrigeration

process, it provides a service to the compressor and aims to improve the safety of the system. An accumulator is a small tank typically installed after the evaporator that provides a small volume that can be filled with liquid refrigerant. As the compressor operates, or more importantly, when the compressor is in an off-mode, it is possible that some liquid refrigerant can escape from the evaporator. Liquid can cause significant damage to the compressor and it is thus vital that only vapor enter the compressor. The accumulator is therefore installed upstream of the compressor in order to act as a collector for any liquid refrigerant that could potentially leave the evaporator and enter the compressor. The effectiveness of the accumulator, however, is generally not well understood as the available volume is fixed and refrigerant flow through the system is variable as the compressor turns on and off. It is also unknown as to whether or not compressor oil enters or remains in the accumulator during operation and whether or not this action affects the available volume able to contain liquid refrigerant.

Understanding the oil and refrigerant distribution within the refrigeration system is important in evaluating the effectiveness and overall performance of the system. In particular, it is of interest to study the accumulator and how well it traps liquid refrigerant from entering the compressor.

## 2 Background

### 2.1 The Working Principle of Vapor Compression Cycles

In order to understand the oil/refrigerant distribution and the effectiveness of the accumulator, it is first necessary to understand the working principles of a traditional vapor compression cycle. A traditional vapor compression cycle is comprised of four main elements: a compressor, condenser, expansion device, and evaporator, as shown in Figure 1.

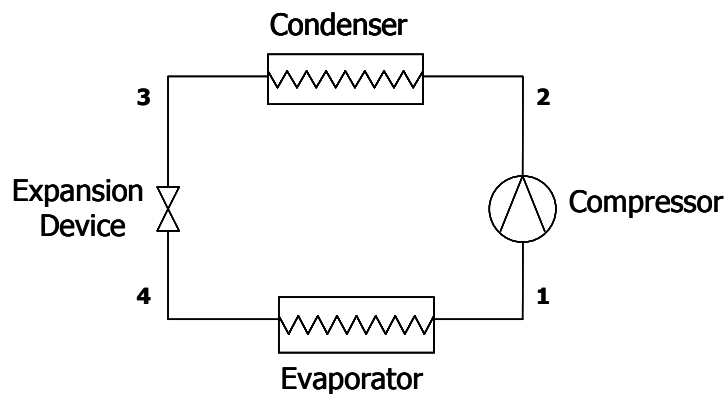


**Figure 1: Schematic of a Vapor Compression System**

For a refrigeration cycle, the evaporator works in the cold space of the refrigerator and/or freezer and the condenser interacts with the warmer ambient air. Starting at the compressor, point 1, refrigerant enters as a gas and is compressed to a higher temperature. In the ideal cycle, this compression is isentropic, as seen on the P-h diagram in Figure 2, and involves a temperature increase. The refrigerant leaves the compressor as a superheated vapor at a temperature above the ambient condition and then enters the condenser. During this phase, the pressure remains relatively constant, dropping only

slightly due to pressure drops through the condenser coils. While the pressure remains constant, the temperature of the refrigerant decreases as the condenser interacts with the ambient air. Heat carried from the refrigerant is rejected to the ambient, consequently lowering the temperature of the working fluid. The refrigerant leaves the condenser as a saturated liquid and then moves through an expansion device, either a valve or capillary tube, where the pressure is lowered to the desired evaporator operating pressure. During this process, the temperature of the refrigerant is lowered to a temperature below the desired temperature of the refrigerated space. For a typical household refrigerator, this value may be anywhere between  $-15$  and  $-30^{\circ}\text{C}$ . The refrigerant enters the evaporator as a vapor-liquid mixture and exchanges heat with the refrigerated space at a near-constant pressure. Because the temperature of the working fluid is below that of the desired temperature of the refrigerated space, the refrigerator is able to accept heat from the cabinet, allowing the refrigerant to warm up and the refrigerated space to cool down. The refrigerant leaves the evaporator as a saturated vapor and returns to the compressor to start the cycle once again.

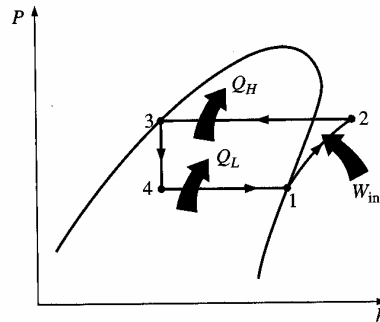


**Figure 2: Sample P-h Diagram for an Ideal Refrigeration Cycle [1]**

In order to ensure proper functioning of the vapor compression cycle, several other features are often included in the system. In order to ensure liquid is fed to the

expansion device and vapor is sent to the compressor, a suction-line heat exchanger (SLHX) is often included in the system. This heat exchanger allows a transfer of heat from liquid coming from the condenser to vapor leaving the evaporator. A transfer between these two stages allows the condenser liquid to be subcooled and the evaporator vapor to be superheated. Adding the SLHX and subcooling or superheating the refrigerant provides some insurance that the expansion device will not see a two-phase mixture at the inlet and that the compressor will not receive any liquid. In addition to the SLHX, an accumulator is also often added after the evaporator, as previously discussed. The accumulator acts as an added security that no refrigerant liquid will enter and damage the compressor. Finally, to remove any debris that may contaminate the refrigerant and block the piping, a filter dryer is typically installed in the system prior to the expansion device. A sample system including all of these features is shown in Figure 3.

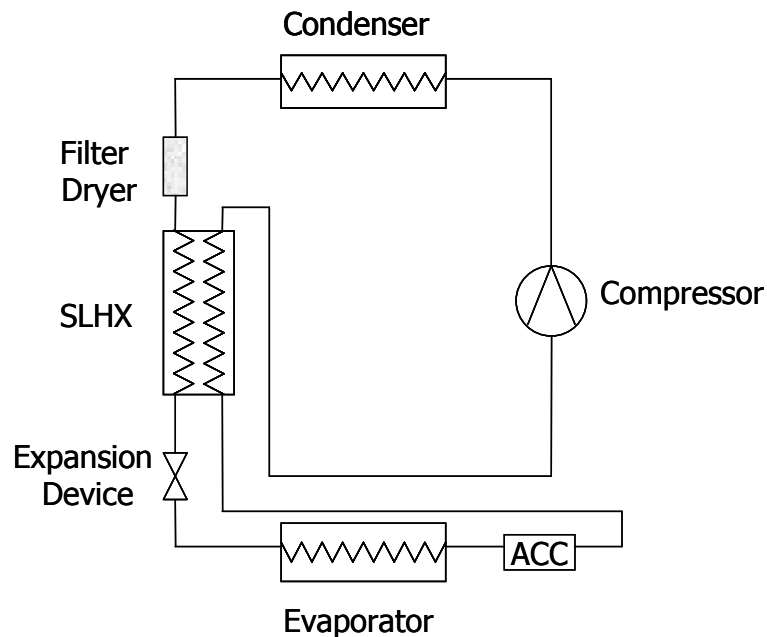


**Figure 3: Sample Schematic with SLHX, Accumulator, and Filter Dryer**

## **2.2 Literature Review**

Before beginning a new research project, it is important to understand prior work related to the area of interest. The following section explores prior research relating to refrigerant flow and migration, the relationship between oil and refrigerant and how to measure their concentration, and the effectiveness of the accumulator and its role in the refrigeration cycle.

### **2.2.1 Effects and Characteristics of Oil and Refrigerant Migration and Distribution**

While the household refrigerator has been in use for the last 80 to 90 years [2], it has not always been well understood how the refrigerant and compressor oil move throughout the system. A general understanding of the main components and their role in the refrigeration cycle has been known for some time; however, the exact movement of the refrigerant fluid through the system and how its movement changes during different periods of the refrigeration cycle is a topic of study for many researchers. A particular area of study within this field is refrigerant migration. When a refrigerator is first turned on, it undergoes a pull-down period in which the compressor is constantly running, working to bring the refrigerator and freezer cabinet temperatures to the desired levels. Once these temperatures have been reached, the compressor then experiences a cycling phase in which the compressor remains on for a given period of time and then turns off. This is due to the fact that the compressor no longer needs to remain on in order to maintain the desired cabinet temperatures. The compressor is able to turn off for a period of time in order to save power. Once the temperatures reach a higher level deemed

unacceptable by the control system of the refrigerator, the compressor will then turn back on and work with the rest of the system to restore the cabinet temperatures.

Refrigerant migration is a problem that occurs during the off-cycle of the compressor. During this time, the refrigerant stops flowing as it normally would through the system because it is no longer driven by the compressor. As has been found by several researchers, the off-cycle causes refrigerant to migrate from the condenser to the evaporator as the system equalizes its high and low pressures. Warmer refrigerant at a high pressure stored in the condenser prefers to move to the cooler and lower pressure evaporator, and thus migrates to this space. In doing so, both the temperature and pressure of the evaporator rise, consequently reducing the performance of the refrigerator when the compressor turns back on for the on-cycle.

As reported by Coulter and Bullard [3], researchers Rubas, Bullard, and Krause first explored this topic by examining a variety of factors that reduce refrigerator performance. Coulter and Bullard later in 1997 expanded upon their prior work in order to determine the detrimental effects of refrigerant migration and what measures could be taken in order to improve performance during the on-cycle. Coulter and Bullard found that the refrigerant migration to the evaporator requires that the on-cycle “must first cool the evaporator, so the thermal capacitance of the evaporator causes an on-cycle loss” [3]. Because the refrigerant migrates to the evaporator, extra work is required to redistribute the refrigerant as necessary. Consequently, at the beginning of the on-cycle period, a decrease in evaporator capacity and an increase in system power is observed. Coulter and Bullard suggested that the accumulator may also have a negative impact in this situation as it may trap needed liquid refrigerant from the evaporator. In total, in order to reduce

the negative effects of refrigerant migration, Coulter and Bullard have suggested the use of a solenoid valve after the condenser to prevent refrigerant migration altogether and the relocation, or even removal, of the accumulator.

Other studies have taken a more general approach to observing refrigerant, and in some cases oil, distribution throughout a refrigeration cycle during operation. It is of interest to know how much refrigerant is in a given component at a given time in order to determine the effectiveness of each component and the overall system as a whole. A number of methods have been used to observe refrigerant flow and some studies, such as those conducted by Manwell and Bergles [4] in 1989, have been set up specifically to examine flow patterns involving oil and refrigerant mixtures.

Asano et al. [5] examined refrigerant flows in a domestic refrigerator in a study completed in 1996. The experiment utilized neutron radiography to observe the refrigerant flow and allowed for real-time measurements and visualization using high speed cameras. The experiment provided images of flow within the compressor, evaporator, condenser, and capillary tube. Flow near the compressor and in the liquid separator included in the experimental set-up showed frothy mixtures due to the presence of oil in the refrigerant. For the condenser in particular, it was found that the orientation and inclination of the condenser tubes are very important and change the flow behavior of the refrigerant.

Inan et al. [6] examined refrigerant flows in a domestic refrigeration system in 2003, but they utilized an x-ray method as opposed to neutron radiography. Images were focused on the filter dryer, capillary tube, evaporator, and accumulator. The condenser and compressor were not examined. The x-ray system utilized for experimentation

provided real-time visualization of the dynamic behavior of the refrigeration system. Video was recorded and reviewed to examine refrigerant trends throughout the system and temperatures were also closely monitored and recorded to understand corresponding trends. In total, Inan et al. were able to show that the x-ray method is an effective way to monitor refrigerant distribution. General flow trends were discovered, more of which are discussed in section 2.2.3.

A number of other studies explore refrigerant flow with direct impact on the compressor. As mentioned above, liquid refrigerant entering the compressor can cause significant damage, leading to ultimate failure of the component. In reciprocating compressors in particular, which are the topic of study for Prasad [7], liquid in the compressor volume leads to excessive pressure build up as the piston cannot expel the liquid through the discharge valve. Excessive pressure within the compressor puts a great amount of strain on the moving parts and can eventually cause them to fail. Liquid capture is thus the most important job of the accumulator, as it can protect the compressor from potential damage, but, as described by Coulter and Bullard [3], this exact capability can also create disadvantages in terms of overall system performance and refrigerant migration.

## **2.2.2 Measurement of Oil and Refrigerant Mixture Concentrations**

In addition to knowing how refrigerant moves throughout the refrigeration cycle and within specific components, it is also extremely important to know how the compressor lubricant and system refrigerant interact and mix. The compressor lubricant is vital for protecting the moving parts of the compressor and preventing long term wear and tear that could threaten compressor efficiency and lifetime. Some oil will inevitably,

however, move with the refrigerant from the compressor to other components within the system. It is important to understand how the oil and refrigerant will interact to ensure that the presence of the oil will not significantly change the working properties of the refrigerant throughout the system. Several studies have been conducted to examine the relationship between oil and refrigerant in refrigeration cycles and researchers have attempted to measure oil/refrigerant mixture concentration. Other researchers have attempted to develop methods to predict oil/refrigerant mixtures and properties, though this practice generally proves very difficult due to the transient nature of the refrigeration cycle. In general, there are two approaches to examining oil and refrigerant mixtures. Some researchers examine oil as a pollutant to the refrigerant that affects refrigerant properties. Other scientists view the oil/refrigerant mixture like a zeotropic mixture, enabling them to review all oil-related effects throughout the entire refrigeration cycle [9].

Real-time measurements of oil/refrigerant concentration were attempted by Lebreton et al. [8] in 2000 using an ultrasonic device. POE oil and R410A were used for the experiment, which was intended to not only determine the characteristics of the oil/refrigerant mixture, but also to verify the method of utilizing the variations of the speed of sound in the mixture to determine concentration. This real-time measurement, along with other real-time methods, is preferred to a sampling technique since samples will remove needed amounts of oil and refrigerant from the system. Most research conducted recently on this topic has focused on the success and utilization of real-time measurements.

Like many other authors, Lebreton et al. believe “that the quantity of oil present in the vapor phase of an oil/refrigerant liquid mixture is negligible” [8]. In many cases, the

boiling point of the oil is much higher than that of the refrigerant, so it is unlikely that the oil will be included in the vapor phase of the refrigerant. The most important mixture, therefore, is that of liquid oil and liquid refrigerant.

In their study, Lebreton et al. were able to successfully use the ultrasonic method to examine oil/refrigerant mixtures and the oil distribution throughout the refrigeration cycle. Characteristics of oil/refrigerant mixtures, however, vary greatly depending on the type of oil and refrigerant used. Therefore, the ultrasonic method is useful, but only with careful and time-consuming calibration conducted specifically for the unique combination of fluids.

Fukuta et al. (2006) [9] also examined real-time measurement of oil/refrigerant mixtures by using a refractive index measure with a laser displacement sensor. Fukuta et al. explain that the inclusion of oil within the refrigerant “affects pressure drop and the heat transfer characteristics of the heat exchangers” [9], thus validating the importance of oil/refrigerant concentration measurements. The principle of Fukuta et al.’s measurement method uses the difference of refractive index between the refrigerant and oil to detect the mixing ratio between them. The principle is outline in Figure 4.

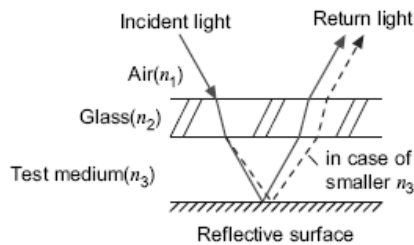


**Figure 4: Measurement Principle for Fukuta et al. Experimentation [9]**

Like Lebreton et al., Fukuta et al. agreed that a sampling technique is generally undesirable for determining the oil/refrigerant concentration in a given mixture. In order

to verify results and the refractive index measurement method, however, samples were also taken during experimentation. A range of concentrations and temperatures were studied in order to obtain a comprehensive understanding of the mixing relationship between oil and refrigerant, which were PVE and R410A, respectively. Equations relating the refractive index, temperature, pressure, mixture density, and concentration were found specific to the experiment. The method proved successful and real-time measurements were taken. No specific results relating the concentrations of the mixtures were provided.

Prior work by Fukuta et al. (2005) [10] explored the relationship between R600a and mineral oils when mixing and separating, an oil/refrigerant combination of particular interest to this project. Two experiments were designed and conducted to test first the transient mixing of R600a with several mineral oils and second the separation of R600a and mineral oil. Mixing was not conducted mechanically, but was rather induced using a change in pressure simulating the off-period in the vapor-compression cycle. Unlike other more traditional oil/refrigerant mixtures, R600a is less dense than the compressor oil and different mixing trends consequently result. Where other mixtures experience mixing by convection due to the differences in density, R600a and mineral oils do not experience this phenomenon and instead mix by diffusion when subject to appropriate changes in pressure. The mixing process, therefore, is very slow. Separation experimentation also only considered decreases in pressure as the motivator for changes in the R600a/mineral oil mixtures. A vessel containing R600a and mineral oil was depressurized and trends in the fluid behavior were observed. The most important observation was bubble formation shortly after the start of depressurization. Bubbles were unstable and unpredictable and

affected the rate at which the vessel completely depressurized. Convection was observed in this condition, unlike the mixing case, because of the density difference between the bottom (high density) and top of the vessel (low density) where the refrigerant escaped. Fukuta et al. (2005) did not explore conditions of mixing or separation where mechanical stimulation occurred, as when the compressor would turn-on during start-up or cycling periods, but a better understanding of transient behavior for R600a/mineral oil solutions during the off-periods was obtained.

While real-time measurements provide experimental data evaluating the concentration of oil/refrigerant mixtures and their fluid behavior, it is ultimately desired to have a basic known relationship for oil/refrigerant mixtures at given pressures and temperatures. Using experimental results and simulation, several researchers have attempted to further understand the relationship between oil and refrigerant and quantify it by creating useful mixture equations. In 1999, Elvassore et al. [11] proposed a method for calculating the vapor-liquid equilibrium for oil/refrigerant mixtures. The method builds upon the classical cubic equation of state but requires the knowledge of all oil properties and the chemical composition. The relationship developed is also specifically for use between hydrofluorocarbons (HFCs) and POE oils, so use of the method with other refrigerants and mineral oils may not hold.

Zhelezny et al. [12] went further in determining mathematical relationships for oil/refrigerant mixtures by using experimental work to backup modeling simulations and previous predictions in work conducted in 2007. Like Fukuta et al. (2005) [10], Zhelezny et al. specifically explored R600a and compressor oil solutions, solutions that are of particular interest to this project. Experiments were conducted to examine the solubility,

mixture density, and capillary constant for such solutions and results were combined with models to develop appropriate relationships. In general, it was found that it takes a significant amount of time for an R600a/oil solution to reach equilibrium, as seen in Figure 5. Thermodynamic properties of an oil/refrigerant solution are best measured under steady conditions. Zhelezny et al. made sure to establish equilibrium before measuring the desired properties, but the length of time to reach this point, which was generally several hours, shows through example the pure difficulty in determining real-time transient oil/refrigerant properties. This result also supports the findings of Fukuta et al. (2005) for the mixing of R600a and mineral oil due to pure temperature and pressure changes. Because of the low density of the R600a refrigerant, the refrigerant and oil are slow to mix as they do so through diffusion alone.

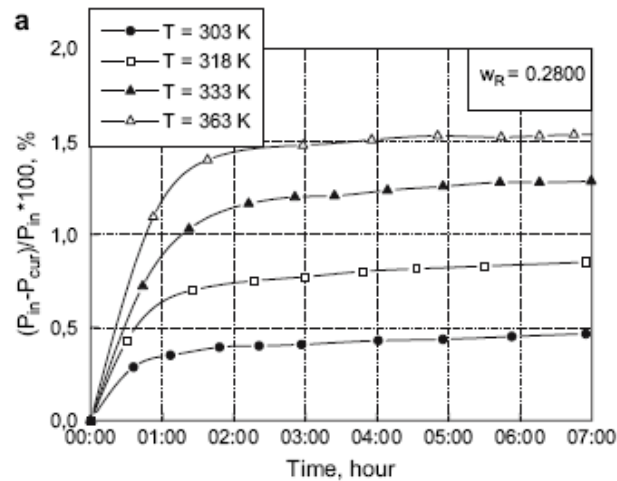


**Figure 5: Changing Vapor Pressure with Time for Different Temperature Conditions [12]**

The mathematical relationships found for the specified R600a/oil mixture were specific to the study conducted by Zhelezny et al. and included several empirical

constants that will vary for other solutions. While the equations established were specific to the tests conducted, results agreed well with the experimental data.

Zhelezny et al. were able to show basic R600a/mineral oil mixture trends in addition to developing mathematical relationships between the desired measurements. As can be seen in Figure 6, the saturated pressure of the R600a/mineral oil solution increases both with increasing temperature and weight fraction, or solubility, of R600a. As shown in Figure 7, the mixture density decreases with increasing temperature and weight fraction of R600a.

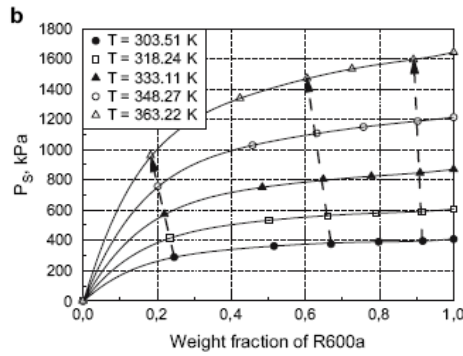


**Figure 6: Concentration Dependence on Vapor Pressure for R600a/Mineral Oil Solution [12]**

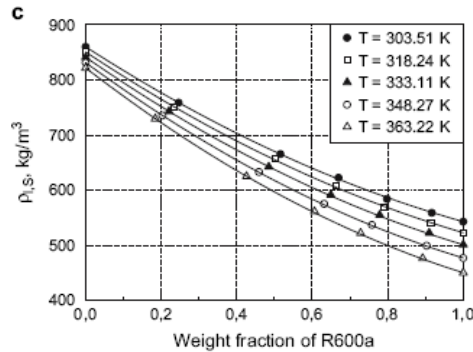


**Figure 7: Concentration Dependence on Density for R600a/Oil Solution [12]**

Finally, the American Society of Heating, Refrigerating, and Air-conditioning Engineers (ASHRAE) has published a detailed reference for refrigerants and lubricants in refrigerant systems [13]. Background information on a number of oils and their potential interaction with various refrigerants is included in the ASHRAE Refrigeration Handbook. The reference provides several data charts for various properties of oil/refrigerant mixtures including mixture viscosity, solubility, and density. Only a handful of refrigerants and oils are represented, however, leaving a large gap in the understanding of other oil/refrigerant solutions. General equations for defining mixture density, for example, are provided for solutions that are not represented in the given data.

Research conducted on oil/refrigerant solutions has proven two things. First, real-time measurements of oil/refrigerant concentrations are possible, but it is important to properly calibrate experiments appropriately for the specific oil/refrigerant solutions that are used. Second, the measurement of thermodynamic properties of oil/refrigerant mixtures is only possible under steady-state conditions, which can take hours to obtain, especially with systems using R600a. It must be understood, therefore, that transient measurement of oil/refrigerant solubility and mixture density is very difficult and subject to inaccuracies.

### **2.2.3 Accumulator Studies**

Because this study also examines the role of the accumulator within the refrigeration cycle, it is important to examine prior studies relating to the accumulator. Several studies outlined above explored the accumulator specifically and their work is further discussed here.

As mentioned above, Coulter and Bullard [3] discussed the accumulator briefly in their study of cycling losses in domestic refrigerators. While the accumulator is generally included to collect liquid refrigerant and keep it from entering and harming the compressor, Coulter and Bullard explained that this exact feature is also a drawback for the refrigeration system. Liquid remaining in the accumulator “starves” the evaporator, contributing to the decrease in evaporator capacity at the start of the on-cycle. Coulter and Bullard predicted from their experimental work that liquid refrigerant can remain in the accumulator for as long as 15 minutes during the beginning of an on-cycle, as shown in Figure 8.

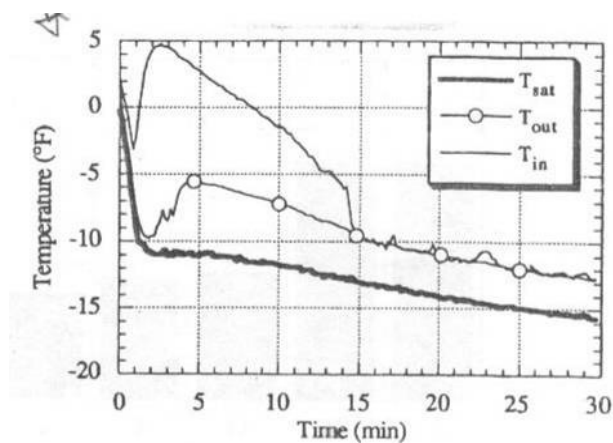


**Figure 8: Accumulator and Saturated Temperatures Showing Refrigerant Trapped in the Accumulator after Start-up [3]**

To help alleviate this problem, Coulter and Bullard have suggested that the accumulator could either be removed, which could compromise the compressor, or moved “outside the cabinet, close to the compressor, where heat conduction from the compressor would quickly evaporate any trapped liquid” [3]. Ultimately, it is of interest to determine if the accumulator is vital to the system in order to determine the best measures to enhance system performance.

Bjork and Palm [14] did not explicitly study the accumulator, but did note another important characteristic of the device. Because the accumulator is able to hold a variable amount of liquid, it is often able to act as a buffer for refrigerant charge within a given range of charges. With a charge that is too low, the system can become further starved and result in a large superheat. With a charge that is too high, the evaporator can overflow and create a cold suction line, which allows for cooling capacity outside of the refrigerator cabinet. The accumulator, however, “explains the rather flat energy minimum in between these two extremes” by providing a buffer volume that can trap a variable amount of fluid.

Inan et al. [6] examined the accumulator more specifically and were able to capture clear pictures of the accumulator and its associated liquid levels using their X-ray technique. They found that the maximum liquid level in the accumulator is achieved approximately one hour and twenty-five minutes after the system is started. Results also indicated that the liquid level in the accumulator is directly associated with the amount of subcooling and the liquid level rises as the amount of subcooling decreases. Flow behavior during the on and off periods also show changes in the liquid level. The liquid level is observed to decrease during the off-cycle as some liquid refrigerant drains back to the evaporator. When the system is started again, refrigerant is quickly pushed through the evaporator shortly after start-up and the accumulator fills with liquid, as shown in Figure 9. The liquid level in the accumulator, indicated by the dark shadow in the pictures of Figure 9, is shown to decrease during the off period in picture (a). As the system is started, liquid levels are observed to increase, as seen by the increase in shadow

in picture (b). Shortly after start-up, however, the liquid level decreases slightly, as seen in picture (d).

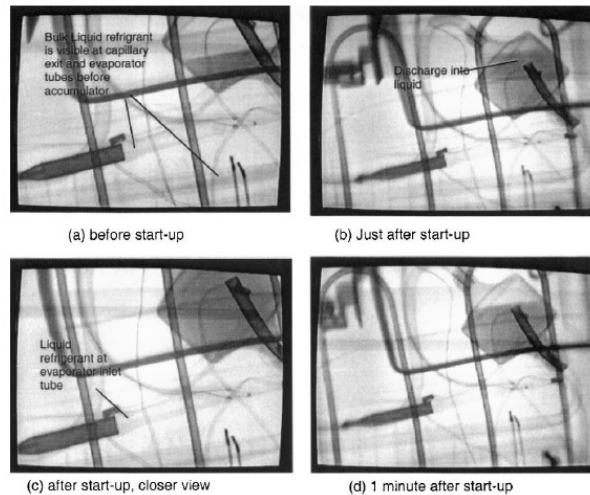


**Figure 9: Accumulator View during Compressor Start-up [6]**

As was found in the experiment conducted by Coulter and Bullard, some refrigerant can become trapped in the accumulator, especially during the off-cycle, but the amount of refrigerant trapped will of course depend on the capacity and orientation of the accumulator.

A study by Lee et al. [15] exclusively looked at oil and refrigerant flow through the accumulator for a rotary compressor. This work, conducted in 2003, was one of the first experiments to examine refrigerant flow through the accumulator in real-time. A transparent accumulator was built for the experiment and high speed cameras were used to capture images of the flow. Lee et al. observed pulsating motions of the oil and refrigerant mixtures moving through the accumulator, which were consistent with the pulsing motions, or phase, of the rotary compressor. It was also discovered that the flow may be affected by the presence of oil within the refrigerant and the entrance pipe of the accumulator is thus critical in the success of the overall design.

### **3 Motivation and Objectives**

The motivations and objectives of the study are outlined below.

#### **3.1 Motivation**

The purpose of studying oil and refrigerant migration within the refrigeration system and focusing on the accumulator is:

1. To improve refrigerator performance and efficiency
2. To possibly eliminate the accumulator, simplifying the refrigerator's design

Little research exists that explores the explicit role of the accumulator and how oil/refrigerant migration is related to its effectiveness.

#### **3.2 Objectives**

The objectives of this study are:

1. To observe the distribution of refrigerant and oil in a household refrigerator during the pull-down, cyclic, and defrost stages of operation
2. To determine the effectiveness and necessity of the accumulator

## 4 Experimentation with the Accumulator

In order to adequately assess the role of the accumulator within the refrigeration system, it is important to evaluate its effectiveness at different stages within the refrigeration cycle. In addition to cycle characteristics such as temperature and pressure, it is also useful to know the estimated volume of liquid enclosed in the accumulator and how much of that liquid is either refrigerant or oil. The experiment described in section 4.1 was designed in order to evaluate the effectiveness of the accumulator and to explore other interests relating to oil/refrigerant distribution. The final aim was to evaluate whether or not the accumulator was vital to the proper functioning of the compressor. If not, the removal of the accumulator could allow for cost reduction and simplification in the refrigerator design.

### 4.1 Experimental Set-up

#### 4.1.1 Refrigerator/Freezer

A commercial frost free bottom freezer refrigerator-freezer intended for an Asian or European market, as shown in Figure 10, was used for this experiment. Specifications are listed in Table 1 below:



**Figure 10: Commercial Frost Free Bottom Freezer Refrigerator-Freezer [16]**

**Table 1: Refrigerator-Freezer Specifications [16]**

Power	230V / 50Hz / .71A
Approximate Price	\$740.00 (USD)
Refrigerant	R600a
Insulation	Cyclopentane
Freezing Capacity	14Kg / 24hrs
Net Volume	Freezer: 104L Refrigerator: 246L
Defrosting Input	300W
Max. Input of Lamp	11W
Freezer Temperature Range	-17°C to -25°C
Refrigerator Temperature Range	+1°C to +6°C

#### 4.1.2 Compressor

The standard compressor used for the test refrigerator-freezer is a reciprocating compressor made for use with R600A. Specifications are listed in Table 2 and a picture of the original unmodified compressor is shown in Figure 11.

**Table 2: Compressor Specifications [16]**

Type	Reciprocating
Refrigerant	R600A
Voltage	220V / 50 Hz
ASHRAE cooling capacity	160 Kcal/Hr / 186 Watt / 635 Btu/Hr
ASHRAE COP / EER	55 W/W / 5.28 Btu/WHr
CECOMAF cooling capacity	118 Kcal/Hr / 138 Watt / 470 Btu/Hr
CECOMAF COP / EER	1.16 W/W / 3.96 Btu/WHr



**Figure 11: Unmodified Commercial Compressor**

Because it is of interest to study the relationship between oil and refrigerant, particularly within the compressor, the compressor was specially adapted for the experiment. A circular visualization port was added to its front and a visualization tube was added to its side. The visualization port was supplied and assembled by the manufacturer. In order to create the visualization tube, two holes were drilled into the compressor, one in the top and one in the bottom. The holes were then tapped and the compressor was flushed with oil to remove any remaining metal shavings. Teflon tape was used to attach NPT fittings to both holes and the visualization tube was attached using standard Swagelok® tube fittings. The installation of the visualization tube is shown in Figure 12. After installing the visualization tube, the compressor was calibrated for oil volume. Table 3 shows the calibration levels of the compressor that were used during experimentation with the accumulator.



**Figure 12: Compressor with Visualization Tube and UV Dye**

**Table 3: Visualization Pipe Liquid Line Levels**

Line Number	Total Volume (mL)	Line Measurement (mm)
1	25	3
2	45	5
3	75	8
4	115	11
5	160	15
6	240	19
7	320	24
8	400	29
9	480	35

The addition of the visualization tube to the compressor changed its overall size. Consequently, it no longer fit in the back of the refrigerator as originally designed. For the purpose of experimentation, the compressor was positioned outside of the back of the refrigerator and new supports and piping were constructed accordingly.

After all changes were made to the compressor, it was charged with 180mL of Freol S-10 mineral oil, as specified by the manufacturer. Oil properties are presented in Table 4 below.

**Table 4: Compressor Oil Specifications [17]**

Oil Name	Jomo Freol S10
Density	0.868 g/cm <sup>3</sup> (15°C)
Specific Gravity	0.8700 g/cm <sup>3</sup> (15°C)
Kinematic Viscosity	10.3 mm <sup>2</sup> /sec (40°C) 2.62 mm <sup>2</sup> /sec (100°C)
Flash Point	160.0°C
Melting Point (pour point)	-30.0°C

In addition to the oil, a UV dye produced by UView [18] was added to the compressor to enhance the visibility of liquid flow during experimentation. This modification is shown in Figure 12.

Properties of the UV dye are shown in Table 5. Using information from the Material Data Safety Sheet for the UV dye and based on test observations, it was assumed that the dye did not change the behavior of the oil or any other features of the system.

**Table 5: Properties of the UView Dye [18]**

Product Name	Universal A/C Dye
Description	Fluorescent Dye
Company	UView Ultraviolet Systems Inc.
COC Flash Point	>100°C
Water Solubility	Insoluble

### 4.1.3 Evaporator and Accumulator

A fin-and-tube heat exchanger provided by the manufacturer was used as the evaporator for the system, as shown in Figure 13. The evaporator was installed in the freezer, which was located in the bottom of the unit. Two plastic panels separated the evaporator from the main freezer cabinet and also provided the evaporator fan and humidity sensors.

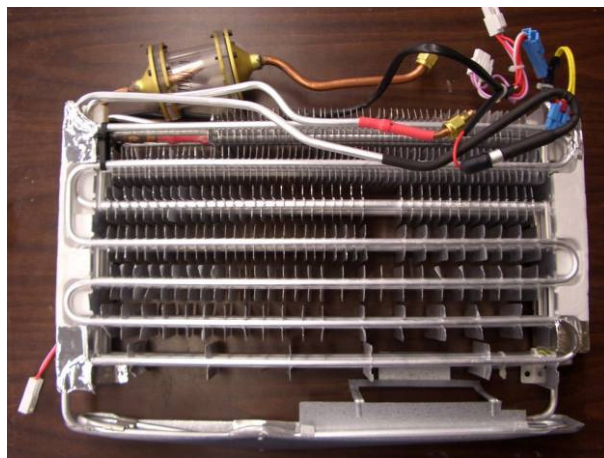


**Figure 13: System Evaporator with Installed Clear Accumulator**

Like the compressor, the accumulator was specially designed for the test. As can be seen in Figure 14, the accumulator was made out of clear plastic in order to allow for liquid visualization during testing. Prior to installation in the system, the accumulator was calibrated for volume level, as indicated by the lines in Figure 14. The calibration is shown in Table 6 and has an error of approximately +/- 2mL. As can be seen in the table, the accumulator is only capable of holding approximately 60mL before liquid will spill over into the exiting pipe. The total volume of the accumulator based on pure measurement and size is approximately 81mL.



**Figure 14: Clear Accumulator Installed with Calibration Lines**

**Table 6: Liquid Level Lines with Corresponding Total Volume for the Accumulator**

<b>Line Number</b>	<b>Total Volume (mL)</b>
1	5
2	10
3	15
4	20
5	25
6	30
7	35
8	40
9	45
10	50
11	55
12	60

#### 4.1.4 System Sight Glasses

After some preliminary testing with the modified accumulator and compressor, it was determined that more points within the system were of interest for observation. Three sight glasses were installed into the system, one at the accumulator outlet, one at the compressor inlet (suction), and one at the compressor outlet (discharge). It was of interest to know whether or not oil could be observed leaving, as well as re-entering, the compressor. The suction line sight glass is indicated by the solid circle and the discharge line sight glass is indicated by the dotted circle in Figure 15.

At specific time intervals within the refrigeration cycle, particularly when the compressor was off due to cycling or defrost, it was of interest to understand what was occurring at the accumulator. While liquid motion was observed in the accumulator itself, it was not clear as to whether or not liquid ever left the accumulator. Consequently, a sight glass was installed at this point in the system as well. The accumulator outlet sight glass is circled in Figure 16.



**Figure 15: Suction (solid circle) and Discharge (dotted circle) Sight Glasses**



**Figure 16: Accumulator Outlet Sight Glass**

#### **4.1.5 Refrigerant and Oil Flow Visualization**

In order to observe oil/refrigerant flow patterns within the system, four video cameras were installed. These cameras periodically recorded liquid activity of the oil and refrigerant within the system at known time periods. Cameras recorded activity at the compressor, accumulator, accumulator outlet, suction line, and discharge line.

##### **4.1.5.1 Compressor Visualization**

In order to view the visualization port and tube during experimentation, a camera was installed in front of the compressor. Liquid levels within the compressor could then be monitored while testing. Figure 17 shows a sample of the camera view during experimentation. The angle changed slightly during the experimentation period due to periodic changes and repairs needed on the system.

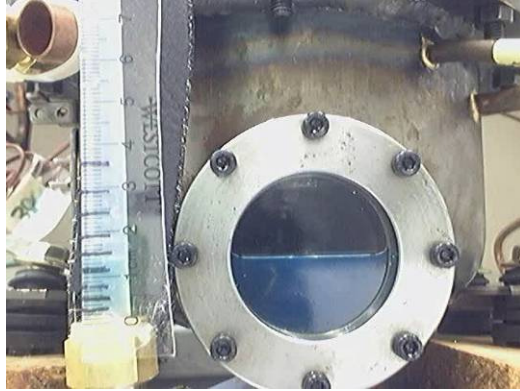


**Figure 17: Camera View of Compressor**

#### 4.1.5.2 Accumulator Visualization

In order to view the accumulator during experimentation, adjustments had to be made to the plastic panels that covered the evaporator at the rear of the freezer cabinet. A hole was cut in both panels, causing the removal of an additional heating agent normally positioned near the side of the accumulator. The original configuration as well as the adjustments made can be seen in Figure 18 through Figure 20.



**Figure 18: Unmodified Evaporator Panels in front of the Accumulator within the Freezer Compartment**

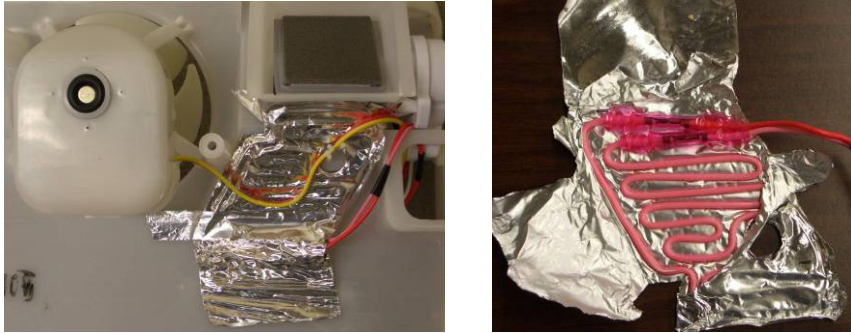


**Figure 19: Heater Removed from the Rear of the Fan Panel**

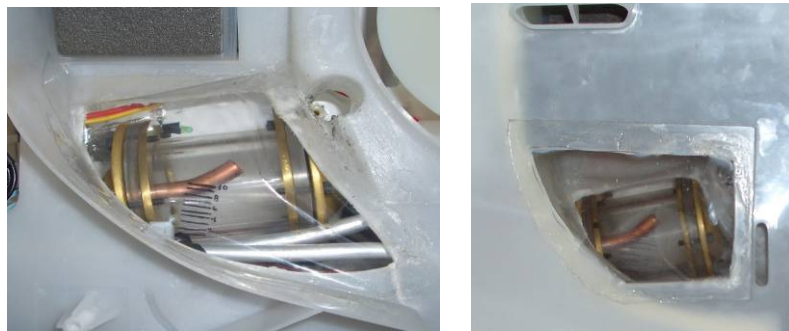


**Figure 20: Modified Evaporator Panels for Accumulator Visualization**

In order to view the accumulator during experimentation, a camera was installed in the freezer compartment. LED lights were installed to enable better visualization of the accumulator and any liquid inside. Figure 21 shows the camera view for experimentation.

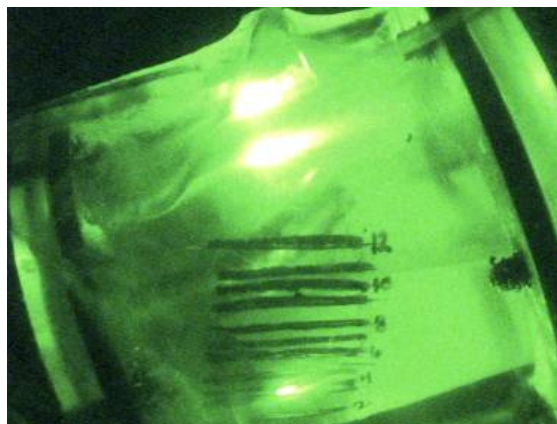


**Figure 21: Camera View of Accumulator with LED Lights**

#### 4.1.5.3 Accumulator Outlet Visualization

In order to view the installed sight glass at the accumulator outlet during testing, a camera was positioned at this location. The freezer panels were modified a second time to include a hole for visualization of the sight glass. An LED light was also used in this location. A picture of the camera view of the accumulator outlet can be seen in Figure 22.



**Figure 22: Camera View of the Accumulator Outlet with LED Lights**

#### 4.1.5.4 Suction and Discharge Line Visualization

One camera was installed to view both the suction and discharge lines during testing. A picture of the camera view for these two sight glasses is shown in Figure 23. The suction line is the lower sight glass, positioned more vertically through the view and the discharge line is the upper sight glass, positioned more horizontally.

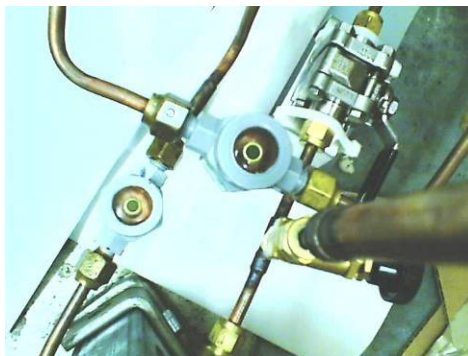


**Figure 23: Camera View of the Suction and Discharge Lines**

## 4.1.6 Experimental Measurements

A number of parameters were measured during the experimental tests to allow for proper analysis of the system.

### 4.1.6.1 Pressure Measurements

Four pressure transducers were installed in the system to aid in determining refrigerant properties at various locations throughout the system. Pressure transducers were installed at the compressor inlet and outlet (suction and discharge lines, respectively), the condenser outlet, and at the evaporator inlet, as shown in Figure 24.

Additional pressure transducers could not be installed due to space limitations.

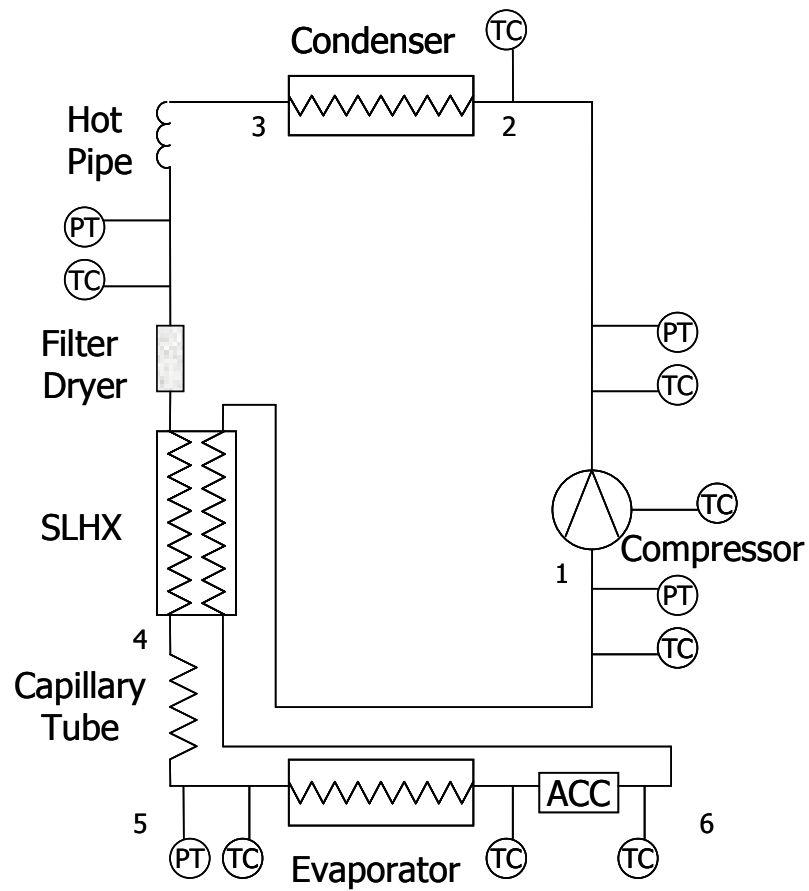


**Figure 24: Pressure Transducer and Thermocouple Placement**

Setra pressure transducers, as shown in Figure 25, were used for each pressure measurement. Specifications of the pressure transducers are shown in Table 7.



**Figure 25: Setra Pressure Transducer [19]**

**Table 7: Pressure Transducer Specifications [19]**

Model	280E
Full Scale Pressure Output	5.03 VDC
Zero Pressure Output	0.03 VDC
Accuracy (RSS Method)	+ - 0.11%
Pressure Type	Absolute
Pressure Range	0 – 250 psia
Operating Ambient Temperature Range	0 – 65°C
Manufacturer	Setra

T-junctions were used to install each of the pressure transducers and all transducers were installed in an appropriate upright orientation, as seen in Figure 26.



**Figure 26: Pressure Transducers Outside of the Unit**

Unlike the three pressure transducer connections near the compressor at the rear of the refrigerator, as shown above in Figure 26, the evaporator inlet pressure transducer could not be directly connected to the evaporator. As mentioned earlier, two panels cover the evaporator, disabling the pressure transducer from fitting in this space. The freezer also reaches cold temperature conditions around  $-19^{\circ}\text{C}$ , which could affect the proper functioning of the pressure transducer. To accommodate, a small hole was drilled into the back of the refrigerator and a pipe was directed through the hole to a location outside of the freezer. The pipe was insulated on the outside of the freezer to minimize temperature and pressure effects from ambient air conditions. This arrangement can be seen in Figure 27.



**Figure 27: Evaporator Inlet Pressure Transducer Connection**

The pressure transducers were calibrated after installation using a digital calibrator. Appropriate calibration equations were entered into the program utilized by the data acquisition system (DAS) to record and display experimental measurements.

#### 4.1.6.2 Temperature Measurements

A total of 33 temperatures were measured in order to fully understand the functioning of the refrigerator during operation. T-type thermocouples, as shown in Figure 28, were used to measure temperature. Thermocouple specifications are given in Table 8.



**Figure 28: T-type Thermocouple [20]**

**Table 8: Thermocouple Specifications [20]**

Model Number	FF-T-24
Temperature Range	-200°C to +350°C
Tolerance (@ 0 to -200°C)	0.75%
Tolerance (@ 0 to 350°C)	1.50%
Manufacturer	Omega Engineering Inc.

##### ***4.1.6.2.1 Refrigeration Cycle Temperature Measurements***

Eight temperature measurements were taken around the refrigeration cycle, as shown in Figure 24. Measurements included temperatures at the compressor inlet, compressor oil inside the bottom of the compressor, compressor outlet, condenser inlet, filter dryer inlet (hot pipe/condenser outlet), evaporator inlet, evaporator outlet, and accumulator outlet.

Surface thermocouples were used to measure the condenser inlet, evaporator inlet, evaporator outlet, accumulator outlet, and condenser outlet temperatures. Surface

thermocouples as well as in-stream thermocouples were used to measure all compressor temperatures.

#### ***4.1.6.2.2 Evaporator Air Side Temperature Measurements***

Five air side temperatures are measured around the evaporator, as indicated by the solid circles in Figure 29.



**Figure 29: Air Side Evaporator Thermocouples**

#### ***4.1.6.2.3 Cabinet Air Temperature Measurements***

Within the food compartment, seven thermocouples were used to measure air temperatures at the vents and sensor controls, as indicated by the dotted circles in Figure 30. Three copper cylinders were suspended in the cabinet to measure the average cabinet air temperature, as indicated by the solid circles in Figure 30. The total height of the food cabinet, length  $L$ , is 97.8 cm (38.5 inches).

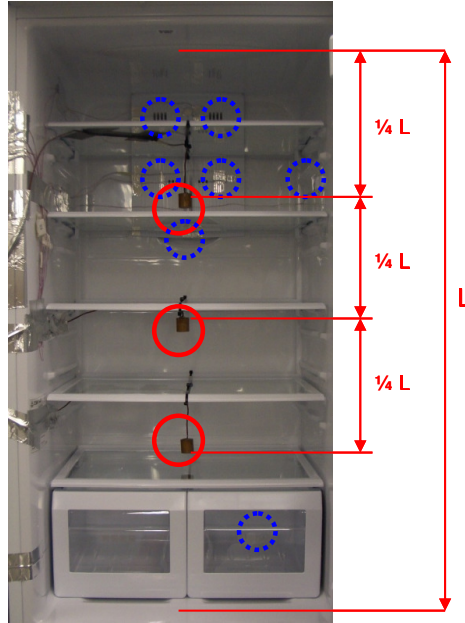


**Figure 30: Food Compartment Thermocouples**

Within the freezer compartment, seven thermocouples were used to measure air temperatures at the vents and sensor controls, as indicated by the dotted circles in Figure 31. Three copper cylinders were suspended in the cabinet to measure the overall cabinet air temperature, as indicated by the solid circles in Figure 31. The total L is 64.8 cm (25.5 inches).

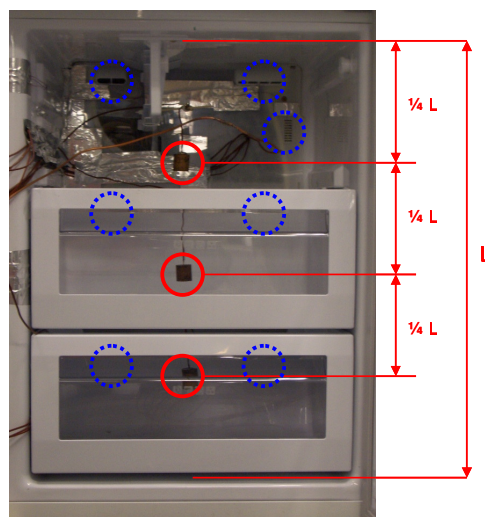


**Figure 31: Freezer Compartment Thermocouples**

#### ***4.1.6.2.4 Ambient Air Temperature Measurements***

Two copper cylinders were hung in the environmental chamber to measure and record ambient temperature. The environmental chamber temperature was also monitored by its own internal thermostat, but this measurement could not be captured by the DAS. A picture of the copper cylinders used to measure ambient temperature is shown in Figure 32.



**Figure 32: Environmental Chamber Temperature Measurements**

#### **4.1.6.3 Power Measurement**

A watt meter, as shown in Figure 33, was connected to the system and recorded power consumption of the entire unit during operation. Power of individual components was not measured. Specifications of the meter are given in Table 9.



**Figure 33: Watt Meter**

**Table 9: Watt Meter Specifications [21]**

Model Number	GW5 – 002X5-51	
Input	Volts AC	0 to 300 VAC
	Amps AC	0 to 5 amps
	Frequency Range	58 to 62 Hz
Output	Watts F.S.	1000 W
	Response time	400 msec
	Voltage DC	0 to 5 VDC
	Accuracy	0.2% Reading.
Manufacturer	Ohio Semitronics	

#### 4.1.6.4 Humidity Measurement

In addition to ambient temperature, humidity levels were specified for each test condition. Relative humidity was controlled within the environmental chamber using two humidifiers, one dehumidifier, and a relative humidity sensor. The sensor was connected to the DAS and allowed the humidity to be monitored and recorded. A program within the DAS also allowed for control of the humidity and turned the humidifiers on or off depending on the relative humidity reading. The specifications for the relative humidity sensor are listed in Table 10. A picture of the humidity sensor can be seen in Figure 34.

**Table 10: Specifications for the Relative Humidity Sensor [22]**

Model	Humidity and Temperature Transmitter HMD 30 YB
Manufacturer	Vaisala (Finland)
Serial Number	657135
Measurement Range	0-100% Relative Humidity
Operation Range	Between -20°C and 80°C
Accuracy	+/- 2% Relative Humidity (at 20°C)



**Figure 34: Vaisala Humidity Sensor**

#### **4.1.7 Environmental Chamber**

The experimental set-up was built in an environmental chamber in order to control and monitor ambient conditions. The environmental chamber is manufactured by Kolpack and has the capability of maintaining temperatures between 5°C and 45°C. The chamber cannot monitor and control humidity itself, thus requiring an additional set-up for humidity conditioning within the chamber, as described above. A picture of the chamber and its computer controls is shown in Figure 35.



**Figure 35: Environmental Chamber and Computer Controls**

#### 4.1.8 Data Acquisition System

All system measurements, including pressure, temperature, and power, sent signals to a DAS. A Hewlett Packard Data Acquisition Unit (HP 3497A), as shown in Figure 36, was used as the DAS and various cards were used for different measurements. Two T-Couple Acquisition cards were used to translate thermocouple inputs and one Guarded Acquisition card was used for pressure transducer and power measurements. A Q-Basic program was used to translate all incoming data, which were displayed on the computer screen during experimentation as actual temperatures, pressures, and power. Data was recorded every 5 seconds and downloaded to another computer for analysis after the completion of a test run.



**Figure 36: Hewlett Packard Data Acquisition Unit (HP 3497A)**

#### 4.1.9 Power Supply

Because the refrigerator used was made for an Asian or European market, the power requirements were different from those that are standard in the United States. The test refrigerator required 220V and 50 Hz. Available voltages within the environmental chamber only provided 120V and 208V and 60 Hz. In order to provide the correct power, two voltage/frequency inverters were connected to the system and adequately transferred 120V/60Hz into 220V/50Hz supply. The inverters used are shown in Figure 37.



**Figure 37: Voltage and Frequency Inverters (Manufactured by LeMarche)**

#### **4.1.10 Cabinet Door Sealing**

The condenser tubes were known to pass through the walls of the refrigerator unit and for safety and security of the system, a hole was not cut in the side walls of the refrigerator to allow for the necessary thermocouple wires. Instead, for both the food and freezer compartments, thermocouple wires were positioned within the door frame, ultimately resulting in poor door seals of the cabinets. To ensure proper door sealing and better test conditions with the given arrangement, notches were cut in the doors to allow space for the passing wires. Silicone was then used to block the notches during testing. An example of the sealant is shown in Figure 38.

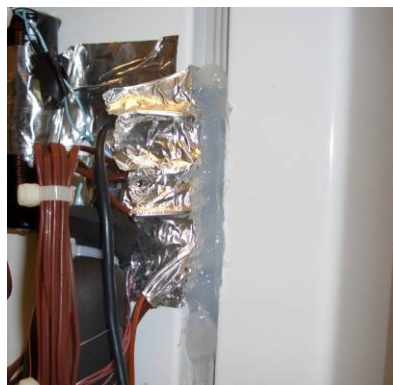


**Figure 38: Silicon Sealant for Refrigerator and Freezer Doors**

### 4.1.11 Refrigerant

R600a was used as the refrigerant for all tests conducted. R600a is highly compatible with the environment, but it is also combustible [23]. R600a is a colorless, odorless gas with a very slight solubility with water. Gas properties are listed in Table 11.

**Table 11: R600a Refrigerant Properties [23]**

Property	Value
Boiling Point	10.9°F / -11.7°C
Melting Point	-255.3°F / -159.6°C
Vapor Pressure (@ 70 °F)	45 psia
Vapor Density (Air = 1)	2.06
Purity	99.0% [22]

A charge of 52.0g R600a was used as the base charge of the system. Exact charges varied slightly for individual tests due to small errors of approximately 1% in charging methods used. Because the gas used is extremely flammable, a hydrocarbon detector was installed within the environmental chamber for safety.

## 4.2 Experimental Method

### 4.2.1 Experimental Procedures

Three different ambient conditions were examined for tests with the accumulator. A summary of the experimental conditions is given in the experimental matrix, shown in Table 12. The 43°C condition was not explored for experiments without the accumulator due to the lack of observed cycling trends, as outlined in sections 4.3.1 and 5.2.1.

**Table 12: Experimental Matrix**

<b>Accumulator</b>	<b>Temperature (°C)</b>	<b>Rel. Humidity (%)</b>
With	5	65
	32	75
	43	
Without	5	65
	32	75

Pull-down, cycling and defrost periods of operation were recorded and observed for each test condition.

#### **4.2.2 Experimental Analysis**

After completing the experiments listed above, data collected by the DAS was transferred to an Excel® file for review and analysis. The same Excel® template was used for each test to allow for easy data downloads and comparisons. A variety of graphs and additional values were plotted and calculated once the data was successfully transferred.

In addition to the data, any video files that were recorded during a test were compressed and reviewed. Trends and observations were noted for each video and compared to any previous videos as well as to the corresponding data.

##### **4.2.2.1 Calculation of the Cycle Properties**

All calculations for the cycle properties were performed automatically using a macro in the Excel® data file. Refprop 7.0 [25] was used to calculate any necessary refrigerant properties using measured temperatures and pressures as known inputs. Calculations using Refprop 7.0 included the enthalpies at each state point in the cycle and the liquid density of R600a for specific locations.

As shown in Figure 24, both pressure and temperature measurements were taken at points 1, 2, 3, and 5 in the system, as labeled in Figure 39. Enthalpies for points 1, 2, and 3 were directly calculated with Refprop 7.0 using the measured pressure and temperature values. Enthalpy at state point 5, however, could not be directly calculated with pressure and temperature as the point is always in a two-phase condition, as indicated by the P-h diagram in Figure 40. Several assumptions were made to evaluate the enthalpies for the remainder of the system.

First, assuming no pressure drop across the SLHX, the enthalpy for point 6 was calculated using the direct temperature measurement at this point and the pressure measurement for state point 1. Assuming the heat transferred across the SLHX is equal on both sides, the following equation was then used to find the enthalpy for state point 4:

$$h_3 - h_4 = h_1 - h_6 \quad (1)$$

Assuming isenthalpic expansion, the enthalpy at state 5 was set equal to the enthalpy at state 4.

The above analysis results in a P-h diagram similar to that shown in Figure 40. Exact pressures and temperatures depend on specific operating conditions and ambient temperature.

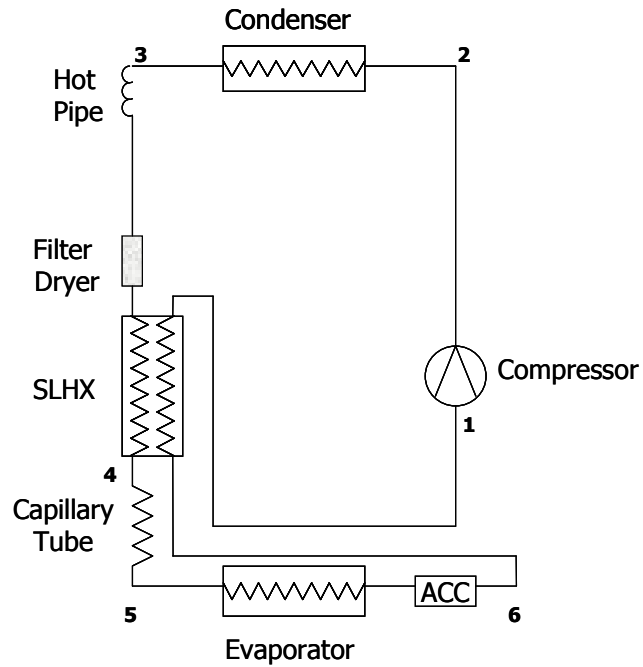


**Figure 39: System Schematic with State Points**

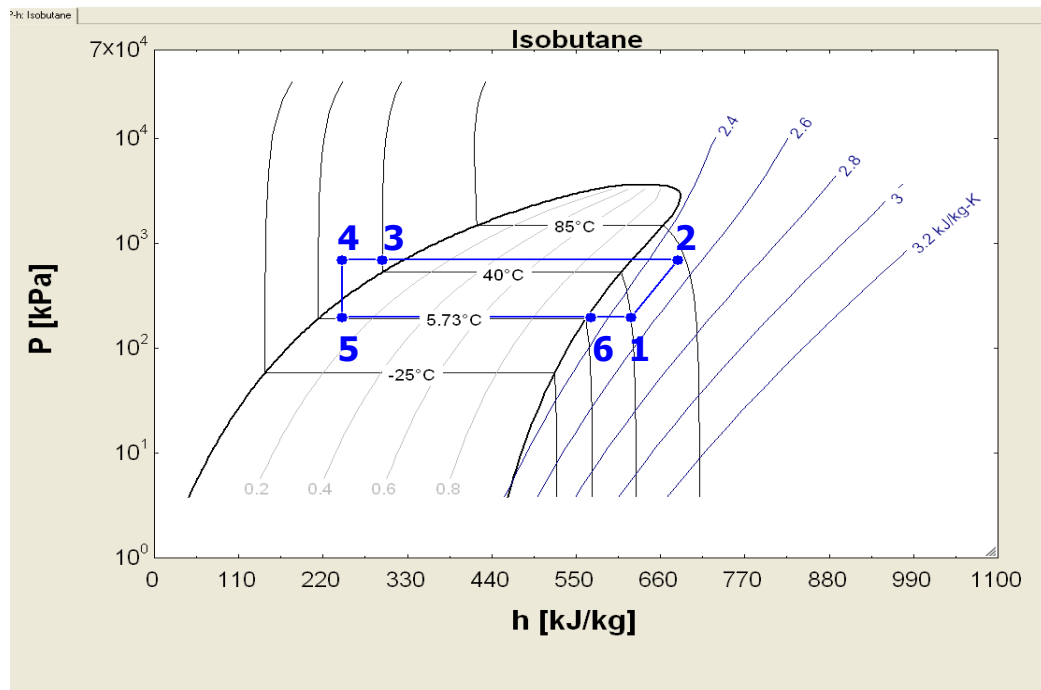


**Figure 40: State Points of the Refrigeration Cycle on a P-h Diagram**

#### 4.2.2.1.1 Superheat and Subcooling Calculations

Total degrees of superheat were calculated using the following equation:

$$T_{\text{superheat}} = T_1 - T_{\text{sat}, P_1} \quad (2)$$

where  $T_1$  is the temperature at state point 1 and  $T_{\text{sat}, P_1}$ , which was calculated using Refprop 7.0, is the saturated temperature at the pressure for state point 1,  $P_1$ .

Degrees of subcooling were calculated using equation 3:

$$T_{\text{subcooling}} = T_{\text{sat}, P_3} - T_4 \quad (3)$$

where  $T_{\text{sat}, P_3}$  is the saturated temperature using the pressure at state point 3,  $P_3$ , and  $T_4$  is the temperature at state 4 calculated by Refprop 7.0 using the known pressure at state point 3,  $P_3$ , and the calculated enthalpy,  $h_4$ .

#### 4.2.2.1.2 Specific Capacity Calculations

Because a compressor map was not provided by the manufacturer, the mass flow was not calculated for the system. Consequently, the units for capacity remain as those for specific capacity, kJ/kg, as opposed to kJ/s. In order to determine evaporator and condenser specific capacity, the following equations were used:

$$q_{\text{evap}} = h_6 - h_5 \quad (4)$$

$$q_{\text{cond}} = h_2 - h_3 \quad (5)$$

where  $q_{\text{evap}}$  is the evaporator specific capacity,  $q_{\text{cond}}$  is the condenser specific capacity, and the  $h$  values correspond to the state points as shown in Figure 39 and Figure 40.

### 4.2.2.1.3 Solubility Calculations

Solubility measurements were desired at both the compressor and accumulator in order to determine oil/refrigerant ratios at these positions in the system. Solubility was calculated using a correlation provided by the oil manufacturer, as shown in Figure 41.

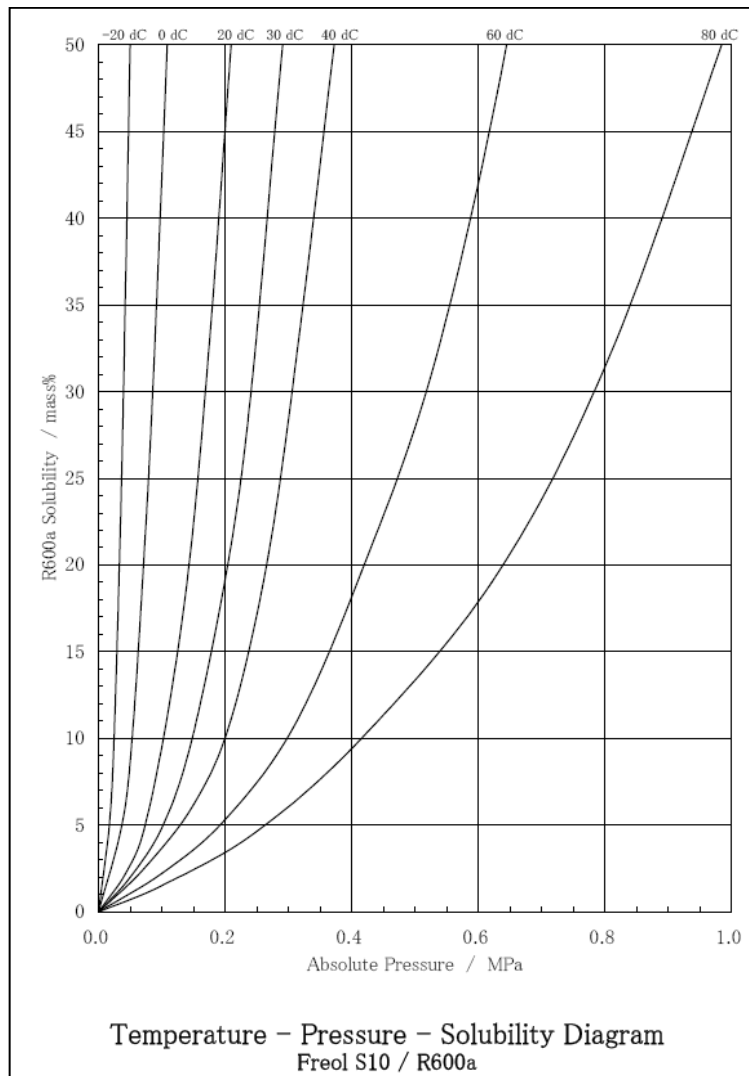


**Figure 41: Original Solubility Data for Freol S-10 Mineral Oil and R600a (Provided by the Manufacturer)**

Data provided by the manufacturer was uploaded in TableCurve® 3D [26], a software program that is able to develop 3D correlations based on input data. From the

provided data, an extended correlation between temperature [K], pressure [kPa], and solubility [mass % R600a] was developed and used for solubility calculations:

$$\ln(z) = 26167 + 0.2 * \ln(P)^2 - 0.1 * P^{0.5} + 1.6 * \ln(P) + 275.9 * \ln(T)^2 - 4665 * \ln(T) - \frac{48721.8}{\ln(T)} \quad (6)$$

where z is the solubility in percent of refrigerant mass, P is the pressure in kPa, and T is the temperature in K. Constants in the above equation are simplified, but the full expression was included in the Excel® macro program. Solubility in percent of refrigerant mass, z, is defined by the following equation:

$$z = \frac{m_r [g]}{m_t [g]} * 100\% \quad (7)$$

where  $m_r$  is the mass in grams of refrigerant and  $m_t$  is the total combined mass in grams of oil and refrigerant. A graphical representation of the solubility correlation developed by TableCurve® 3D is shown in Figure 42.

**Freol S10 / R600a Solubility Diagram**  
 Rank 7 Eqn 156444404  $\ln z = a + b(\ln x)^2 + cx^{0.5} + d \ln x + e(\ln y)^2 + f \ln y + g / \ln y$   
 $r^2 = 0.99251206$  DF Adj  $r^2 = 0.99172974$  FitStdErr = 1.2739668 Fstat = 1502.211  
 $a = 26167.366$   $b = 0.1636556$   $c = -0.098086017$   $d = 1.0652598$   
 $e = 275.94017$   $f = -4664.9882$   $g = -48721.794$

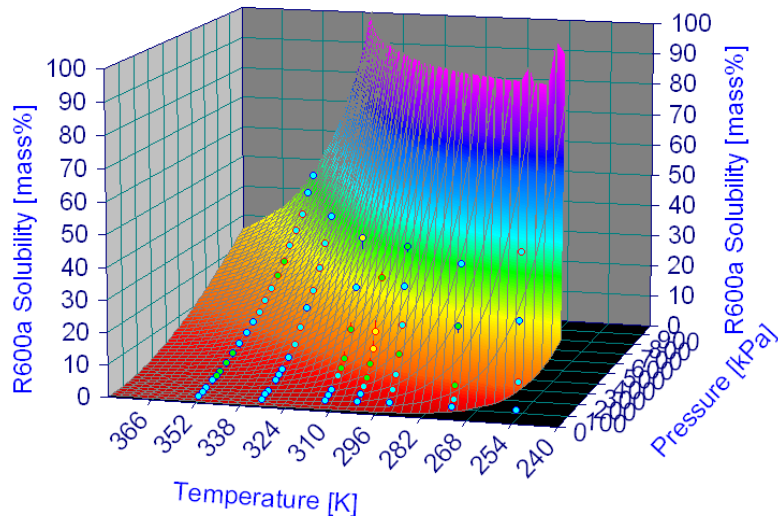


**Figure 42: Solubility Curve Developed in TableCurve® 3D**

In order to produce understandable data, the correlation was capped at 100% in the Excel® macro program. Any value calculated to be greater than 100% solubility was assumed to have a solubility of 100%.

As can be seen by the expression in equation 6 and the graph in Figure 42, an input temperature and pressure are required to calculate solubility. Solubility in the accumulator was calculated using the average of the accumulator inlet and outlet temperatures and the suction pressure. Solubility in the compressor was calculated using the inside compressor oil temperature and the suction pressure.

#### ***4.2.2.1.4 Mixture Density Calculations***

Like solubility, data for the mixture density of oil and refrigerant was provided by the oil manufacturer, given in Figure 43.

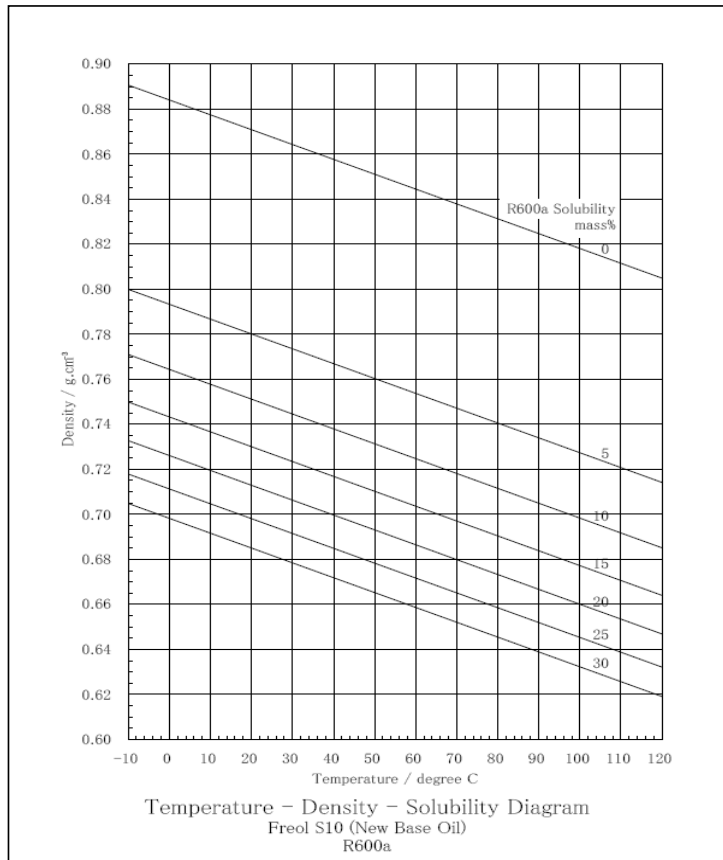


**Figure 43: Original Mixture Density Data Provided by the Manufacturer for Freol S-10 Oil and R600a**

A correlation for this property was also developed using TableCurve® 3D and implemented into the Excel® macro analysis. Figure 44 shows the Chebyshev correlation that was used to determine mixture density given the temperature [K] and solubility [mass % R600a] at the compressor and accumulator. It is important to note that the original mixture density and the following correlation have higher error at high solubility when the mixture is assumed to be all or mostly R600a. At these solubilities, the correlation does not always produce the liquid density of R600a at the appropriate temperature and often assumes the density to be lower. Mixture densities around this

level were thus assumed to be the actual liquid density of the refrigerant rather than the correlation value.

Rank 15 Eqn 1404 Chebyshev X,Y Rational Order 4/5  
 $r^2=0.99979977$  DF Adj  $r^2=0.99976807$  FitStdErr=0.0018405992 Fstat=33566

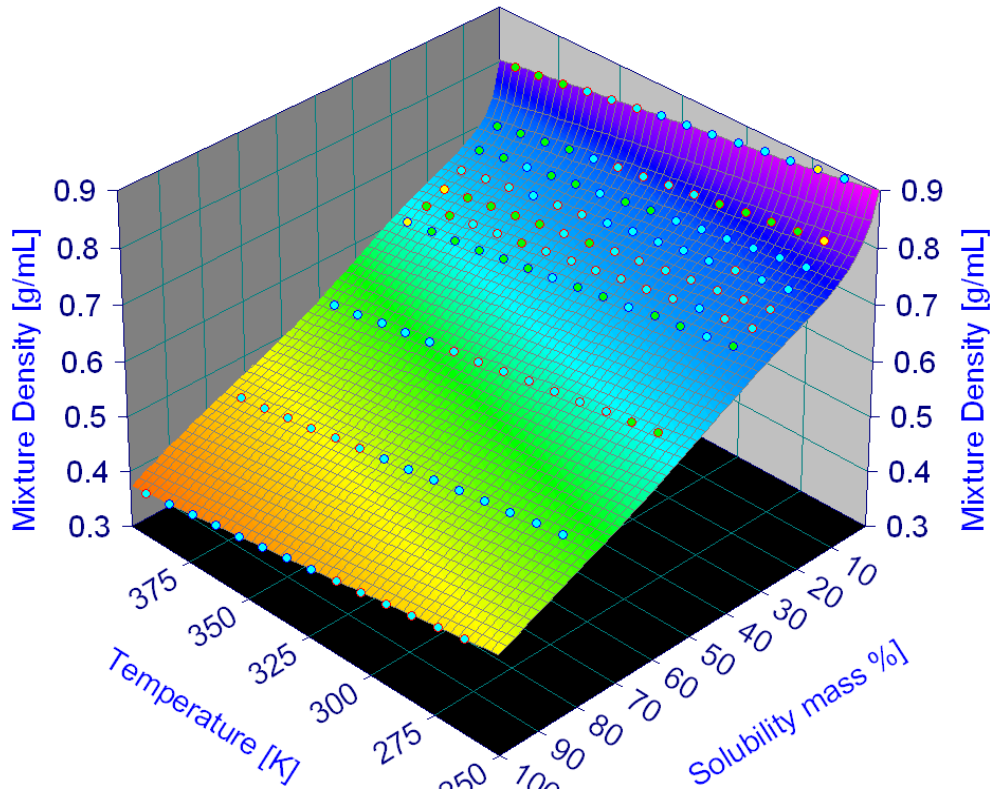


**Figure 44: Mixture Density Correlation Developed by TableCurve® 3D**

Mixture density in the accumulator was calculated using the previously calculated accumulator solubility and the average of the accumulator inlet and outlet temperatures.

Mixture density in the compressor was calculated using the previously calculated compressor solubility and the inside compressor oil temperature.

#### ***4.2.2.1.5 Ideal Density and Correction Factor Calculations***

ASHRAE, which publishes and develops a number of standards for testing and analyzing refrigeration and HVAC equipment, states that the ideal mixture density for an oil and refrigerant mixture is as follows:

$$\rho_{id} = \frac{\rho_o}{1 + w\left(\frac{\rho_o}{\rho_r} - 1\right)} \quad (8)$$

where  $\rho_{id}$  is the ideal density,  $\rho_o$  is the density of the pure oil at the solution temperature,  $\rho_r$  is the density of the pure liquid refrigerant at the solution temperature, and  $w$  is the mass fraction of refrigerant in the solution [6]. Most actual mixture densities are found from ASHRAE using this equation and dividing it by a correction factor. Because actual mixture density data was available for these experiments, both the actual density based on the correlation and the ideal density based on equation 8 were calculated. A correction factor was then calculated using equation 9:

$$A = \frac{\rho_{id}}{\rho_m} \quad (9)$$

where  $A$  is the correction factor and  $\rho_m$  is the actual mixture density found using the correlation outlined above.

#### ***4.2.2.1.6 Refrigerant and Oil Mass Calculations***

It was ultimately desired to know the approximate amount of oil and refrigerant in the compressor and accumulator during each stage of the refrigeration cycle, including the pull-down, cycling, and defrost periods. In order to calculate the mass of refrigerant and oil in each localized volume, information corresponding to specified data points was gathered from the video files. Using the video images, an approximate volume of total

liquid ( $V_t$ ) was estimated for both the compressor and accumulator. Knowing the mixture density from the above correlation, the total mass of oil and liquid refrigerant ( $m_t$ ) can be determined from the following equation:

$$\rho_m = \frac{m_t}{V_t} \quad (10)$$

Because the solubility at a given temperature and pressure is also known using the given correlation in equation 6, the refrigerant mass ( $m_r$ ) can be calculated from equation (7). The oil mass ( $m_o$ ) is calculated by subtracting the refrigerant mass from the total mass ( $m_t$ ). These calculations are represented below:

$$m_r = \rho_m * V_t * \left(\frac{z}{100\%}\right) \quad (11)$$

$$m_o = m_t - m_r \quad (12)$$

#### 4.2.2.2 Uncertainty Analysis

Uncertainty analysis was completed for a 5°C and 32°C ambient condition test with the accumulator. The 5°C test used had an approximate charge of 52.0g and the 32°C test had an approximate charge of 52.8g. Random and systematic errors for representative pressures, temperatures and power were calculated. Specifically, the suction pressure ( $P_{suc}$ ), discharge pressure ( $P_{dis}$ ), instream discharge temperature ( $T_{dis, i}$ ) and surface evaporator inlet temperature ( $T_{evap, s}$ ) were used for error analysis. For random error calculations, average values were calculated during the compressor-on time period for a series of 5 consecutive cycles, as shown in Figure 45 and Figure 46. Average values for the compressor-on time period are shown in Table 13 and Table 14 and the error analyses are given in Table 15 and Table 16.

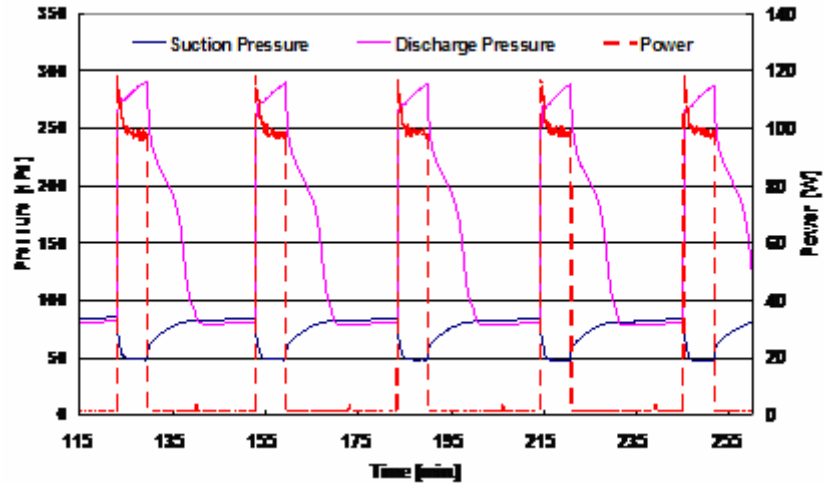


Figure 45: Cycles Used for Random Error Calculations from a 5°C Ambient Test

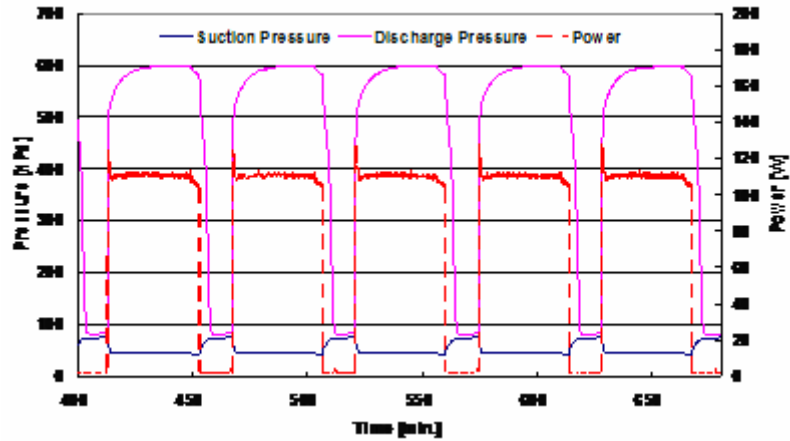


Figure 46: Cycles Used for Random Error Calculations from a 32°C Ambient Test

Table 13: Average Cycle Properties for 5°C Ambient Condition

Cycle	Time [min.]	Power [W]	Psuc [kPa]	Pdis [kPa]	Tdis, i [°C]	Tevap, s [°C]
1	6.7	99.6	52.0	280.6	23.6	-29.4
2	6.6	99.4	51.4	278.3	22.8	-30.2
3	6.6	99.7	50.8	277.4	22.3	-30.5
4	6.7	99.9	50.5	276.3	22.0	-31.0
5	6.7	99.8	50.1	275.4	21.2	-30.9

**Table 14: Average Cycle Properties for 32°C Ambient Condition**

Cycle	Time [min.]	Power [W]	Psuc [kPa]	Pdis [kPa]	Tdis, i [°C]	Tevap, s [°C]
1	40.1	110.3	46.0	584.9	64.7	-27.2
2	39.4	110.2	46.0	584.3	64.3	-27.2
3	39.2	110.2	45.9	584.2	64.0	-27.2
4	39.3	110.3	45.9	583.6	64.0	-27.2
5	39.2	110.1	45.8	583.3	63.9	-27.3

**Table 15: Error Analysis for 5°C Ambient Condition**

	Time [min.]	Power [W]	Psuc [kPa]	Pdis [kPa]	Tdis, i [°C]	Tevap, s [°C]
All Cycle Averages	6.6	99.7	51.0	277.6	22.4	-30.4
Random Error (Standard Deviation)		0.2	0.7	2.0	0.9	0.6
Systematic Error		0.2	0.1	0.3	0.3	0.5
% Random Error of Mean		0.2	1.4	0.7	4.0	2.1
% Systematic Error of Mean		0.2	0.1	0.1	1.5	1.5
<b>% Total Error</b>		<b>0.4</b>	<b>1.6</b>	<b>0.8</b>	<b>5.5</b>	<b>3.6</b>

**Table 16: Error Analysis for 32°C Ambient Condition**

	Time [min.]	Power [W]	Psuc [kPa]	Pdis [kPa]	Tdis, i [°C]	Tevap, s [°C]
All Cycle Averages	39.4	110.2	45.9	584.1	64.2	-27.2
Random Error (Standard Deviation)		0.1	0.1	0.6	0.3	0.04
Systematic Error		0.2	0.1	0.6	1.0	0.4
% Random Error of Mean		0.1	0.2	0.1	0.5	0.1
% Systematic Error of Mean		0.2	0.1	0.1	1.5	1.5
<b>% Total Error</b>		<b>0.3</b>	<b>0.3</b>	<b>0.2</b>	<b>2.0</b>	<b>1.6</b>

As can be seen in Table 15 and Table 16, the error for the power and pressures are relatively low, always less than 2% for the 5°C ambient condition and less than 0.5% for the 32°C ambient condition. While the temperature measurements have larger errors as

high as 5.5% in the 5°C ambient condition, these errors are within reasonable limits and are conservatively high. Systematic error for the pressure and temperature is dependent upon the actual reading value, as outlined in sections 4.1.6.1 and 4.1.6.2. Consequently, the total error for the pressure and temperature at the 32°C test condition are slightly lower than they are for the 5°C case. Note that at the 5°C ambient condition, the ambient operating temperature is near the low end of the appropriate operating range for the pressure transducer, increasing the likelihood of systematic error for those measurements.

#### 4.2.2.3 Sample Collection

After some preliminary testing to ensure that the system was working properly, it was suggested that the experimental set-up be altered to allow for the removal of an oil/refrigerant mixture sample. This was desired in order to verify the correlations developed in TableCurve® 3D for solubility and mixture density for R600a and mineral oil. While sample collection is not ideal for verifying mixture properties for reasons suggested by Lebreton et al. [8] and other researchers, real-time measurement methods were unavailable.

##### ***4.2.2.3.1 Sample Collection Set-up***

To allow for the removal of oil/refrigerant samples from the system, two sample removal ports were fabricated; one at the compressor and one at the accumulator. Samples were taken from these two locations because the compressor and accumulator were the main areas of interest and contained the largest volumes of oil and refrigerant, both of which were monitored with video cameras. The first collection vessel was connected to the bottom portion of the visualization tube at the bottom of the compressor

using a thin copper pipe that was inserted into the visualization tube without causing an obstruction, as shown in Figure 47. The sample collection vessel was thus able to take oil/refrigerant mixture samples from the middle of the bottom of the compressor shell.



**Figure 47: Sample Collection Pipe through the Sight Tube at the bottom of the Compressor**

In addition to the compressor sample collection pipe, a sample collection pipe was added to the accumulator. A hole was cut into the end of the accumulator and a small copper pipe was inserted and brazed in place, as seen in Figure 48 and Figure 49.



**Figure 48: Sample Pipe in the Accumulator (front view)**



**Figure 49: Sample Pipe in Accumulator (rear view)**

Because the accumulator resides in the freezer, the sample pipe was routed outside of the refrigerator through a small hole that was drilled in the back of the unit. The copper pipe was insulated to minimize temperature change and the evaporation of any refrigerant taken in the sample.

After conducting a few test runs, it was determined that several samples within close time intervals were needed to improve the accuracy of sample collection. Three collection vessels of similar size and shape were built to replace the original collection vessel. Each vessel held between 6.9 and 8.2mL of liquid, depending on the specific vessel; therefore no more than 8.2mL (approximately 7.1g or 4.5% of the total oil charge) of oil or 8.2mL (approximately 4.7g or 9% of the total refrigerant charge) of liquid refrigerant could be removed from the system with any given sample. A picture of one of the collection vessels is shown in Figure 50. These collection vessels could be used to take samples at either the compressor or accumulator ports.



**Figure 50: Oil/Refrigerant Collection Vessel**

A series of valves were used to connect the collection vessels to the system, though only one vessel could be connected at any given time. The valve system allowed the vessel and the connecting tube to the system to be evacuated prior to sample collection to eliminate the possibility of air entering the system or sample. The valve system used is shown in Figure 51 and was implemented at both the compressor and accumulator locations.

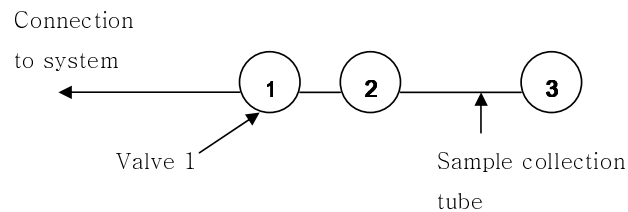


**Figure 51: Valve System for Sample Collection**

In addition to the oil/refrigerant sample collection ports, an oil charging port was added to the system. Multiple removals of samples resulted in a relatively large decrease of the compressor lubricant. Consequently, a method of recharging lost oil was needed. To do so, a U-tube was inserted into the suction line. This method allowed for oil to be added to the tube first, then evacuated to eliminate air within the oil and tubes, then opened to the system so incoming refrigerant could push the added oil back into the compressor. A picture of the added U-tube is shown in Figure 52. The U-tube was installed in the suction line, as shown in Figure 53, and, like the collection vessels, contained a valve system to allow the addition of the oil, as shown in Figure 54.



**Figure 52: Oil Charging "U" Tube**



**Figure 53: Oil Port U-tube Assembly in the Suction Line**

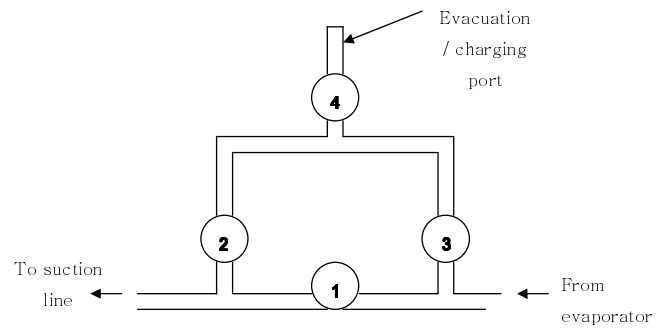


**Figure 54: Valve System for the Oil Port U-tube Assembly**

A method for recharging refrigerant was not incorporated, as the samples taken generally contained very little refrigerant. Any refrigerant that did need to be re-charged could be done through the original charging port of the compressor.

The collection vessels and samples were weighed using a high accuracy scale in order to capture small changes in weight. Measurements of weights up to four decimal places were recorded. A picture of the scale is shown in Figure 55 and specifications are listed in Table 17.

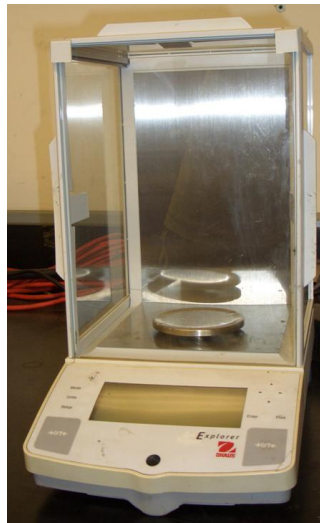


**Figure 55: Ohaus Explorer High Accuracy Scale**

**Table 17: Specifications for the Ohaus Explorer High Accuracy Scale [27]**

Model Name, Number	Explorer, E12140
Manufacturer	Ohaus Corporation
Operating Temperature Range	10-50°C
Maximum Weight	210 g
Accuracy	0.0001g

#### ***4.2.2.3.2 Sample Collection Method***

Several samples were taken at both the compressor and accumulator for several tests, at both the 32°C and 5°C ambient conditions. Three samples were collected at the same location, either the compressor or accumulator, within a 15 minute time frame. The following procedure was followed when collecting the samples:

1. Clean the collection vessel with acetone to eliminate any trace amounts of oil or refrigerant.
2. Evacuate the collection vessel.
3. Weigh the collection vessel and record the result. Attach the vessel to the system.
4. The collection vessel is initially closed from the system using valve 1 in Figure 51. Valves 2 and 3 are also closed as the vessel should be under vacuum.
5. Evacuate the collection vessel again and open valve 2 to evacuate the connecting pipe between the system and the collection vessel. Evacuate for approximately 1 minute.
6. Once evacuated, close valve 3 to maintain vacuum in the tube and connecting line.
7. Open valve 1 to allow the sample into the collection tube.
8. Close valves 1 and 2 after approximately 15 seconds. Close valve 1 first and then valve 2.
9. Remove the collection vessel from the system. Less than 1mL of sample will be lost in the connecting pipe.
10. Weigh the total oil/refrigerant mixture weight in the collection tube and record the result.
11. Hold the collection vessel vertically and evacuate again, removing any refrigerant from the vessel. The vessel can also be opened directly to atmosphere to allow the refrigerant to escape and let oil run back down into the bulk of the collection vessel. Evacuate again after opening the vessel to atmosphere to maintain vacuum and consistent weighing methods.
12. Weigh the collection vessel with just oil and record the result.

13. Purge the oil sample into a graduated cylinder. Record the amount of oil retained.

If the amount of oil is small, clean the vessel and collect the waste. Heat the mixture so that the waste solvent will evaporate and measure the pure oil collected. Compare to previous weights and density calculations for liquid volume.

14. Repeat steps 1-13 for the remaining two collection vessels.

When significant amounts of oil were lost from sample collection, the following procedure was followed to add oil back to the system:

1. The “U” is initially closed from the system. Valve 1, as in Figure 54, is open and valves 2, 3 and 4 are closed.
2. Calculate how much oil should be added based on prior sample removal.
3. Charge oil through the top port, valve 4. Be sure to charge slowly to allow for air bubbles to escape.
4. Add a vacuum connection to valve 4.
5. Evacuate the top portion of the “U” for at least 5 minutes to remove excess air from the pipes and the oil.
6. Close valve 4.
7. Open first valve 2 and then valve 3.
8. Periodically close valve 1. Watch the suction line sight glass for oil addition. Open and close valve 1 several times until you believe all of the oil has been added.

9. After several minutes of opening and closing valve 1, keep valve 1 open and close first valve 3 and then valve 2.
10. Check camera visualization for the compressor and the suction and discharge line sight glasses to determine the success of oil addition.

#### ***4.2.2.3.3 Sample Collection Results***

Unfortunately, the sample collection method did not prove to be as useful as originally hoped. There was a large amount of error associated with the samples collected and no conclusive results were gained from the sample collection method. Solubility data could not be verified or refuted as sample collection measurements varied greatly between one another despite the precautions taken to reduce or eliminate this problem. Of 21 samples taken at the compressor, only 2 measurements showed agreement within 10% of the calculated solubility. While this may suggest that the solubility correlation needs adjustment, the average standard deviation between compressor sample measurements was 6.4%. Considering that the sample size was relatively small (at most a total of 8.2mL of oil/refrigerant mixture), the error and standard deviations for these samples do not provide enough conclusive evidence to make a statement on the validity of the solubility data.

Results for the accumulator were worse than those for the compressor given that the accumulator was often at temperatures near -20°C. Collecting samples while the system was running proved to be quite difficult as refrigerant would evaporate as soon as it would enter the warmer collection vessel. Methods of cooling the collection vessel prior to collecting the sample were attempted but were ultimately unsuccessful. Of 16 samples collected at the accumulator, only 4 measurements showed agreement within

10% of the calculated solubility. 10 of the measurements had an error between 28 and 75% of the calculated value and 2 of the measurements showed very poor agreement with an error greater than 75%. The average standard deviation for the accumulator sample measurements was 28.8%, much higher than that for the compressor sample measurements. This is partially due to the difficult nature of collecting accumulator samples at low temperatures.

After collecting a number of samples and reviewing work done by Zhelezny et al. [12], which shows that sample collection must be very precise and that solubility data is only relevant for steady-state operations, the sampling method was abandoned. The given solubility correlation was used for experimental analysis with the understanding that results were not necessarily accurate and may not apply appropriately for when the system is running and continuously changing temperature and pressure.

### **4.3 Experimental Results**

A total of six tests at the 5°C ambient condition, three tests at the 32°C and two tests at the 43°C were conducted with the accumulator. A summary of the tests conducted and their key characteristics and results are shown in Table 18. As can be seen from the table, the defrost period was not often captured in the 5°C case due to the length of time required to reach this stage. Also, cycling did not occur during the length of the testing periods for experiments at the 43°C ambient condition because of the high ambient temperature.

**Table 18: Test Results Summary**

Test No.	Average Ambient Temp.	Average Relative Humidity	Approximate Refrigerant Charge	Time to Pull-down	Cycling Comp. On Time	Cycling Comp. Off Time	Time before 1 <sup>st</sup> Defrost	Length of Defrost
1	5°C	70.3%	51.0	50 min.	7 min.	23.4 min.	N/A	N/A
2	5°C	64.0%	51.0	48.1 min.	7.6 min.	24.0 min.	N/A	N/A
3	5°C	69.3%	51.0	48.8 min.	8.0 min.	24.0 min.	807.5 min.	15.7 min.
4	5°C	69.1%	51.0	N/A	7.6 min.	24.5 min.	N/A	19.4 min.
5	5°C	69.4%	52.0	42.3 min.	6.9 min.	24.2 min.	N/A	N/A
6	5°C	69.4%	52.0	48.2 min.	7.4 min.	24.7 min.	N/A	N/A
1	32°C	71.9%	52.8	335.6 min.	39.4 min.	14.3 min.	243.6 min.	16.6 min.
2	32°C	68.9%	52.8	333.5 min.	39.2 min.	15.3 min.	243.7 min.	16.7 min.
3	32°C	67.8%	49.9	337.7 min.	41.2 min.	15.2 min.	243.8 min.	17.0 min.
1	43°C	55.1%	52.0	N/A	N/A	N/A	229.8 min.	14.5 min.
2	43°C	65.6%	52.0	N/A	N/A	N/A	228.0 min.	14.3 min.

### 4.3.1 Data Results and Trends

The following section outlines data collected for each of the three ambient conditions. Key trends are also noted.

#### 4.3.1.1 Pressure Results

System pressures, temperatures, and power levels all varied depending on the given ambient condition. As would be expected, discharge pressures increased with increasing ambient temperature. As the ambient temperature increases, the compressor must work harder to achieve the desired refrigerator and freezer cabinet temperatures and the consequent increased power input increases the discharge pressure. Changes in the low-side pressure, however, were not as pronounced and varied as little as 2%. The small change in low side pressure between ambient conditions can be seen in Figure 56. The suction pressure for the 5°C ambient condition is indicated by the solid line with many

cycling periods, the suction pressure for the 32°C ambient condition is indicated by the longer dashed line with longer cycles following a long pull-down period, and the 43°C ambient condition is indicated by the short dotted line with no cycling periods. In general, when the compressor was on, the suction pressure was between 40 and 45 kPa. When the compressor was off, the suction pressure would rise to 75-80 kPa during cycling periods and above 225 kPa during a defrost period.

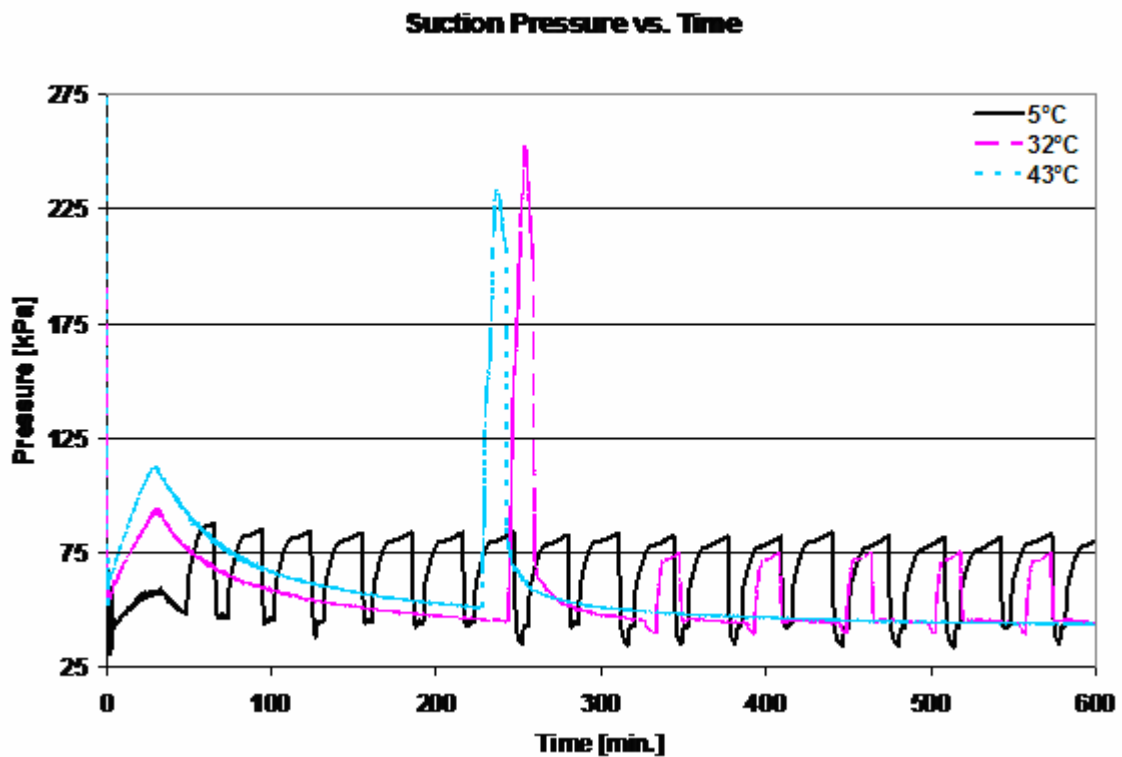


**Figure 56: Suction Pressure for Each Ambient Condition for Testing with the Accumulator**

The change in operating pressure due to the change in ambient temperature is best shown with the discharge pressure, as can be seen in Figure 57. Discharge pressures were generally around 270kPa at the 5°C ambient condition and 600kPa at the 32°C ambient condition when the compressor was on during cycling. Discharge pressure at the 43°C

ambient condition was as high as 1175kPa and as low as 760kPa during pull-down. The same indicators as were used in the above graph for suction pressure for each ambient condition are used in Figure 57.

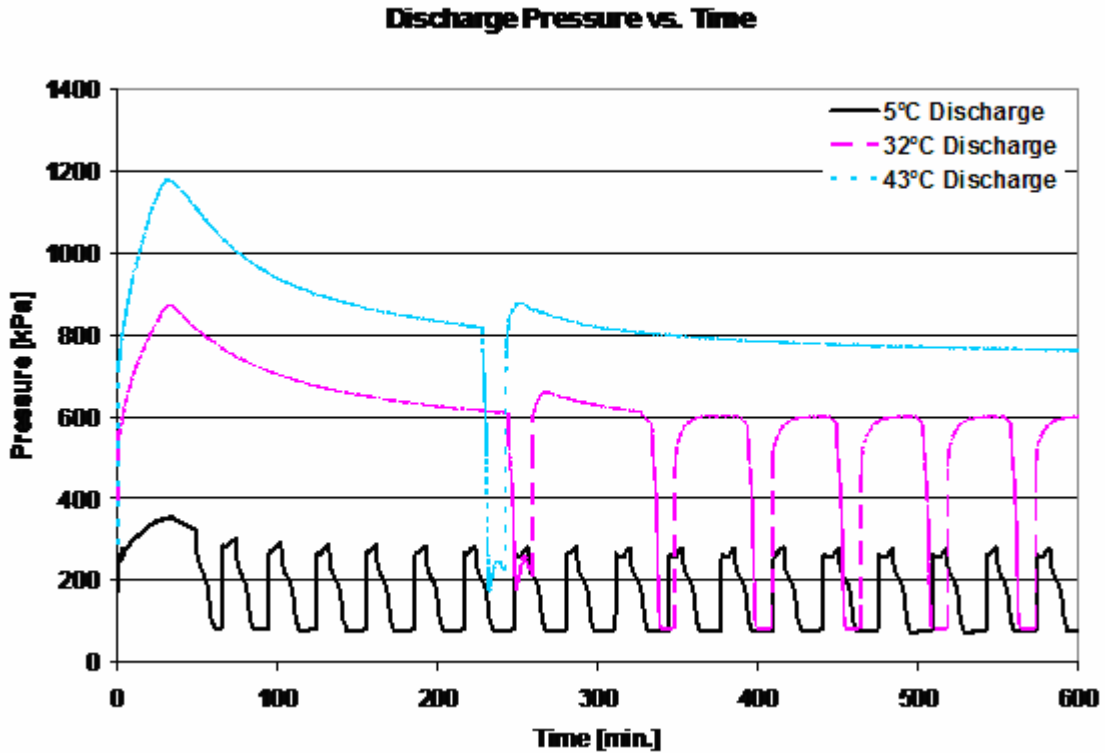


**Figure 57: Discharge Pressure for Each Ambient Condition for Testing with the Accumulator**

The changes in pressure can also be observed on a P-h diagram for each of the ambient conditions. This is shown in Figure 58, which illustrates the P-h diagram for each ambient condition while the compressor is on during a cycling period. The labeled state points correspond to those outlined in Figure 39 and Figure 40. As mentioned before, the high side pressure increases with increasing ambient temperature. This is illustrated not only through Figure 58, but also through the pressure ratio, defined as the discharge

pressure divided by the suction pressure. Average pressure ratios for the system during cycling when the compressor is on for each ambient condition are given in Table 19.

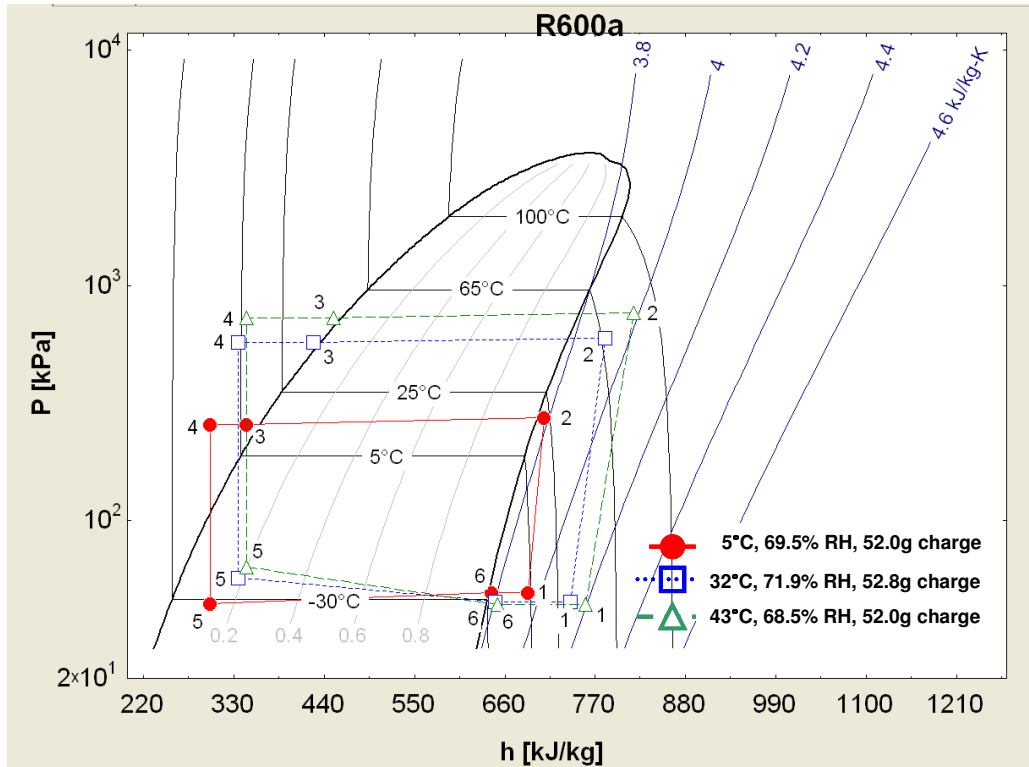


**Figure 58: P-h Diagram for Each Ambient Condition at Averaged Values for Compressor-On Time Periods for Testing with the Accumulator**

**Table 19: Pressure Ratios for Each Ambient Condition with the Accumulator**

Ambient Condition	Pressure Ratio
5°C	5.6
32°C	12.6
43°C	17.5

#### 4.3.1.2 Temperature Results

System cycle temperatures also increased with increasing ambient temperature, though the degree of change varied depending on the location of the temperature measurement. The temperature inside the compressor shell increased from as low as 15°C

at the 5°C ambient condition to as high as 90°C in the 43°C tests, as shown in Figure 59. Like pressure, increases in compressor temperature are due to the increased compressor work associated with increasing ambient temperature.

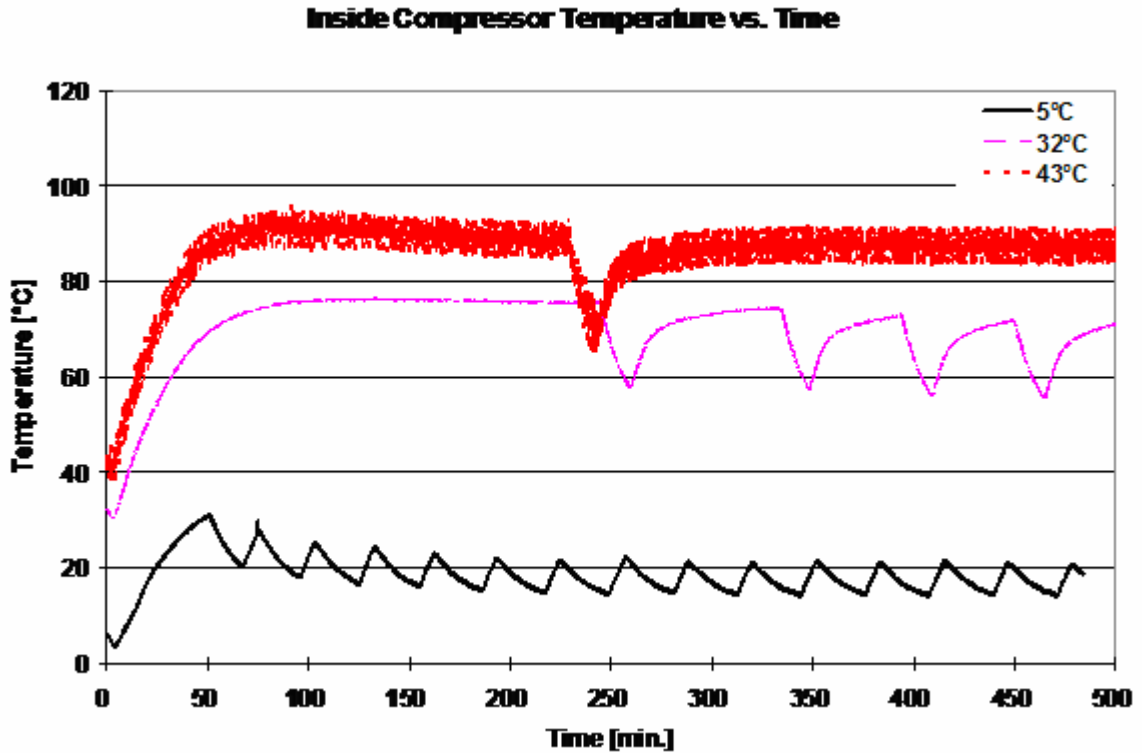


**Figure 59: Inside Oil Temperature at the Base of the Compressor for Each Ambient Condition for Testing with the Accumulator**

Accumulator temperatures during periods when the compressor was on were approximately the same, around -20°C, and varied only by about 2K between ambient conditions, as shown in Figure 60. Results shown are only given for the 5°C and 32°C tests for the sake of graphing. Results for the 43°C case were very close to those values for the 32°C tests.

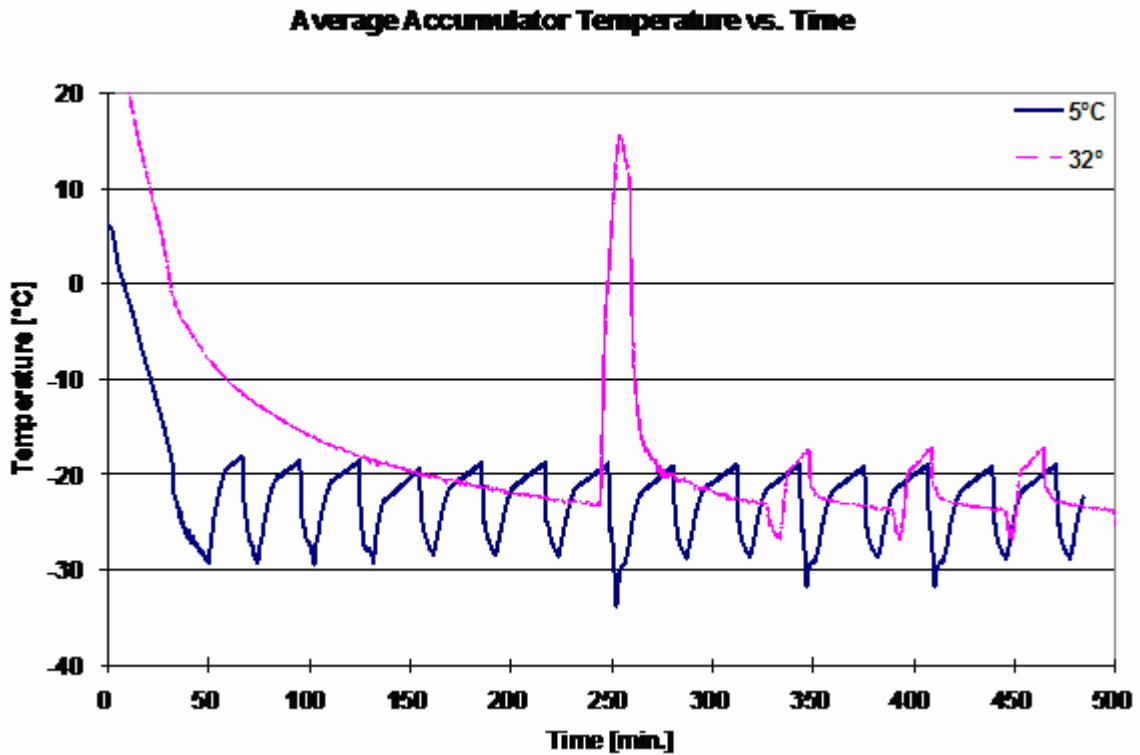


**Figure 60: Average Accumulator Temperature for the 5°C and 32°C Conditions for Testing with the Accumulator**

When looking specifically at the accumulator inlet and outlet temperatures, there is a 0-2K difference between the two measurements, depending on the point of operation. As shown for the 5°C case in Figure 61, the accumulator outlet temperature, indicated by the lighter line, was always slightly higher by approximately 2K than the inlet temperature, indicated by the darker line. Only for brief periods shortly after the compressor was turned back on was the inlet temperature slightly higher than the outlet temperature. Similar trends were also found at the higher ambient conditions and, in general, accumulator temperatures increased significantly during defrost periods. Notice that the difference in accumulator inlet and outlet temperatures does not compare favorably with those presented by Coulter and Bullard [3] outlined in section 2.2.3.

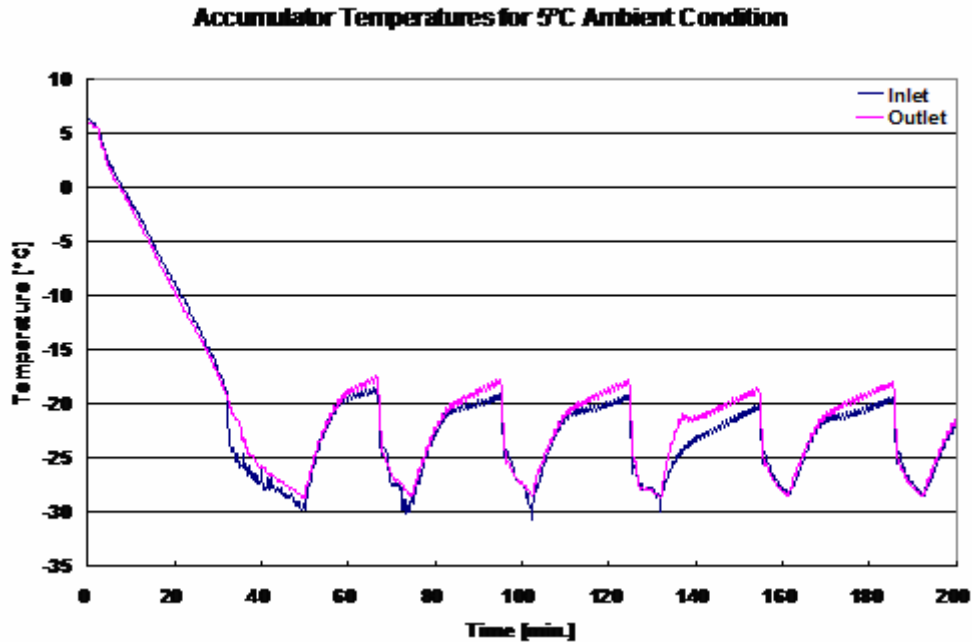


**Figure 61: Accumulator Inlet and Outlet Temperatures for the 5°C Ambient Condition for Testing with the Accumulator**

Evaporator inlet and outlet temperatures increased from around -33°C for 5°C tests to -27°C for 32°C tests. While the compressor is off, the inlet and outlet temperatures approach the same value. While the compressor is on, there is approximately a 5K difference between the inlet and outlet temperature, with the inlet temperature being the colder temperature of the two. The difference between the evaporator inlet and outlet temperatures for the 5°C ambient condition is shown in Figure 62. Similar trends are observed for the other ambient conditions and, like the accumulator temperatures, the evaporator temperatures increase significantly during defrost periods as heating was applied to the freezer cabinet.

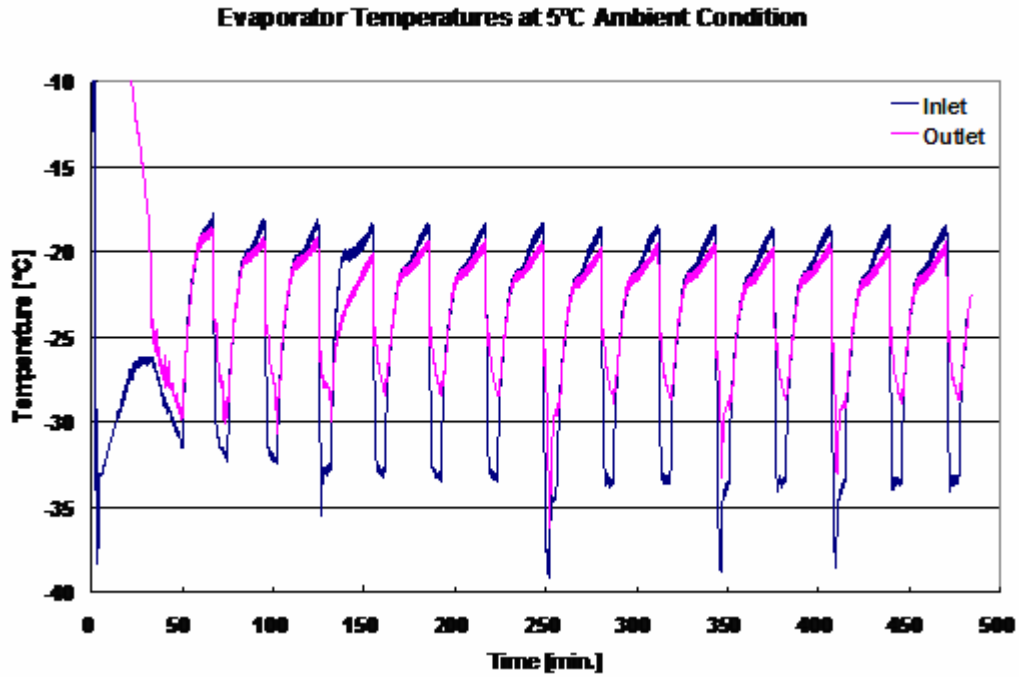


**Figure 62: Evaporator Inlet and Outlet Temperatures for the 5°C Ambient Condition for Testing with the Accumulator**

#### 4.3.1.3 Power Results

Like pressure and temperature, power also increased with increasing ambient temperature. Increased ambient temperature demanded more of the compressor thus requiring more overall power to the system. The power increase with respect to ambient temperature is shown in Figure 63 with the same indications for each ambient as used for compressor pressures and temperature.

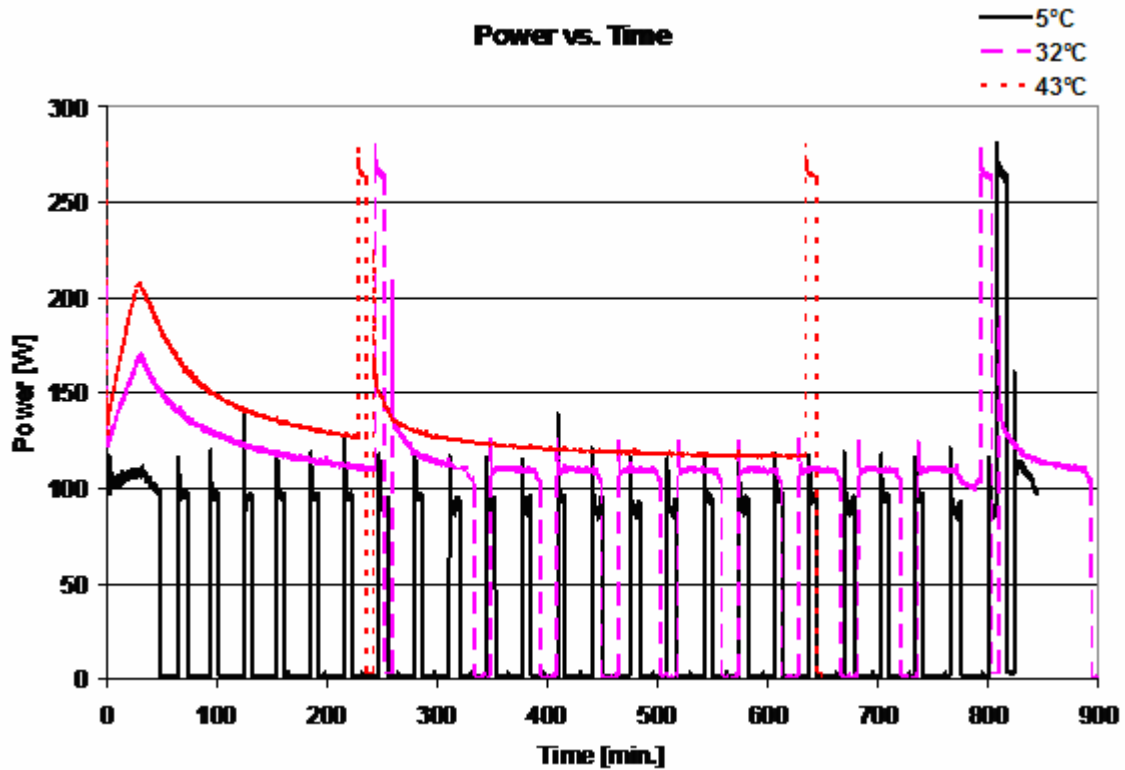


**Figure 63: System Power for Each Ambient Condition for Testing with the Accumulator**

As can be seen in Figure 63, each ambient condition experienced a difference in the timing of the refrigeration cycles. Pull-down, cycling, and defrost time periods all varied depending on the ambient condition. The variation between these times is noted in Table 18 and relates to the increased demand on the compressor associated with increasing ambient temperature. An example of each time period for the 32°C condition is shown in Figure 64. Note that for the 5°C case, the pull-down does not include a defrost period. As mentioned above, there is no cycling in the 43°C condition for the length of time during which data was collected, so the system does not complete a full pull-down period as defined in the other cases.

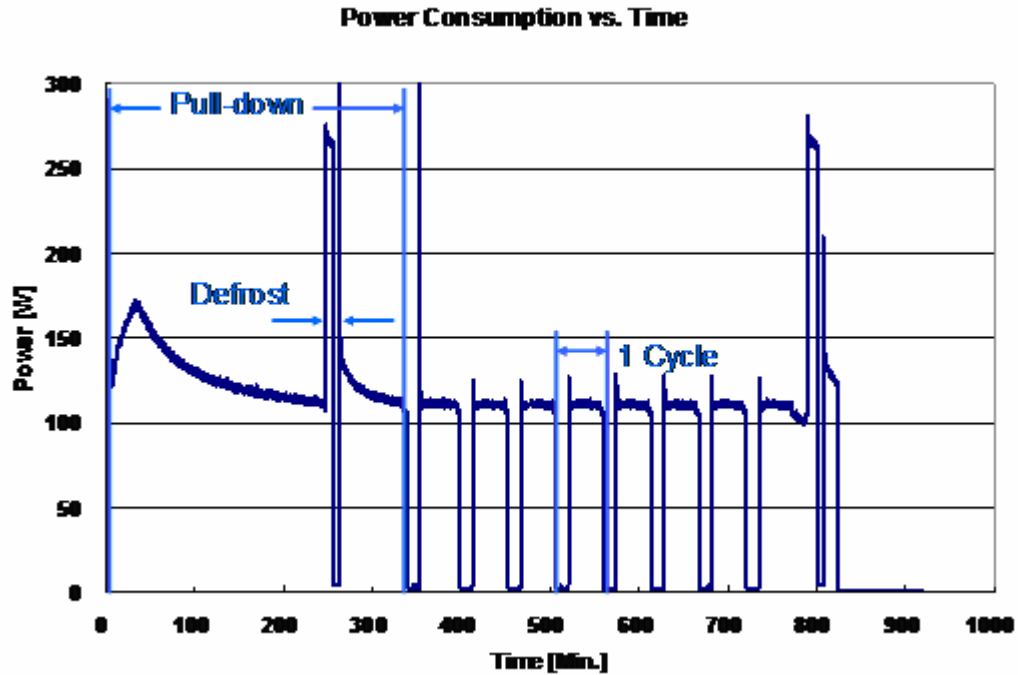


**Figure 64: Pull-down, Cycling, and Defrost Periods for the 32°C Condition for Testing with the Accumulator**

#### 4.3.1.4 Specific Capacity Results

Evaporator and condenser specific capacity results for the 5°C and 32°C ambient conditions are shown in Figure 65 and Figure 66, respectively. As can be seen in the figures, evaporator capacity decreases and condenser capacity increases slightly with increasing ambient temperature. The decrease in evaporator capacity is best seen with the P-h diagram shown in Figure 40. This diagram shows the shift in state point 5, the evaporator inlet, as the ambient temperature increases. With lower ambient conditions, especially for the 5°C case, low evaporator temperatures are easier to obtain as the temperature difference between the ambient and desired evaporator temperature is low. As the ambient temperature increases, however, so does this difference, causing more

work for the compressor and a decrease in the evaporator capacity. As mentioned in section 2.2, a decrease in evaporator capacity is expected at the beginning of a cycle as the compressor is turned back on. This decrease is due to the fact that the system has to work harder to bring the evaporator back down to the appropriate temperature quickly as the compressor is turned back on. Once the compressor has been running again for a few minutes, the system no longer has to work as hard to establish the low temperature, and the evaporator capacity increases. This trend can be seen by the small dips in capacity for both the 5°C and 32°C ambient conditions shown in Figure 65.

Condenser capacity also varies with increasing ambient temperature though the trend is somewhat reverse. As the ambient temperature increases and the compressor works harder to operate the system, more heat is available to exchange with the environment. Because the condenser temperature is generally close to the ambient temperature, however, changes between condenser capacities for each ambient condition are less than 1%, as shown in Figure 66. Results for the 43°C ambient condition are not shown as there is too much noise in the data, but trends were observed to be the same. Noise in the 43°C data was due to a grounding issue with the DAS that was resolved for following tests.

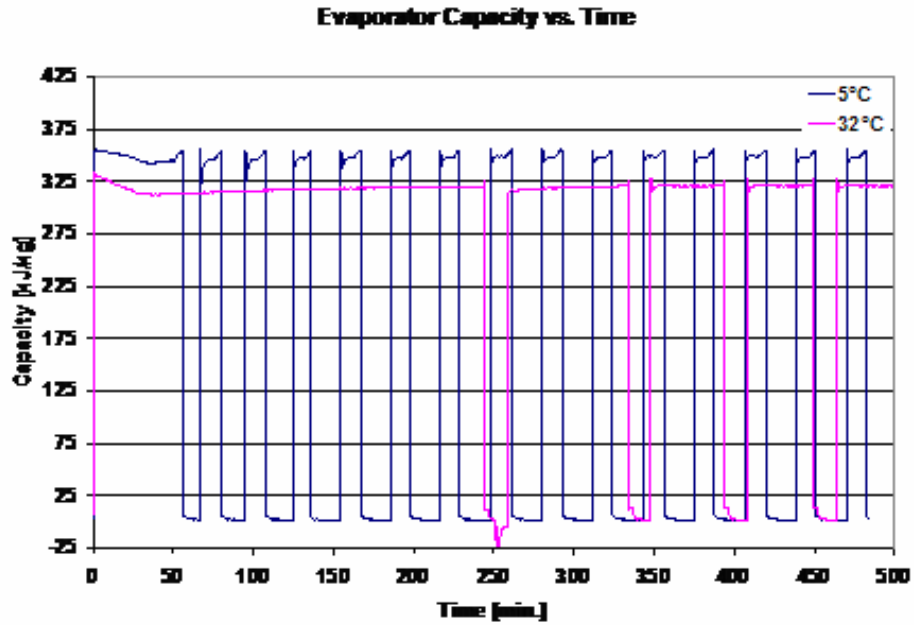


Figure 65: Evaporator Specific Capacity vs. Time for 5°C and 32°C Conditions for Testing with the Accumulator

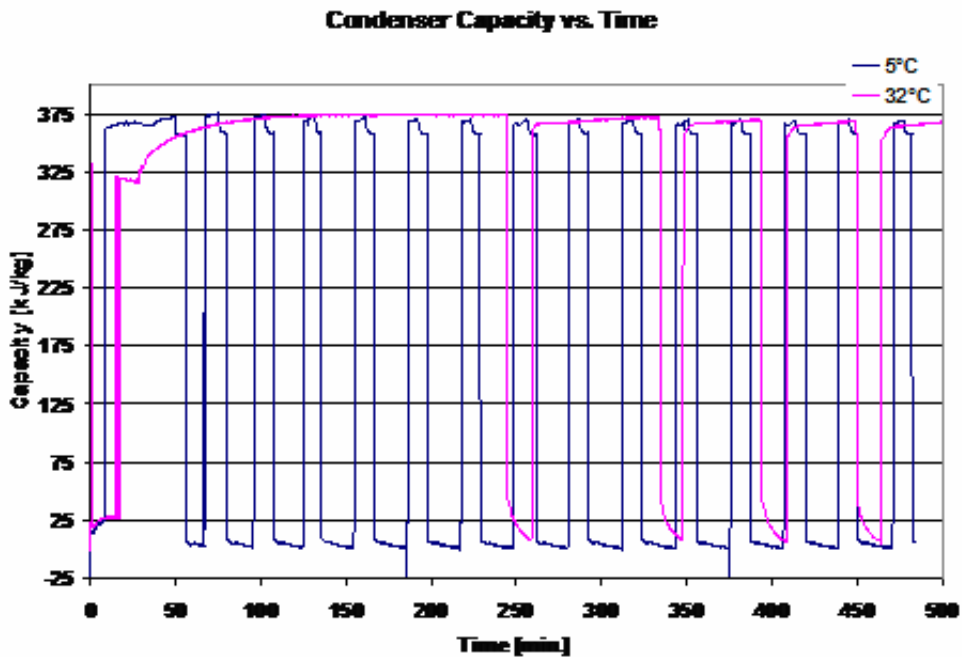
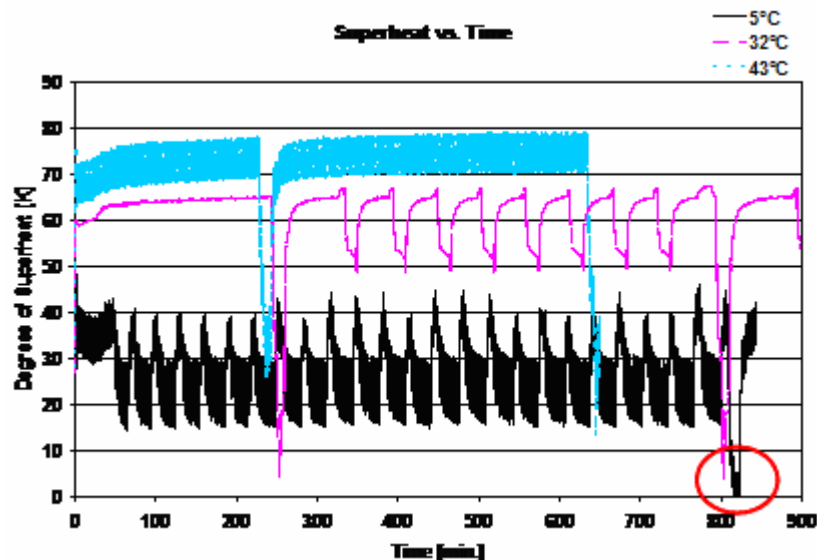


Figure 66: Condenser Specific Capacity vs. Time for 5°C and 32°C Conditions for Testing with the Accumulator

#### 4.3.1.5 Total Superheat Results

The total degrees of superheat increased with increasing ambient temperature, as expected. Even at the 5°C condition, there is a sufficient amount of superheat to ensure that any escaping liquid refrigerant from the accumulator could be evaporated prior to entering the compressor. This can be seen in Figure 58. Degrees of superheat ranged between 0 and 40K for the 5°C condition, between 5 and 65K for the 32°C condition, and between 25 and 80K for the 43°C condition, as seen in Figure 67. Periods of lower degrees of superheat occurred when the compressor was off either due to cycling or a defrost period. The only time when there was a lack of superheat was during the defrost period at the 5°C ambient condition. During this time, the superheat was calculated to be negative, as seen in the figure. Lower superheat is further verified by the appearance of more liquid in the suction line sight glass, particularly as the system is started after the defrost period at the 5°C ambient condition. This is further discussed in section 4.3.2.4



**Figure 67: Degrees of Superheat for Each Ambient Condition for Testing with the Accumulator**

#### 4.3.1.6 Solubility Results

Solubility decreased with increasing ambient temperature, as shown in Figure 68 and Figure 69, as would be expected given the system solubility correlations which show a decrease in solubility with increasing temperature or decreasing pressure. The solubility in the compressor experiences a more significant change from near 0% solubility at higher ambient temperatures to 2-3% solubility at the low ambient condition. This difference is primarily due to the increase in inside compressor temperature, which increased with increasing ambient temperature as outlined above. For a given ambient condition, the compressor solubility increased slightly during the off periods, from 0.1% to 0.5% for the 32°C ambient condition and from 2.0% to 10.0% for the 5°C ambient condition, as suction pressure increased due to system equalization.

For the accumulator, while pressures and temperatures were similar regardless of the ambient condition, solubility decreased with increasing ambient temperature as even small changes in the accumulator region would cause larger changes in overall accumulator solubility. Solubility in the accumulator increased when the compressor was off, from 67% to 100% during 5°C tests and from 55% to 100% during 32°C tests, due to the corresponding increase in pressure from system equalization. From the correlation found using TableCurve® 3D, the solubility during off periods in the accumulator is estimated to be 100% R600a, suggesting all mass observed within the accumulator is liquid R600a. Given the transient nature of the system, however, it is questionable as to whether or not the accumulator was full with only refrigerant and no oil at these times. This issue is further discussed in section 4.3.3.4.

Solubility values for each ambient condition in the compressor are shown in Figure 68 and solubility values for each ambient condition in the accumulator are shown in Figure 69. Note that the solubility also increases when the compressor is off during defrost periods at both locations.

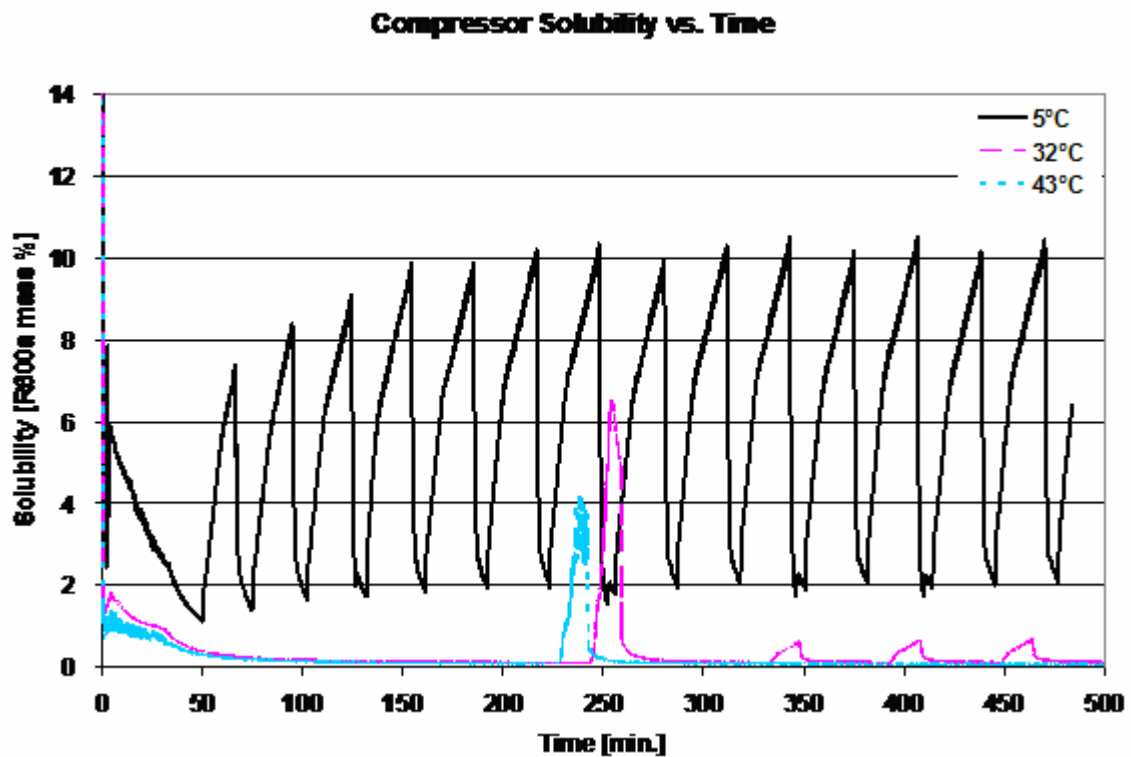
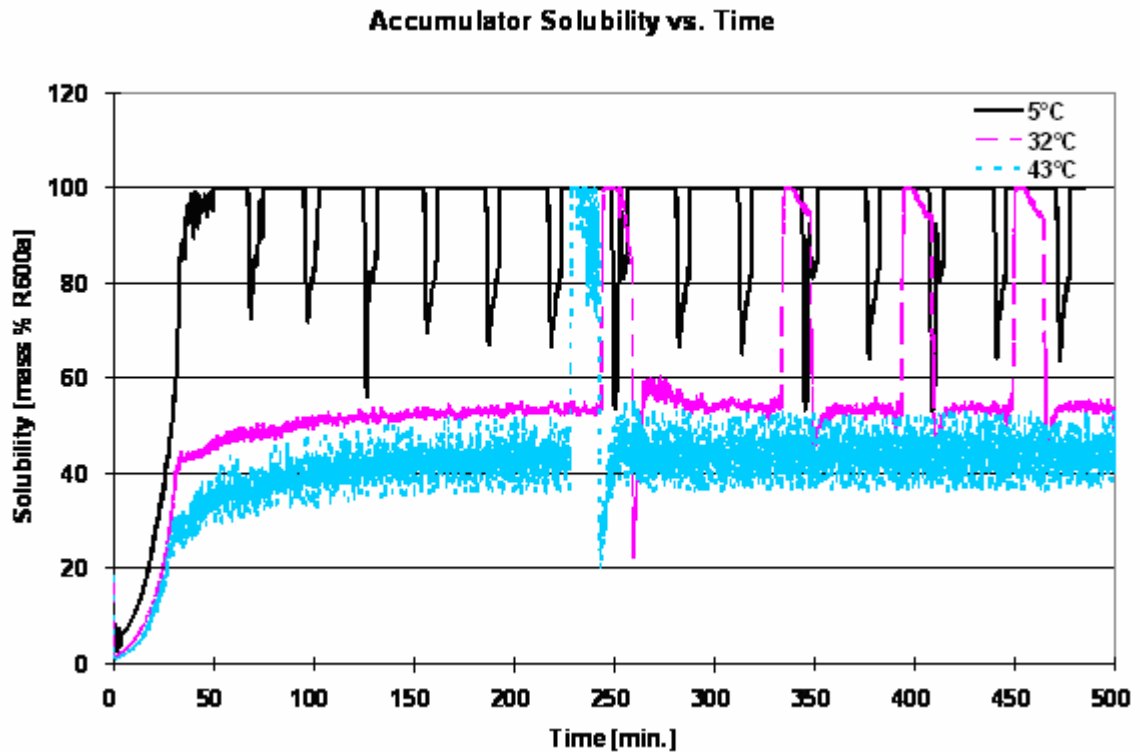


Figure 68: Compressor Solubility for Each Ambient Condition for Testing with the Accumulator



**Figure 69: Accumulator Solubility for Each Ambient Condition for Testing with the Accumulator**

#### 4.3.1.7 Mixture Density and Correction Factor Results

In the compressor, the mixture density does not experience much fluctuation. The solubility is always less than 15% mass R600a in the compressor, less than 2% if the compressor is on, regardless of the ambient temperature, and consequently, the mixture density tends to remain around the oil density level. The 5°C ambient condition results in greater fluctuation in the mixture density than in either of the other two cases due to the increased time in cycling, the increased length in off-cycle, and the larger fluctuation in solubility. During the off-cycle, the solubility increases, causing a consequent decrease in the mixture density. Similar decreases are observed in the 32°C and 43°C conditions during the defrost periods when the compressor is turned off.

Mixture density in the accumulator, however, increased with ambient temperature. With small changes in suction pressure, increasing ambient temperature lowers the solubility, which in turn increases the mixture density. With a lower solubility, less refrigerant and more oil is assumed to be present, thus the density is higher as the density of pure oil is greater than the pure liquid density of R600a. Note that mixture density for the compressor and accumulator solutions is assumed to be homogeneous despite the transient nature of the system. Further comments addressing this assumption can be found in sections 2.2.2 and 4.3.3.4. Compressor mixture density trends are given in Figure 70 and accumulator mixture density trends are given in Figure 71. Again, large fluctuations observed for the accumulator mixture density at the 43°C ambient condition are due to grounding issues with the DAS that were resolved for subsequent tests.

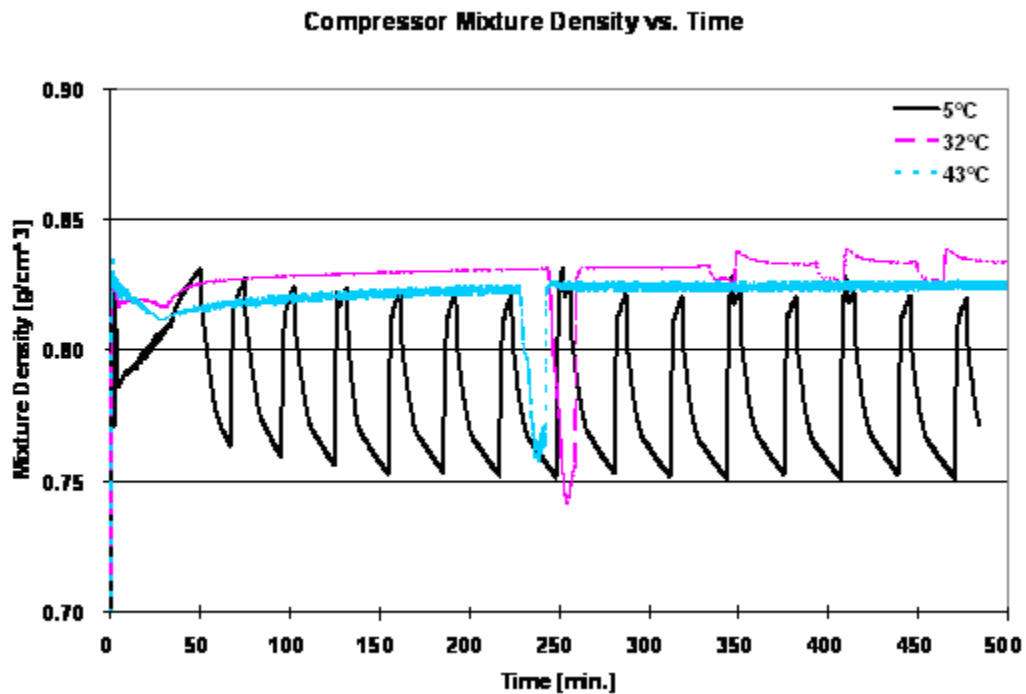
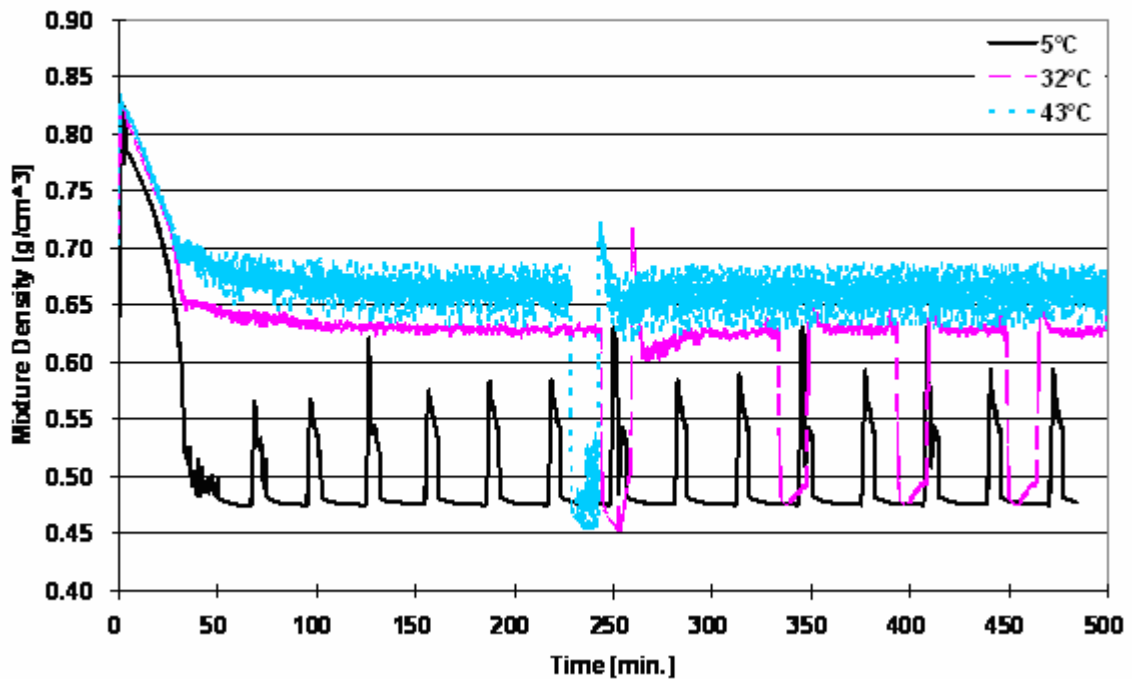


Figure 70: Compressor Mixture Density for Each Ambient Condition

**Accumulator Mixture Density vs. Time**



**Figure 71: Accumulator Mixture Density for Each Ambient Condition**

As outlined in section 4.2.2.1.5, ideal density as defined by ASHRAE was calculated in addition to the mixture density. As can be seen by the example in Figure 72, the calculated ideal and actual mixture densities vary by a constant value. This constant, or correction factor, is known for a variety of oil and refrigerant mixtures, but no known data has been published for the correction factor for R600a and Freol S-10 mineral oil. The correction factor relationship between R600a and Freol S-10 mineral oil is shown in Figure 73.

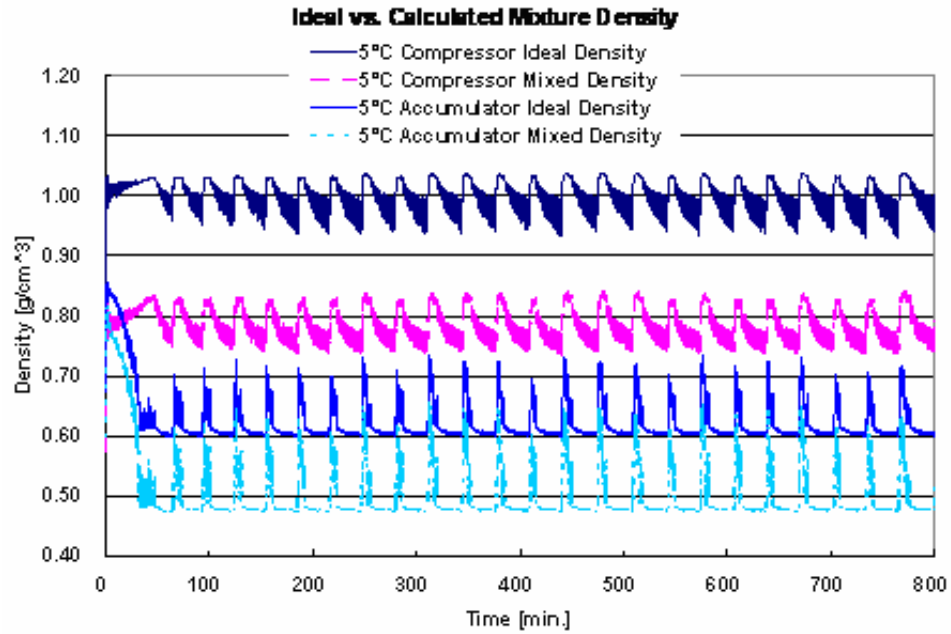


**Figure 72: Ideal and Actual Mixture Density for the 5°C Condition for Testing with the Accumulator**

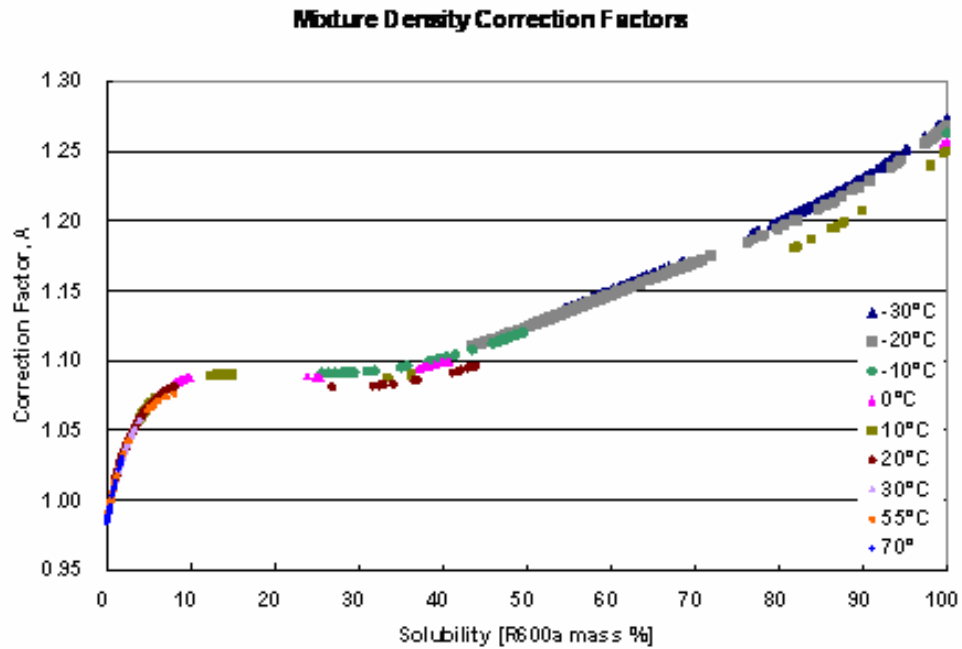


**Figure 73: Correction Factors for R600a and Freol S-10 Mineral Oil Based on Calculated Ideal and Mixture Densities**

## **4.3.2 Visualization Results and Trends with the Accumulator**

Visualization trends for each ambient condition, each video location, and each time period, including pull-down, cycling, and defrost, are outlined below.

### **4.3.2.1 Compressor Visualization Results**

#### ***4.3.2.1.1 Start-up and Pull-down***

Liquid levels in the compressor are approximately the same during the start-up and pull-down periods for each of the ambient conditions. The liquid level starts around 160mL and is sometimes as high as 180mL. In the 5°C ambient condition test, bubbles are observed when the system is started and the compressor turns on. The bubbles form and pop quickly, but there is no foaming of the bubbles as the refrigerant escapes from the oil. A liquid film is observed on the top portion of the compressor visualization port, which dispenses fluid into the liquid volume on the bottom portion of the sight glass. As the bubbling in the liquid level subsides within 7-10 minutes after start-up, the liquid level is observed to decrease. Fluctuations of the liquid surface level continue during the pull-down period around 90-115mL. Start-up trends for the 32°C and 43°C conditions are similar, but the warmer ambient conditions experience more foaming of the refrigerant bubbles when the compressor is first turned on. The foaming action causes the liquid level to drop significantly at first, but as the foaming and bubbling subsides, the liquid level increases again, though not back to its original level of 160-180mL. Instead, the liquid level stays primarily around 115mL while the compressor continues to operate. The difference in start-up trends between the different ambient conditions is shown in Figure 74.

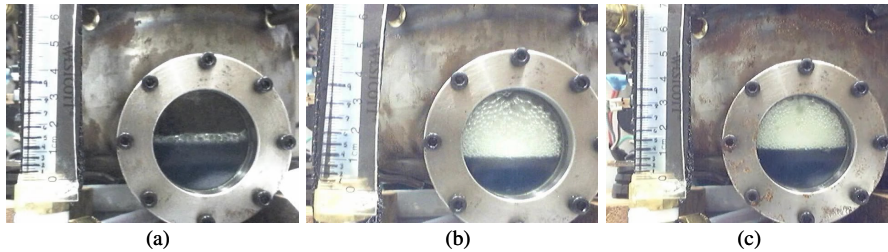


**Figure 74: Start-up Trends in the Compressor for a) 5°C, b) 32°C and c) 43°C**

### **Ambient Conditions for Testing with the Accumulator**

#### ***4.3.2.1.2 Cycling***

When the compressor is on, small waves or fluctuations in the liquid surface level in the compressor visualization port are observed. For the 32°C ambient condition, these fluctuations vary around the 115mL mark. Tests at 5°C experience fluctuations at slightly lower levels, around 100mL. When the compressor turns off, the liquid motion stops, the liquid film from the top portion of the visualization port drains to the top of the liquid surface and consequently, the overall liquid level rises. Increases in the liquid level also occur as refrigerant is able to absorb into the oil during the off period. During this time, the solubility increases, as discussed above, and without agitation from the compressor motor, refrigerant within the compressor is able to absorb into the lubricant. In the 5°C ambient condition, the liquid level rises from 100mL to approximately 115mL. In the 32°C, the liquid level rises from 115mL to 130mL. As can be seen in Figure 75, these changes in liquid level are very small and coarse given the large volume of the compressor. This trend was not observed for the 43°C condition as cycling did not occur at that ambient temperature.

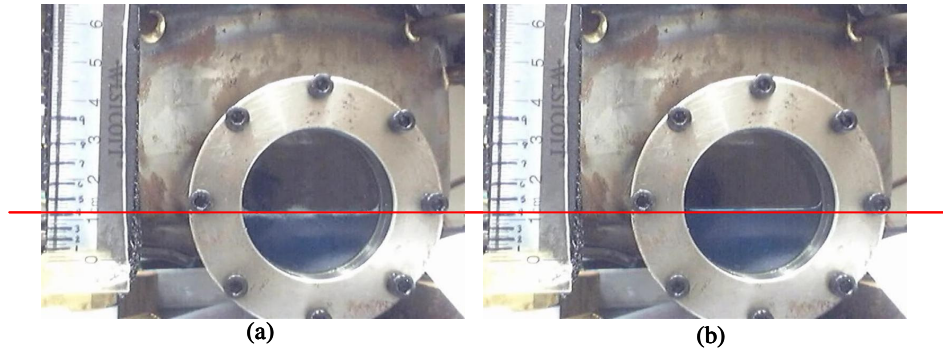


**Figure 75: Cycling Trends for the Compressor at the 32°C Condition while a) Compressor is on and b) Compressor is off for Testing with the Accumulator**

#### ***4.3.2.1.3 Defrost***

No liquid movement or fluctuations within the compressor visualization port are observed during the defrost period. For the 5°C and 32°C ambient conditions, the liquid level rises; the liquid level rises from 100mL to 120-130mL for the 5°C condition and from 115mL to 140mL for the 32°C condition. The liquid level remains around the 115mL mark during tests at the 43°C condition. Some bubbling is observed when the compressor is turned back on, but no foaming is observed for any ambient condition as in the system start-up. Fluctuations in the surface liquid level continue, first at a higher level close to that during defrost, then gradually decreasing back to the normal fluctuation level experienced during cycling.

A summary of the observed liquid levels in the compressor during each period at each ambient condition is given in Table 20. For the cycling condition, (on) represents the time when the compressor is on and (off) represents the time when the compressor is off.

**Table 20: Compressor Liquid Level Results for Each Ambient Condition for Testing  
with the Accumulator**

<b>Ambient Condition</b>	<b>Start-up/Pull-down</b>	<b>Cycling</b>	<b>Maximum Level during Defrost</b>
5°C	160-180mL (start) 90-115mL (pull-down)	100mL (on) 115mL (off)	120-130mL
32°C	160-180mL (start) 115mL (pull-down)	115mL (on) 130mL (off)	140mL
43°C	160-180mL (start) 115mL (pull-down)	115mL (on)	115mL

#### 4.3.2.2 Accumulator Visualization Results

##### ***4.3.2.2.1 Start-up and Pull-down***

Trends in the accumulator during the start-up period vary depending on the individual test and not necessarily on ambient temperature. In initial tests where the system was newly charged with both oil and refrigerant, fluid motion within the accumulator is not observed at the beginning of the test. Little to no liquid is observed in the accumulator at the start of these tests as all oil and most of the refrigerant begins in the compressor. As the test continues, however, liquid begins to enter the accumulator and the liquid level slowly rises. Small fluctuations in the liquid surface level are then observable. At the 5°C condition, the liquid level reaches 40-50mL by the end of the pull-down period, which was typically around 50 minutes. For tests at the 32°C condition, the liquid level approaches 50mL prior to the defrost period and remains at this level whenever the compressor is on. Trends for the 32°C ambient condition within the accumulator are shown in Figure 76. At the 43°C condition, a liquid level between 40-50mL is also achieved. In subsequent tests after which the system has been operated and oil and refrigerant have been distributed throughout the system, liquid remains trapped in

the accumulator at the end of a test. With approximately 20-30mL of liquid initially present in the accumulator, some bubbling within the liquid is observed when the system is first started. As in the compressor, this initial bubbling observed is due to the boiling of refrigerant from the oil as the solubility in the accumulator initially decreases. As in the other tests, the liquid level slowly rises during the pull-down period as more fluid enters the accumulator, ultimately reaching a level around 50mL.

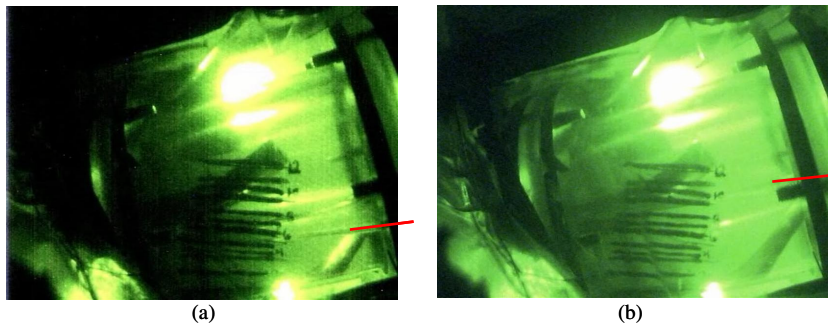


**Figure 76: Accumulator Start-up Trends at the 32°C Condition at a) initial start-up and b) just prior to defrost**

#### ***4.3.2.2.2 Cycling***

No motion is observed in the liquid in the accumulator while the compressor is off during cycling periods for the 5°C and 32°C ambient conditions. Liquid droplets are occasionally observed falling down the sides of the accumulator walls, particularly just after the compressor turns off and the liquid begins to settle. For the 32°C condition, there is no change in the liquid level, so it remains around 50mL. For the 5°C condition, however, the liquid level initially drops to around 40mL as the compressor is turned off. During the off period, there is a possible slow increase in liquid level back up to 50mL. There are two possible causes for this increase in liquid volume. The first is similar to the rise observed in the compressor. When the compressor is off, the solubility rises,

allowing refrigerant to absorb within the oil. Also during this time, liquid flow-back from the accumulator outlet piping into the accumulator is possible, adding liquid volume to the vessel. While this trend is expected based on prior the results of prior research, this trend was not observed first-hand.

When the compressor is turned on, bubbling is observed in the liquid within the accumulator for both ambient conditions. Observations at the 5°C condition show a more violent motion with a sudden surge in liquid level up to 55mL as the compressor is turned on. Liquid that was trapped within the bottom tubes of the evaporator may be suddenly sucked into the accumulator as the compressor turns on and the suction pressure quickly drops. This liquid motion gradually subsides and the liquid level drops back down to around 50mL after several minutes. In both ambient conditions, the liquid motion is observed to be around 50mL while the compressor is on. Liquid motion is also observed around 50mL for the 43°C condition, though these tests did not experience a compressor-off time period other than during defrost, as indicated previously.

#### ***4.3.2.2.3 Defrost***

Similar to trends during the cycling off-period, the liquid level in the accumulator initially drops to around 40mL for tests at the 5°C ambient condition during the defrost period. Droplets are seen raining down the sides of the accumulator walls and shortly thereafter sudden increases and decreases in the liquid level of the fluid occur as large bubbles form and pop within the liquid and/or more liquid enters the accumulator. The sudden changes in liquid level bring the total liquid level volume to 50 and 55mL, and sometimes as high as 60mL, the maximum capacity of the accumulator for its installed orientation. The surges in liquid level continue but the camera visualization grows poor

due to the frost accumulated on the freezer panels during this time. Results for the 32°C case are similar to the 5°C condition, but the liquid level rises completely to 60mL during the defrost period. Similar surges in the liquid level are observed in the 32°C condition as well. A defrost heater is used in the freezer compartment on the evaporator during the defrost period, quickly raising the temperature within the accumulator. The increase in temperature may cause some R600a to boil, causing the sudden pops and surges observed in the accumulator. At the same time, however, the pressure, and consequently the solubility, increase, suggesting that the liquid level rise is due to R600a absorbing within any oil captured within the accumulator.

When the compressor is turned back on at the end of the defrost period, bubbling and large fluctuations are observed, but the liquid level drops back to its usual 50mL mark within several minutes. The same trend is observed for the 43°C condition. Bubbling is again due to the evaporation of refrigerant from the oil and fluctuations resume with the movement of oil and refrigerant through the system.

A summary of the observed liquid levels in the accumulator during each period at each ambient condition is given in Table 21.

**Table 21: Accumulator Liquid Level Results for Each Ambient Condition for**

**Testing with the Accumulator**

<b>Ambient Condition</b>	<b>Start-up/Pull-down</b>	<b>Cycling</b>	<b>Maximum Level during Defrost</b>
5°C	Start at 20-40mL Rises to 40-50mL	50-55mL (on) 40-50mL (off)	Up to 55-60mL
32°C	Start at 10-30mL Rises to 40-50mL	50mL (on/off)	Up to 60mL
43°C	Start at 20-25mL Rises to 40-50mL	50mL (on)	Up to 60mL

### 4.3.2.3 Accumulator Outlet Visualization Results

#### ***4.3.2.3.1 Start-up and Pull-down***

For each of the ambient conditions, there is a small pool of liquid observed in the accumulator outlet sight glass prior to the start of the system. This liquid is assumed to be trapped oil and/or liquid R600a due to the orientation of the sight glass. In general, little motion is observed when the system is turned on though some liquid fluctuation and bubbling is occasionally visible. For some of the 5°C condition tests, however, more violent motion within the sight glass and lots of bubbling are observed at the system start-up. This variation depends on when the system was stopped in previous tests. Depending on the amount of oil and refrigerant available in the sight glass, more or less bubbling is observed as refrigerant boils out of the oil. During the pull-down period, liquid motion and fluctuation continues to be observed, but liquid generally only fills 1/4-1/3 of the sight glass, which is positioned in a vertical orientation. As with other locations within the system, bubbling observed at start-up is consistent with a decrease in solubility and the boiling of refrigerant from the oil.

#### ***4.3.2.3.2 Cycling***

As is observed towards the middle and end of the pull-down period, fluctuations of liquid are observed in the accumulator outlet sight glass while the compressor is on. Liquid fills approximately 1/4-1/3 of the sight glass and bounces as oil and/or refrigerant passes through. In the 5°C condition, a lot of motion and bubbling are initially observed when the compressor is first turned on after an off-period. For the 5°C and 32°C conditions when the compressor is off, liquid motion initially stops. After a few minutes,

however, bubbling and “popping” of the liquid is observed in the accumulator outlet sight glass. Bubble formation is slow at first and gradually increases in size and frequency as the compressor off-period comes to an end. While solubility is suggested to increase with increasing temperature and pressure within the accumulator, the increase in temperature at the evaporator and accumulator outlet may also cause boiling of any liquid refrigerant left in the accumulator outlet sight glass or piping. Because the accumulator has a large mass of fluid of both oil and refrigerant, boiling of any refrigerant within the accumulator is not observed as the temperature at this location does not change as rapidly. With little liquid to retain temperature, however, refrigerant just outside of the accumulator may boil out through the sight glass during off periods. Bubbling motion stops just briefly before lots of liquid and bubbles are observed through the sight glass as the compressor is turned back on.

#### ***4.3.2.3.3 Defrost***

Visualization is generally poor during the defrost period as noted with the accumulator. For the 32°C and 43°C conditions, liquid motion within the sight glass initially stops when the defrost period begins. Several minutes later, lots of bubbling and liquid popping begins and continues until liquid motion can no longer be observed due to poor visualization. Similar behavior is observed in the 5°C test, though there is a lot of motion at the start of the defrost and foamy bubbles fill the sight glass similar to when the compressor is turned on after an off-period. Again, bubbles during the defrost period when the compressor is off are assumed to be due to the boiling of refrigerant from a large increase in temperature due to the defrost heater.

#### 4.3.2.4 Suction and Discharge Line Visualization Results

##### ***4.3.2.4.1 Start-up and Pull-down***

For all ambient conditions, liquid motion, assumed to be mostly compressor oil, is observed in both the suction and discharge line at the beginning of a test. Liquid in the discharge line is only observed for a brief period and then is assumed to subside along the very bottom of the sight glass. Liquid motion is more easily observed in the suction line, though it is assumed that some oil continues to leave the compressor through the discharge line throughout the test.

##### ***4.3.2.4.2 Cycling***

For the 5°C and 32°C conditions, no motion is observed in either the suction or discharge line when the compressor is off during cycling. When the compressor turns back on, liquid is observed in the suction line. It is assumed that some liquid oil flows through the discharge line as well, but liquid motion is not as prominent in the discharge line for either ambient condition. As the compressor remains on in the 43°C test, liquid flow through the suction line is not as pronounced as it is during the start of the test. Little to no motion is observed in the discharge line, as in the other ambient conditions.

##### ***4.3.2.4.3 Defrost***

For all ambient conditions, liquid motion stops in both lines as the defrost period begins. Occasional bubbles and surges of liquid are observed through the suction line for all conditions. Lots of liquid motion is observed in the suction line when the compressor is turned back on, especially for the 5°C ambient condition, and some of the liquid has a green tint, suggesting that it may be the mineral oil with the UV dye. It is unknown,

however, whether or not refrigerant may also be included in this liquid returning to the compressor. Superheat results suggest that liquid R600a flow back to the compressor through the suction line is only a concern during and after defrost for the 5°C ambient condition.

### **4.3.3 Refrigerant and Oil Mass Analysis Results**

Using the method outlined in section 4.2.2.1.6, the approximate mass of oil and refrigerant were calculated for the compressor and accumulator volumes during pull-down, cycling, and defrost periods. Snapshots of data were taken at pre-determined time intervals and matched with corresponding video results. Using the data for those points and the liquid level in the compressor and accumulator at those times, the mass of the oil and refrigerant were calculated. Different trends were noted for each ambient condition during each period of interest. These results are outlined in the following section.

#### **4.3.3.1 Mass Balance Trends during Pull-down**

As mentioned above, data were noted at specific time intervals throughout the pull-down period. Data was used in conjunction with solubility, mixture density, and volume level information to determine the mass of oil and refrigerant in the compressor and accumulator. A sample of data collected for the 5°C condition is provided in Table 22 and Table 23 and corresponds to the graph in Figure 77.

**Table 22: Compressor Data Points for Mass Balance for Pull-down at the 5°C  
Ambient Condition for Testing with the Accumulator**

Measurement	Point 1	Point 2	Point 3	Point 4	Point 5	Point 6
Point Description	System start up	10 min after start	20 min after start	30 min after start	40 min after start	48 min after start (comp. off)
Suction Pressure [kPa]	138.1	51.2	56.2	57.9	52.1	53.6
Inside Compressor Temperature [°C]	9.0	7.5	17.5	19.6	30.0	30.5
Compressor Solubility [mass %]	43.9	6.4	3.7	3.4	1.4	1.4
Liquid Level inside Compressor [mL]	180	115	115	115	115	115
$\rho_{mix}$ at Compressor [g/mL]	0.64	0.78	0.80	0.80	0.83	0.82
Approx. $m_{R600a}$ at Compressor [g]	50.6	5.7	3.4	3.1	1.3	1.3
Approx. $m_{oil}$ at Compressor [g]	64.6	84.0	88.6	88.9	94.1	93.0
Total Mass in the Compressor [g]	115.2	89.7	92.0	92.0	95.4	94.3

**Table 23: Accumulator Data Points for Mass Balance for Pull-down at the 5°C  
Ambient Condition for Testing with the Accumulator**

Measurement	Point 1	Point 2	Point 3	Point 4	Point 5	Point 6
Point Description	System start up	10 min after start	20 min after start	30 min after start	40 min after start	48 min after start (comp. off)
Suction Pressure [kPa]	138.1	51.2	56.2	57.9	52.1	53.6
Ave. Accumulator Temperature [°C]	5.2	-2.6	-11.2	-17.2	-25.4	-30.1
Accumulator Solubility [mass %]	58.2	13.6	32.0	54.8	84.1	100
Liquid Level inside Accumulator [mL]	20	20	20	25	35	38
$\rho_{mix}$ at Accumulator [g/mL]	0.59	0.75	0.70	0.62	0.53	0.48
Approx. $m_{R600a}$ at Accumulator [g]	6.7	2.0	4.5	8.5	15.6	18.2
Approx. $m_{oil}$ at Accumulator [g]	4.9	13.0	9.5	7.0	2.9	0.0
Total Mass in the Accumulator [g]	11.6	15.0	14.0	15.5	18.5	18.2
Total Mass in both Acc. And Comp. [g]	126.8	104.7	106.0	107.5	113.9	112.5

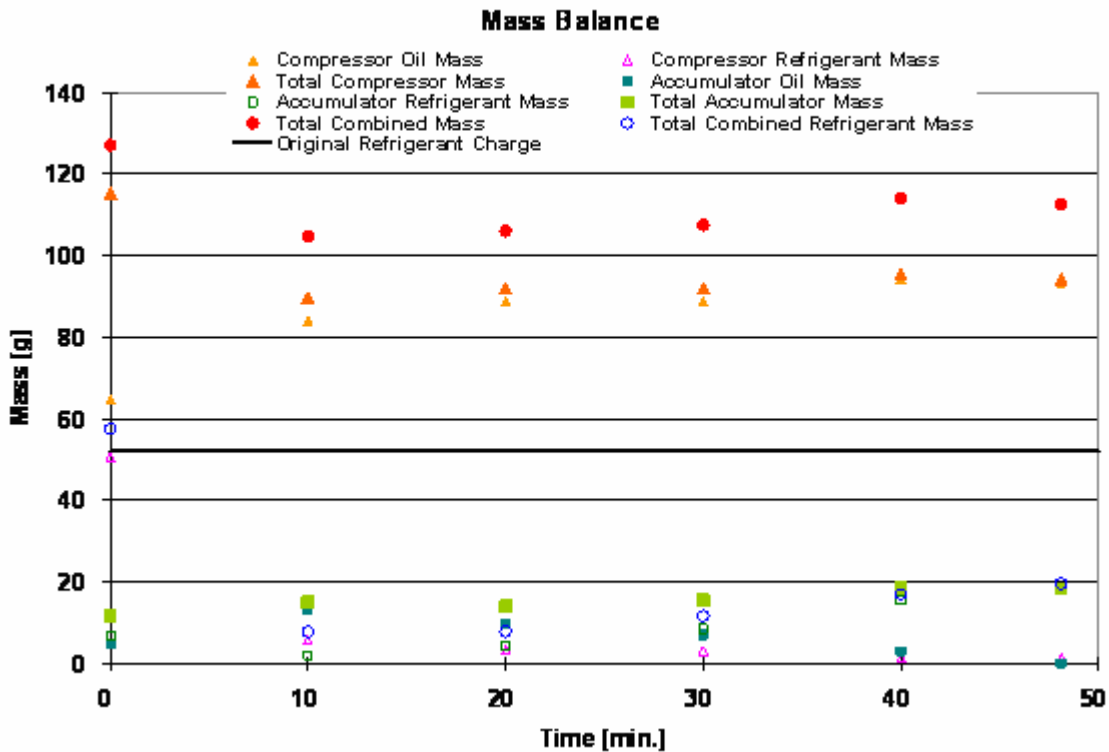


**Figure 77: Mass Balance for the Pull-down Period for the 5°C Ambient Condition for Testing with the Accumulator**

As can be seen in the above tables and graph, the total amount of mass accountable in the compressor and accumulator starts around 125-130g and decreases as the system is started. The largest decrease occurs within the first 10 minutes that the system is running, most likely as refrigerant and oil are quickly distributed throughout the system and any liquid refrigerant dissolved in the oil boils out. Following the initial start and decrease, the total mass in the compressor and accumulator increases throughout the pull-down period. This increase is due primarily to the increase of liquid in the accumulator. After the initial start-up, the amount of oil and refrigerant within the compressor remains fairly constant as a majority of the liquid mass is oil and remains within the compressor for lubrication. Liquid volume in the accumulator, as noted in the

section above, however, increases during the pull-down period, contributing to the overall increase in total combined mass of the two components. This increase is primarily expected to be due to an increase in liquid refrigerant leaving the evaporator and entering the accumulator, though some oil may contribute as well. The solubility within the accumulator also increases as the pull-down period continues, contributing to the notion that more liquid refrigerant becomes trapped inside any existing oil within the accumulator. Note that, at the beginning of the test, the total overall refrigerant mass in the 5°C condition is calculated to exceed the original charged amount of refrigerant to the system by 10%. This is due to error in the correlations and method of calculation.

Results for the mass analysis for the pull-down in the 32°C ambient condition are shown in Figure 78. As seen in the case of the lower ambient, the total mass starts high, this time closer to 140g, and decreases shortly after the initial start of the system. Compressor oil and refrigerant mass then remains fairly constant while again the accumulator mass begins to increase. Mass in the compressor increases during the defrost stage that occurs during the pull-down period 250 minutes after the initial start-up in the 32°C ambient condition as solubility levels rise and refrigerant dissolves back in the oil, raising the liquid level and consequent amount of mass calculated. Accumulator liquid levels increase slightly during the defrost period, but settle back to previous levels afterwards, thus not showing much of a difference in oil or refrigerant mass as the pull-down period continues. More comments about the defrost stage in particular are described in section 4.3.3.3. Data charts outlining each of the assessed points for this and all other cases are shown in Appendix 7.1.

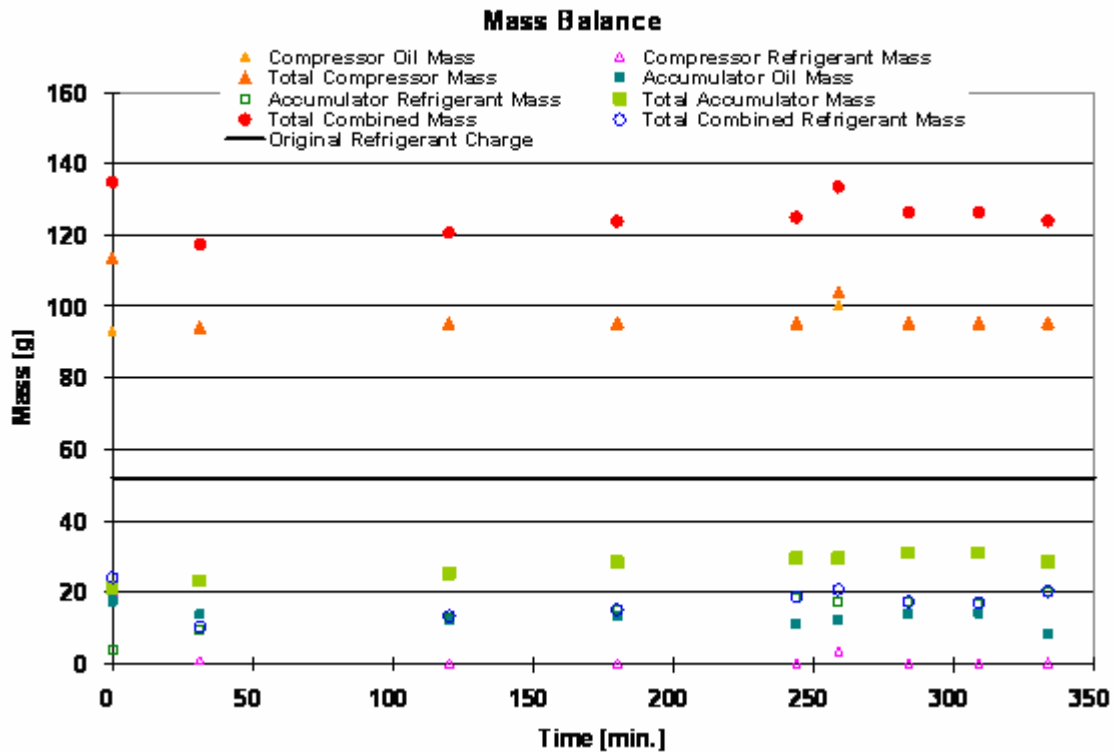


**Figure 78: Mass Balance for the Pull-down Period for the 32°C Ambient Condition for Testing with the Accumulator**

Pull-down for the warmest, 43°C, ambient condition was only considered until the first defrost period. As mentioned above, cycling was never achieved in this condition and thus pull-down was never completed as defined for the other ambient conditions. As seen for the cooler ambient conditions, total oil and refrigerant mass starts around 130g and decreases when the system turns on. Again, total compressor mass remains fairly constant and is mostly oil as the solubility is low and most refrigerant is vapor within the compressor vessel, as is desired. Accumulator mass continues to increase as time progresses as the solubility increases with decreasing temperature. Originally, more oil than refrigerant is calculated to be present within the accumulator. As the system

approaches the first defrost, however, this trend reverses and more liquid refrigerant than oil is expected to be present within the accumulator. These trends are shown in Figure 79.

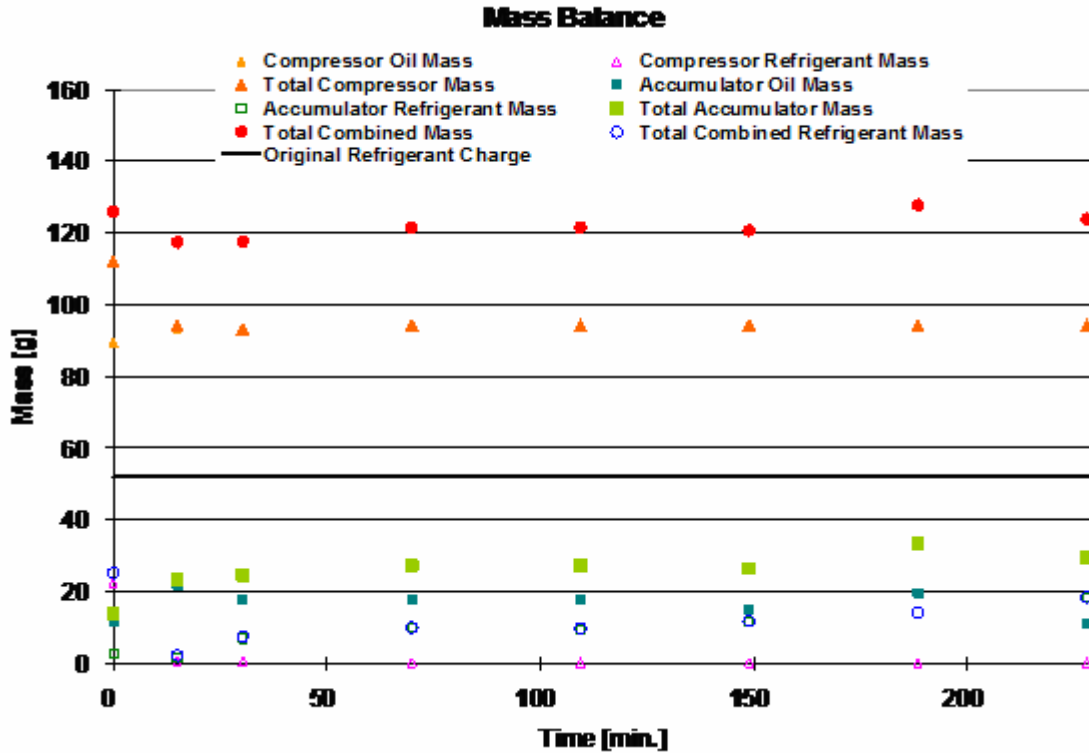


**Figure 79: Mass Balance for the Pull-down Period for the 43°C Ambient Condition for Testing with the Accumulator**

#### 4.3.3.2 Mass Balance Trends during Cycling

In addition to pull-down, cycling mass balance trends were noted. Only the 5°C and 32°C cases were examined as cycling did not occur at the 43°C ambient condition. Cycling included time when the compressor was on, during which the amount of refrigerant liquid decreased in the compressor and fluctuated slightly in the accumulator; and time when the compressor was off, during which the amount of refrigerant increased in comparison to the on period because of increases in solubility and possible liquid flow-back through the system.

In the 5°C ambient condition for cycling, depicted in Figure 80, the compressor and accumulator mass remained relatively constant during the off-period, which consists of data points between 7 and 32 minutes. In the 32°C condition, however, shown in Figure 81, the compressor and accumulator mass remained relatively constant during the on-period, depicted by points between 0 and 45 minutes. This is most likely due to the amount of time spent in each condition for each ambient case. Cycling on-time for the 5°C condition was considerably shorter than that for the 32°C condition and just the opposite was true for the off-time. As the off-period was longer for the 5°C condition, the system was able to stabilize during that time, showing little changes in mass trends. The similar is true for the 32°C condition during on-time. For both conditions, mass within the compressor was always mostly oil at all times, as expected, and mass within the accumulator was calculated to be mostly refrigerant during the off-periods and a combination of oil and refrigerant during the on-periods.

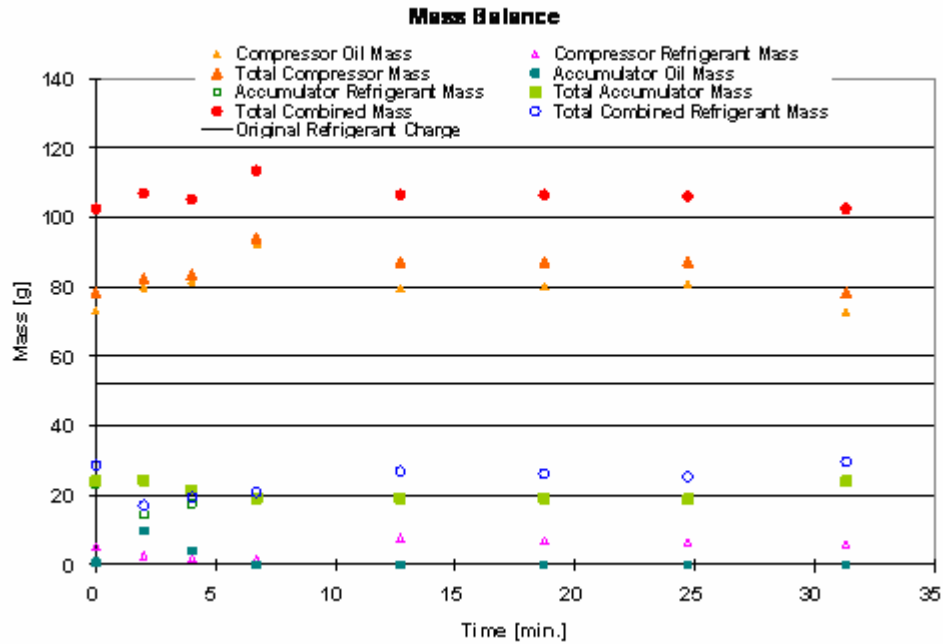


**Figure 80: Mass Balance for the Cycling Period at the 5°C Ambient Condition for Testing with the Accumulator**

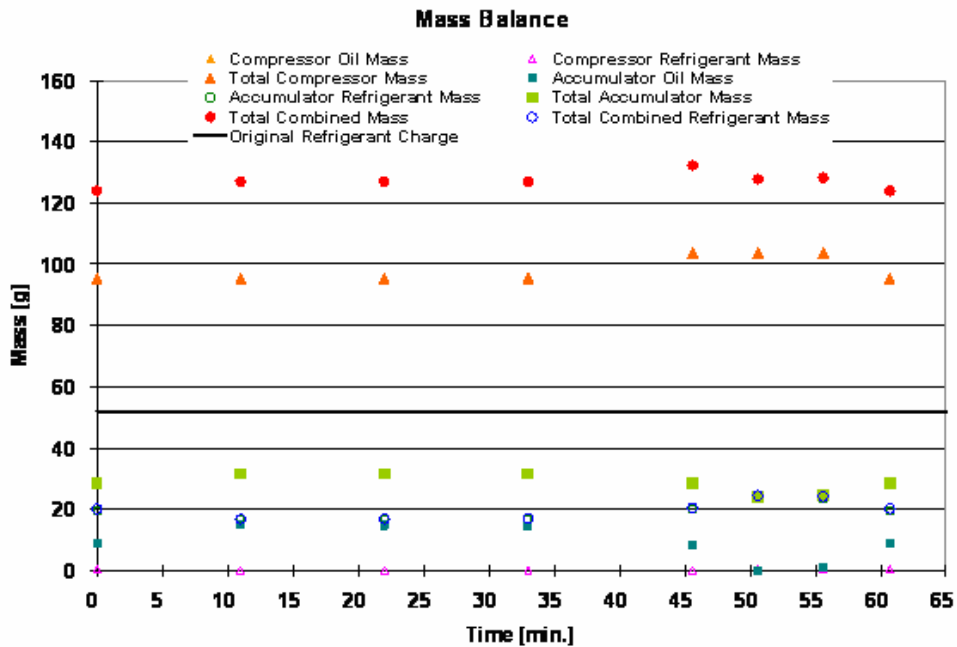


**Figure 81: Mass Balance for the Cycling Period at the 32°C Ambient Condition for Testing with the Accumulator**

#### 4.3.3.3 Mass Balance Trends during Defrost

Finally, mass balance was also examined during the defrost period. Due to poor visualization that often occurred during this time, the liquid level in the accumulator was estimated based on observed trends before and after the period of poor visualization. These points occurred most often towards the end of the defrost period.

Results for the 5°C ambient condition are given in Figure 82. During the initial stage of the defrost period, depicted through points between 0 and 12 minutes, the compressor is turned off, power is high due to the engagement of a heater, pressure increases at the suction side, and inside compressor temperature decreases as the compressor is no longer running. During this time, solubility increases and refrigerant mass in the compressor is consequently calculated to increase with the observed rise in liquid level. During the second half of the defrost period, depicted through points between 12 and 20 minutes, the power level is low, the compressor remains off, and pressure and temperature fluctuate slightly. Solubility consequently fluctuates as well, producing the fluctuation in refrigerant and mass observed in the later portion of Figure 82. Combined mass within the compressor and accumulator, despite observed increases in liquid levels, remains relatively constant during the defrost period.

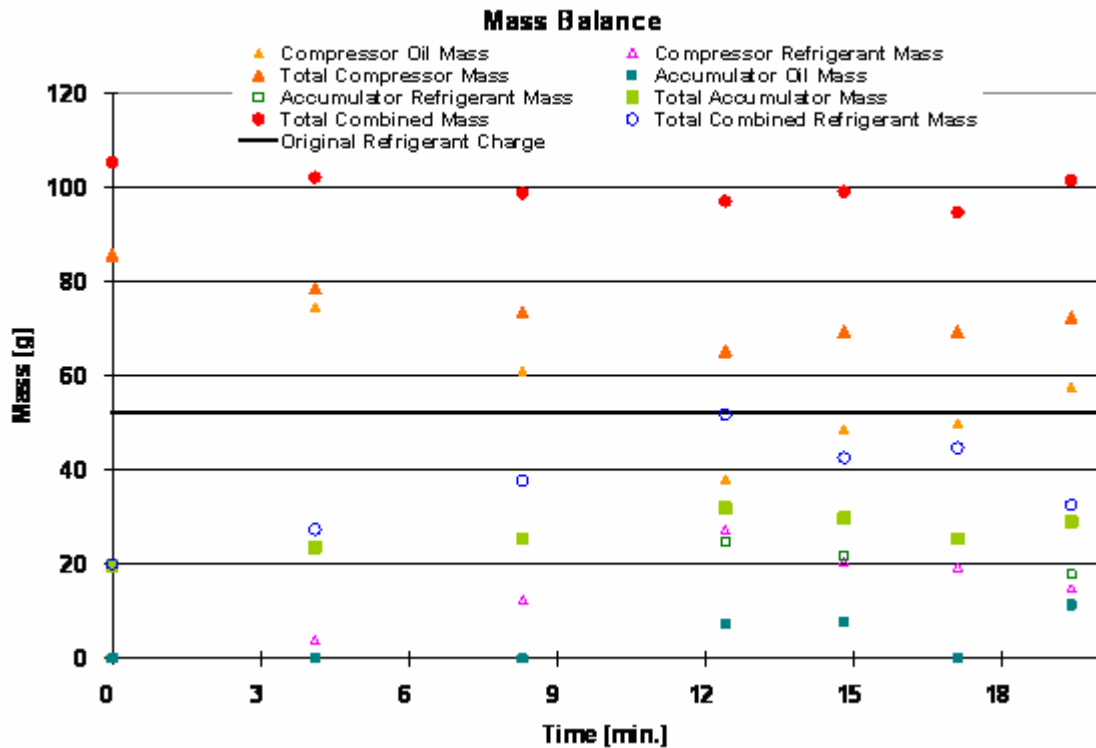


**Figure 82: Mass Balance for the Defrost Period at the 5°C Ambient Condition for Testing with the Accumulator**

Defrost results for the 32°C and 43°C ambient conditions, shown in Figure 83 and Figure 84 respectively, are relatively similar. During the defrost period, the system experiences the highest solubility levels within the compressor other than when the system is first turned on. This occurs because of the increase in pressure and the decrease in temperature that occurs more drastically than during cycling off-periods. On the accumulator side, an increase in pressure and an increase in temperature increase the solubility to 100%. Liquid levels are also observed to increase dramatically in the accumulator during the defrost period and while most likely not all of the liquid is actually liquid refrigerant, a larger portion of the liquid volume is liquid refrigerant than is experienced during the cycling period. For both Figure 83 and Figure 84, the first three

points correspond to high power and the last four correspond to low power during the defrost period.

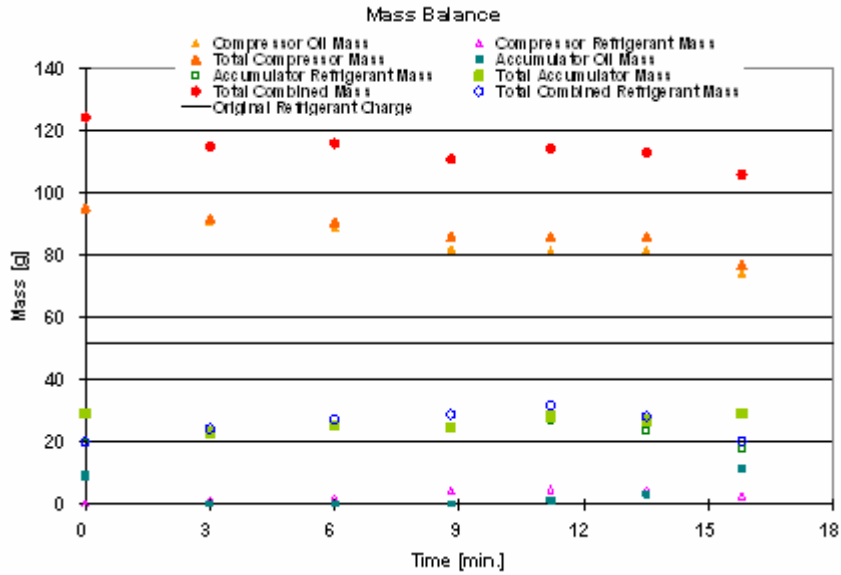


**Figure 83: Mass Balance for the Defrost Period at the 32°C Ambient Condition for Testing with the Accumulator**

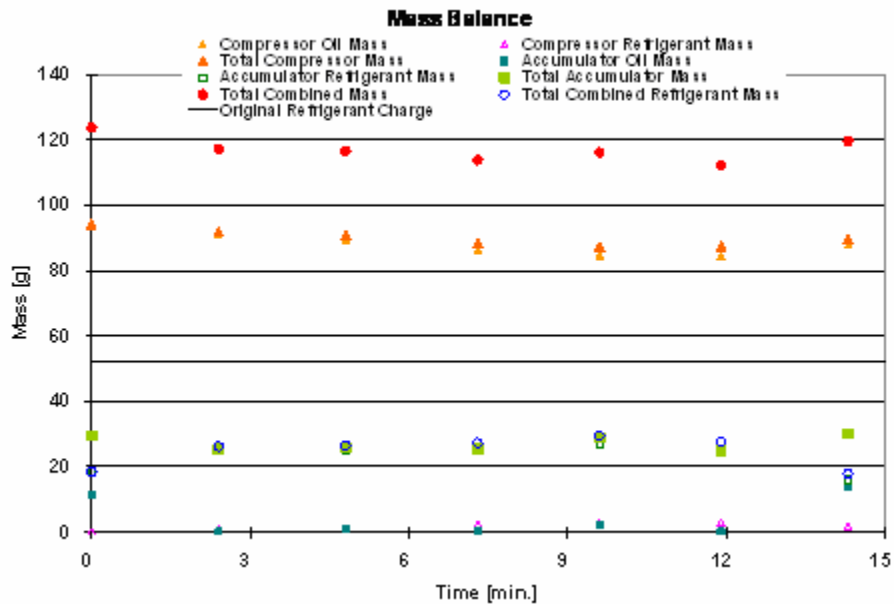


**Figure 84: Mass Balance for the Defrost Period for the 43°C Ambient Condition for Testing with the Accumulator**

#### 4.3.3.4 Issues with mass balance calculations

Because of the unknown errors associated with the solubility and mixture density, as well as the errors in determining liquid level from video observation, the accuracy of mass balance calculations is a large concern. While the correlation often suggested that the solubility in the accumulator was 100%, it is not safe to assume that all liquid present in the accumulator is consequently liquid refrigerant at these times. Between tests, when the system was off, oil was observed to be trapped in the bottom of the accumulator. Whether this oil remained trapped in the accumulator or was able to re-circulate throughout the system when it was turned back on is unknown, though it is likely that much of it remained within the accumulator. The horizontal orientation of the accumulator most likely prohibited large amounts of oil from leaving the accumulator during operation. Thus, a solubility of 100% should not assume a total volume of pure liquid refrigerant. Unfortunately, the method of analysis does not allow for such considerations and assumptions about the available amount of oil or liquid refrigerant in the accumulator or compressor would only contribute to larger analysis error. Consequently, the above calculations and analysis should be reviewed with caution and absolute numbers should not be taken as exact measurements.

In addition to the correlation challenge, it is also important to note the variability and sensitivity of the liquid level measurements. While certain levels may have been observed in the compressor and accumulator during on-periods, more liquid could have been present in these components on the walls of the vessels, particularly in the compressor. Noted liquid level rise during the off-periods, particularly within the compressor, may have just accounted for the liquid that had previously been coating the

walls of the vessel and not necessarily represent “new” liquid coming from other components of the system. This is not true in the accumulator during the defrost period, however, as liquid was observed actually entering the accumulator at that time. Also note that oil and refrigerant mass calculated was only for liquid volume and did not consider the amount of refrigerant vapor mass that could have also been residing in the compressor or accumulator.

#### **4.4 Summary of Oil and Refrigerant Flow with the Accumulator**

Despite the challenges in the analysis method, the above results allow for basic statements and conclusions about oil and refrigerant distribution throughout a household refrigeration system. The following section summarizes the observations that were noted during the pull-down, cyclic, and defrost periods for oil and refrigerant flow.

Prior to the very first start-up, all of the oil and liquid refrigerant are located in the compressor, as both liquids are originally charged to this location. Some R600a dissolves into the compressor oil and the system equalizes to a pressure lower than the saturation pressure of R600a at the given ambient temperature. At the 5°C ambient condition, for example, the starting pressure for the system is around 140kPa whereas the saturation pressure for R600a at 5°C is 187kPa. Similarly, the starting pressure at the 32°C condition is around 245kPa while the saturation pressure is 427kPa. Such a decrease in starting pressure due to the dissolved refrigerant in oil greatly reduces the amount of torque and power required for the start of the compressor.

As the system is started, bubbling occurs in the compressor as the solubility decreases and refrigerant boils out of the oil. For the very first test, bubbling only occurs at the compressor as this is the only location where both oil and refrigerant are present. In

subsequent start-up periods, after the system has circulated both oil and refrigerant, bubbling occurs at other locations, including the accumulator. Warmer ambient conditions experience more foaming action as more power is required at start-up, resulting in increased agitation of the fluid. Solubility at higher ambient temperatures also drops to lower levels than that at lower ambient temperatures, resulting in more refrigerant boiling out of the oil.

During the pull-down period, a small amount of oil leaves the compressor and circulates throughout the system. Some of the oil becomes trapped in the accumulator and other locations where orientation and gravity may prevent it from returning to the compressor. Total liquid volume in the compressor decreases as refrigerant boils out of the oil and small amounts of oil leave to circulate through the system. In total, as described by the above results, it is suggested that 15-20% of the original oil charge leaves the compressor and circulates through the system once it is started. Some of this oil continuously moves throughout the system, but at least 10% of the original oil charge may become trapped within the accumulator. Fluctuations in liquid volumes occur when the compressor is on as oil and refrigerant continue to move throughout the system.

As in pull-down, liquid fluctuations continue during the cycling period whenever the compressor is on. When the compressor is off, liquid motion stops and any fluid that previously traversed on pipe or vessel walls settles to the lowest point of the occupied space. Solubility rise causes stationary liquid volumes to slowly increase as refrigerant is able to absorb with any available oil. When the compressor turns back on, bubbling occurs within the accumulator and compressor as refrigerant boils back out of the oil and returns to movement throughout the system. Whenever the compressor is turned back on,

sudden surges of fluid move quickly through the accumulator and suction line during the first few seconds after turning on as the change in low-side pressure draws this liquid quickly to the compressor. For experiments with the accumulator, enough superheat is available to ensure that any liquid drawn back to the compressor is purely oil and not liquid refrigerant.

The defrost period causes the compressor to turn off, stopping active motion of the oil and refrigerant throughout the system. Bubbling at the accumulator and accumulator outlet occurs, however, as large temperature increases from the defrost heater cause some liquid refrigerant to evaporate. As with the off-period during cycling, liquid volumes in the compressor and accumulator increase due to an increase in solubility and the opportunity for refrigerant to absorb within the oil. Solubility increases during the defrost period are generally greater than during the cycling period, so bubbling that follows when the compressor turns back on is more violent and pronounced than that which occurs during cycling periods. Any bubbling that does occur in the compressor or accumulator settles after several minutes as the system liquid distribution stabilizes.

## **4.5 Conclusions**

Information about a household refrigerator compressor and accumulator was gained through a series of tests at three different ambient conditions. Temperature, pressure, and power data were collected together with visualization results to analyze system solubility and oil and refrigerant mass within both the compressor and accumulator. Liquid levels and liquid flow patterns were observed through clear visualization ports with video camera imaging. Sampling methods were attempted to verify mixture density and solubility data, but were ultimately unsuccessful due to the

small size and number of samples taken. Correction factors for R600a and Freol S-10 mineral oil were established based on experimental data and calculated densities.

Variations in pull-down and cycling times were observed with shorter pull-down and on-time associated with colder ambient temperatures. Low side pressure remained relatively the same for all ambient conditions, but high side pressure increased with increasing ambient temperature. While power also increased with ambient temperature, so did superheat, ensuring that any liquid that might escape the accumulator would evaporate prior to entering the compressor. The only time when superheat was observed to be inadequate was at the 5°C ambient condition during and shortly after the defrost period.

Visualization results showed variable amounts of bubbling and/or foaming within the compressor depending on the ambient temperature and time of cycle. Liquid levels in the accumulator varied and the greatest amount of liquid, reaching the full accumulator capacity of 60mL, was observed during defrost periods. Liquid motion was usually observed in both the suction and discharge lines, suggesting the movement of oil continuously throughout the system while the compressor was on.

In total, the accumulator does an adequate job of trapping liquid refrigerant and ensuring enough superheat to protect the compressor from liquid slugging. Oil is observed circulating throughout the system and may also become trapped in the accumulator, decreasing the overall effective volume of the accumulator for excess refrigerant liquid from the evaporator.

## **5 Experimentation without the Accumulator**

After completing baseline experimentation with the accumulator, the accumulator was removed from the test refrigerator and a new set of tests was conducted. Changes to the experimental set-up and methods are described below, followed by the experimental analysis and results.

### **5.1 Experimental Set-up**

While the same type of refrigerator was used for both experimental set-ups, the refrigeration unit was replaced following tests with the accumulator due to a system blockage and failure. Tests with the accumulator were repeated with the new unit to ensure repeatability and adequate results for later comparison. Besides the refrigeration unit as a whole, specific changes were made to the compressor and evaporator.

#### **5.1.1 Compressor**

The compressor used for experimentation with the accumulator experienced failure in an early test without the accumulator. The compressor was replaced with a back-up compressor of the same type and with the same visualization port. The sight tube, however, was removed due to problems obtaining proper air seals around the plastic tubing. The compressor visualization port was recalibrated so liquid measurements from both sets of experiments could be compared. A picture of the new compressor and new scale is shown in Figure 85 and the calibrated liquid level scale is given in Table 24.



**Figure 85: New Compressor with Modified Sight Glass Liquid Level Scale**

**Table 24: Liquid Level Scale for New Compressor**

<b>Line Number</b>	<b>Total Volume (mL)</b>
1	25
2	45
3	65
4	85
5	105
6	130
7	150
8	170
9	200
10	235
11	270
12	300

### **5.1.2 Evaporator**

The accumulator was removed from the system evaporator outlet and replaced by a straight copper pipe, as indicated by the oval in Figure 86. Slight changes were also made to the piping for the sight glass at the evaporator outlet.



**Figure 86: Accumulator Removal and Pipe Replacement**

### 5.1.3 System Sight Glasses

Other than small piping changes, no alterations were made to the position or placement of the suction, discharge, or evaporator outlet (previously called the accumulator outlet) sight glasses. A diagram of the new set-up without the accumulator depicting the appropriate changes is shown in Figure 87.

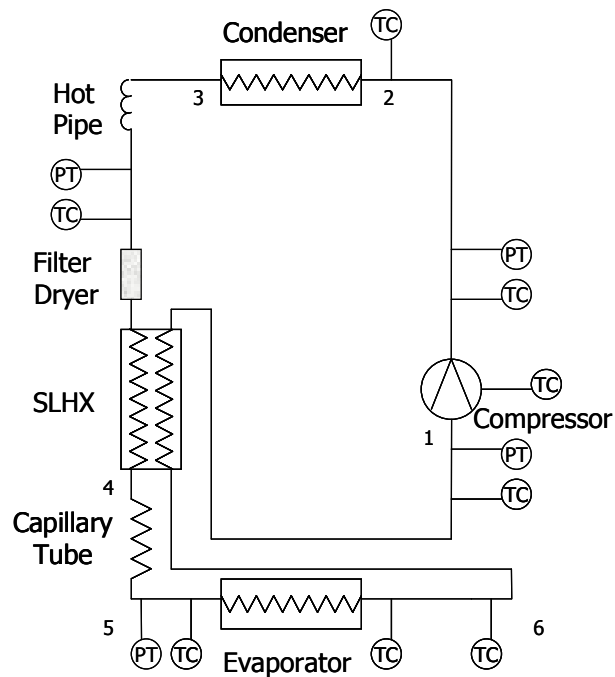


**Figure 87: System Schematic for Testing without the Accumulator**

#### **5.1.4 Refrigerant and Oil Flow Visualization**

Video cameras were again used at the compressor visualization port, suction and discharge sight glasses, and evaporator outlet sight glass for visualization during experimentation. The fourth camera for accumulator visualization was removed as it was no longer necessary.

#### **5.1.5 Experimental Measurements**

The same experimental measurements as described in section 4.1.6 were taken for experiments without the accumulator. Temperature measurements that were previously taken around the accumulator were replaced by temperature measurements on the copper pipe that replaced the accumulator in the new set-up. The same DAS and environmental chamber for ambient control were also used for experiments without the accumulator.

### **5.2 Experimental Methods**

#### **5.2.1 Experimental Procedures**

Because the 43°C ambient condition did not allow for cycling of the compressor, this condition was skipped for tests without the accumulator. Only the 5°C and 32°C ambient conditions were explored, as indicated by the experimental matrix in Table 12. Pull-down, cycling, and defrost periods were again recorded and observed for each test condition. In addition, different refrigerant charges were explored at each ambient condition in order to better understand the effects of the charge on the system without the accumulator. The charges tested are outlined in Table 25. Note that the original charge to the system with the accumulator was 52.0g of R600a.

**Table 25: Extended Experimental Matrix**

<b>Accumulator</b>	<b>Temperature [°C]</b>	<b>Refrigerant Charge [g]</b>
Without	5	44
		48
		50
		52
	32	44
		48
		50
		52

### **5.2.2 Experimental Analysis**

The same analysis method as outlined in section 4.2.2 was used for experimentation without the accumulator. Sample verification without the accumulator, however, was not attempted based on challenges experienced in testing with the accumulator.

### **5.3 Experimental Results**

A complete list of tests conducted both with and without the accumulator is shown in

Table 26 and Table 27 for the 5°C and 32°C ambient conditions, respectively. Results from tests conducted with the accumulator were included for means of comparison. Tests are listed in the order in which they were conducted. As can be seen in the tables, the initial investigation of charges without the accumulator did not produce results similar to those that were found with the accumulator. Consequently, a lower charge of 44.0g was explored. This system refrigerant charge proved to provide better results that matched previous results obtained in experimentation with the accumulator within 2-6%, depending on the ambient condition.

As can be seen in both tables, the timing of pull-down and cycling periods varied depending on the refrigerant charge as well as on the individual test. Tests were conducted for variable amounts of time and the system was never turned off at the same point, leading to differences in the oil and refrigerant distribution within the system for the start of each test. This difference consequently had an effect on the time for the system to obtain pull-down and continue to distribute refrigerant in subsequent tests.

**Table 26: Comparison of Test Results for Tests completed with and without the Accumulator at the 5°C Ambient Condition**

Test No.	Acc.	Average Relative Humidity	Approximate Refrigerant Charge	Time to Pull-down	Cycling Comp. On Time	Cycling Comp. Off Time	Time before 1 <sup>st</sup> Defrost	Length of Defrost
1	With	70.3%	51.0 g	50.0 min.	7.0 min.	23.4 min.	N/A	N/A
2	With	64.0%	51.0 g	48.1 min.	7.6 min.	24.0 min.	N/A	N/A
3	With	69.3%	51.0 g	48.8 min.	8.0 min.	24.0 min.	807.5 min.	15.7 min.
4	With	69.1%	51.0 g	N/A	7.6 min.	24.5 min.	N/A	19.4 min.
5	With	69.4%	52.0 g	42.3 min.	6.9 min.	24.2 min.	N/A	N/A
6	With	69.4%	52.0 g	48.2 min.	7.4 min.	24.7 min.	N/A	N/A
1	Without	78.2%	48.0 g	52.2 min.	5.1 min.	23.2 min.	N/A	N/A
2	Without	76.5%	48.0 g	53.2 min.	5.2 min.	23.6 min.	1099.1 min.	16.3 min.
3	Without	76.1%	50.2 g	89.3 min.	7.1 min.	23.7 min.	751.6 min.	19.6 min.
4	Without	76.3%	50.2 g	89.3 min.	7.2 min.	22.9 min.	719.0 min.	18.8 min.
5	Without	75.0%	52.0 g	91.8 min.	7.2 min.	22.3 min.	728.7 min.	16.9 min.
6	Without	75.3%	52.0 g	90.2 min.	7.1 min.	21.9 min.	721.2 min.	17.3 min.
7	Without	75.8%	44.0 g	49.5 min.	5.4 min.	22.6 min.	N/A	N/A
8	Without	77.0%	44.0 g	50.5 min.	5.4 min.	22.7 min.	N/A	N/A
9	Without	76.5%	44.0 g	49.2 min.	5.3 min.	22.7 min.	Manual	Manual

**Table 27: Comparison of Test Results for Tests completed with and without the Accumulator at the 32°C Ambient Condition**

Test No.	Acc.	Average Relative Humidity	Approximate Refrigerant Charge	Time to Pull-down	Cycling Comp. On Time	Cycling Comp. Off Time	Time before 1 <sup>st</sup> Defrost	Length of Defrost
1	With	71.9%	52.8 g	335.6 min.	39.4 min.	14.3 min.	243.6 min.	16.6 min.
2	With	68.9%	52.8 g	333.5 min.	39.2 min.	15.3 min.	243.7 min.	16.7 min.
3	With	67.8%	49.9 g	337.7 min.	41.2 min.	15.2 min.	243.8 min.	17.0 min.
1	Without	74.8%	48.0 g	360.1 min.	42.2 min.	13.9 min.	243.8 min.	15.7 min.
2	Without	75.8%	48.0 g	330.8 min.	33.5 min.	14.2 min.	243.8 min.	17.0 min.
3	Without	73.7%	50.2 g	377.3 min.	47.7 min.	14.3 min.	243.7 min.	16.8 min.
4	Without	74.4%	50.2 g	375.5 min.	40.6 min.	14.2 min.	243.8 min.	16.9 min.
5	Without	75.5%	50.2 g	369.8 min.	37.2 min.	14.0 min.	243.8 min.	16.2 min.
6	Without	74.3%	52.0 g	382.8 min.	51.7 min.	14.1 min.	243.7 min.	18.2 min.
7	Without	74.2%	52.0 g	384.1 min.	49.3 min.	14.1 min.	243.7 min.	17.3 min.
8	Without	73.8%	44.0 g	342.3 min.	34.9 min.	14.1 min.	243.8 min.	16.4 min.
9	Without	75.2%	44.0 g	377.4 min.	30.7 min.	13.7 min.	243.7 min.	24.2 min.

Averages of tests completed with the same refrigerant charge are shown in Table 28 and Table 29, providing for an easier means of comparison between conditions with and without the accumulator.

**Table 28: Average Comparison of Test Results for Tests completed with and without the Accumulator at 5°C**

Acc.	Approximate Refrigerant Charge	Time to Pull-down	Cycling Comp. On Time	Cycling Comp. Off Time	Time before 1 <sup>st</sup> Defrost	Length of Defrost
With	51.0 g	49.0 min.	7.6 min.	24.0 min.	807.5 min.	17.6
With	52.0 g	45.3 min.	7.2 min.	24.5 min.	N/A	N/A
Without	44.0 g	49.7 min.	5.3 min.	22.7 min.	N/A	N/A
Without	48.0 g	52.7 min.	5.2 min.	23.4 min.	1099.1 min.	16.3 min.
Without	50.2 g	89.3 min.	7.2 min.	23.3 min.	735.3 min.	19.2 min.
Without	52.0 g	91.0 min.	7.2 min.	22.1 min.	725.0 min.	17.1 min.

**Table 29: Average Comparison of Test Results for Tests completed with and without the Accumulator at 32°C**

Acc.	Approximate Refrigerant Charge	Time to Pull-down	Cycling Comp. On Time	Cycling Comp. Off Time	Time before 1 <sup>st</sup> Defrost	Length of Defrost
With	52.8 g	334.6 min.	39.3 min.	14.8 min.	243.7 min.	16.7 min.
With	49.9 g	337.7 min.	41.2 min.	15.2 min.	243.8 min.	17.0 min.
Without	44.0 g	359.9 min.	32.8 min.	13.9 min.	243.8 min.	20.3 min.
Without	48.0 g	345.5 min.	37.9 min.	14.1 min.	243.8 min.	16.5 min.
Without	50.2 g	374.2 min.	41.8 min.	14.2 min.	243.8 min.	16.6 min.
Without	52.0 g	383.5 min.	50.5 min.	14.1 min.	243.7 min.	17.8 min.

### 5.3.1 Data Results and Trends

The following sections contain data for a test with the accumulator, a test without the accumulator with a 44.0g system refrigerant charge, and a test without the accumulator with a 48.0g system refrigerant charge. Results with the accumulator are included to provide a basis for comparison. Results for tests conducted with larger refrigerant charges, including 50.2g and 52.0g, without the accumulator were not included to allow for better readability of the graphs. In general, these refrigerant charges produced results that followed trends similar to those shown between the results for the 44.0g and 48.0g experiments.

#### 5.3.1.1 Pressure Results

Suction and discharge pressure results for the 5°C ambient condition are given in Figure 88. As can be seen in the graph, results without the accumulator at a 44.0g refrigerant charge provided the greatest similarity with results from experiments with the accumulator. Suction pressure for the 44g test was approximately 5.4% higher than the suction pressure for tests with the accumulator based on values when the compressor was

on during a cycling period. Suction pressure for the 48g test was 10% higher than that with the accumulator. Higher charges without the accumulator also produced higher discharge pressure by as much as 7% for the 48g test. These trends also occurred at the 32°C condition, but to a greater extent, as shown in Figure 89. Here the increase in suction pressure was as much as 20% and the increase in discharge pressure was as much as 18% during compressor on-time for the 48g test compared to baseline tests with the accumulator.

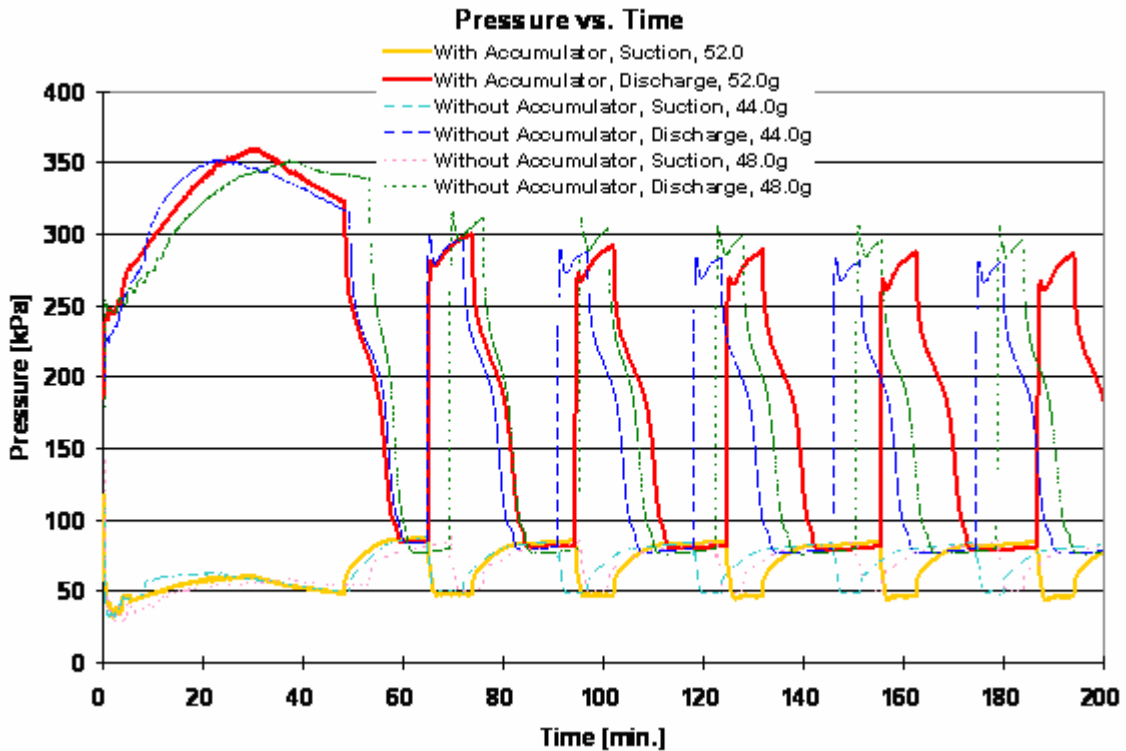


**Figure 88: Suction and Discharge Pressures for Tests with and without the Accumulator at Various Charges at the 5°C Ambient Condition**

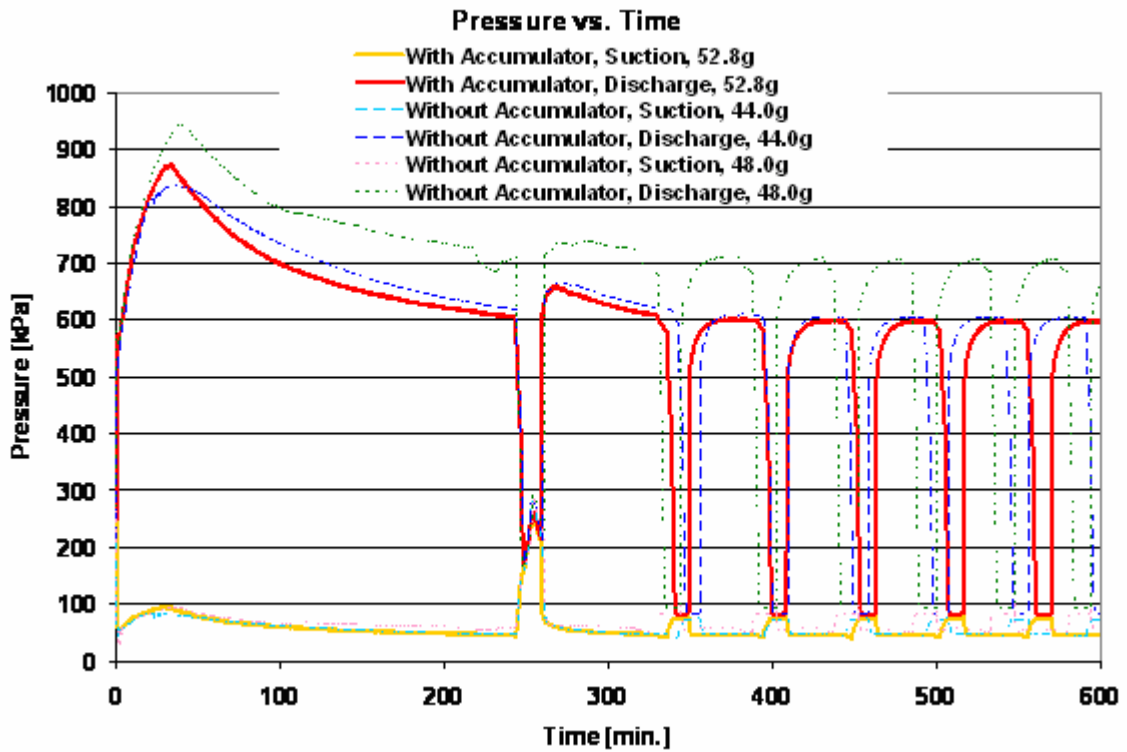


**Figure 89: Suction and Discharge Pressures for Tests with and without the Accumulator at Various Charges at the 32°C Ambient Condition**

**Table 30: Pressure Ratios for Conditions without the Accumulator**

Ambient Condition	Charge	Pressure Ratio
5°C	44 g	5.2
	48 g	6.4
	52 g	7.3
32°C	44 g	12.6
	48 g	12.3
	52 g	12.5

The corresponding pressure ratios for both ambient conditions without the accumulator are given in Table 30. Note that the 44.0g charge at the 5°C ambient condition produced a pressure ratio of 5.2, compared to 5.6 with the accumulator. The 44.0g charge also produced the best results at the 32°C ambient condition with a

matching 12.6 pressure ratio with and without the accumulator. Pressure ratios for different refrigerant charges at the 32°C condition varied slightly as discharge pressure saw large increases and suction pressure saw variable amounts of increase with increasing charge.

Similarities between results with and without the accumulator at various charges are also depicted in Figure 90 and Figure 91. These figures show a sample vapor compression cycle on a P-h diagram for each test case for when the system is on and the compressor is running. Average values during on-time were used to estimate point temperatures, pressures, and enthalpies and are given in Table 31 and Table 32 for the 5°C and 32°C ambient condition, respectively. Note that at the 5°C ambient condition, the ambient temperature is at the low range for the accuracy of the pressure transducers. Averages for the high and low side pressures, specifically for the 48g and 52g tests, were used were appropriate to better represent the cycles and provide a means for comparison.

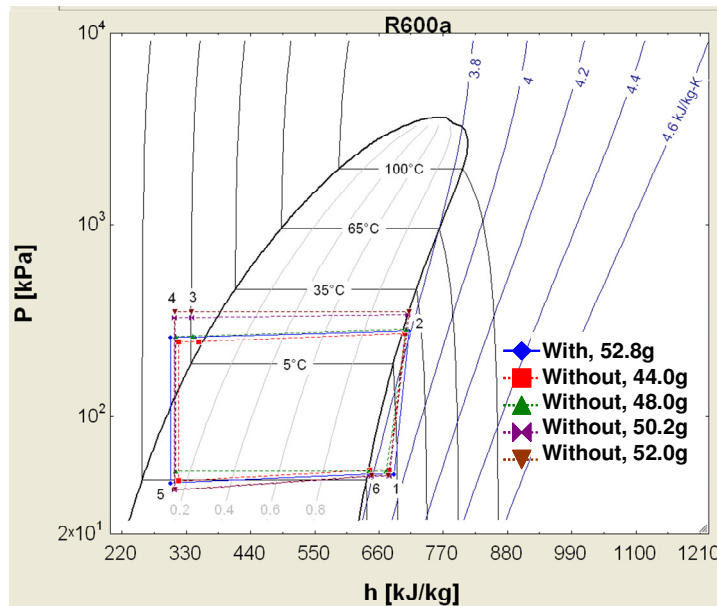


**Figure 90: P-h Diagram for Tests with and without the Accumulator at Various Charges at the 5°C Ambient Condition**

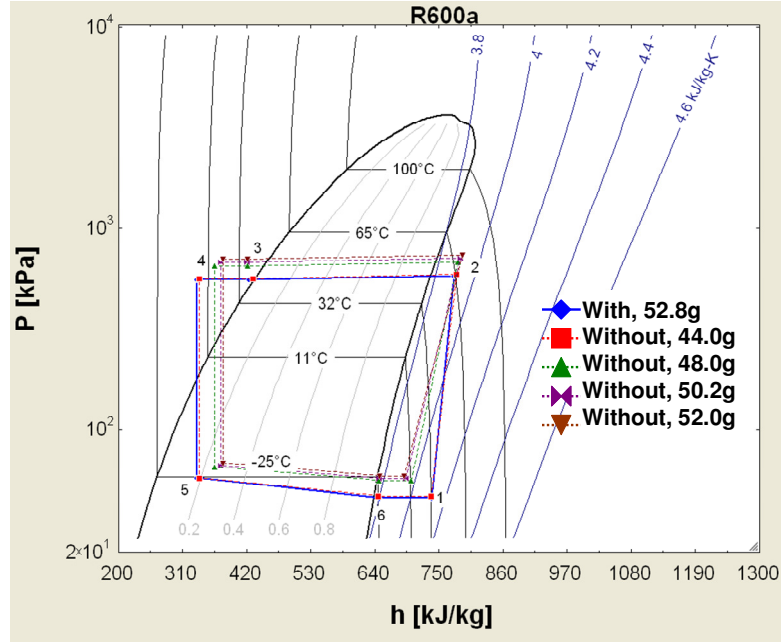


**Figure 91: P-h Diagram for Tests with and without the Accumulator at Various Charges at the 32°C Ambient Condition**

**Table 31: Data Comparison with and without Accumulator for Compressor On-Time during Cycling at the 5°C Ambient Condition**

	With Acc., 51.0g, Test 1	Without Acc., 44.0g, Test 9	Without Acc., 48.0g, Test 2	Without Acc., 50.2g, Test 3	Without Acc., 52.0g, Test 6
Suction Pressure [kPa]	49.7	52.4 (+5.4%)	54.7 (+10%)	48.7	49.2
Discharge Pressure [kPa]	279.9	270.3 (-3.4%)	285.6 (+2%)	339.7	357.6
Condenser Outlet Pressure [kPa]	259.3	244.2 (-5.8%)	261.1 (+7%)	328.3	346.7
Evaporator Inlet Pressure [kPa]	44.9	46.1 (+2.7%)	48.3 (+7.6%)	41.4	41.9
Suction Temperature [°C]	1.7	-3.5	-6.9	-4.3	-4.8
Inside Compressor Temperature [°C]	20.4	9.3	8.9	10.0	10.0
Discharge Temperature [°C]	23.4	19.1	21.2	24.2	25.5
Condenser Outlet Temperature [°C]	8.1	10.1	6.5	5.5	5.4
Evaporator Inlet Temperature [°C]	-30.9	29.1	-29.0	-32.9	-33.3
Evaporator Outlet Temperature [°C]	-26.5	25.8	-26.6	-23.9	-23.7
Compressor Solubility [mass %]	2.5	6.0	6.8	5.4	5.3
Degrees of Superheat [K]	30.3	24.0	19.8	25.2	24.5
Time of Negative Superheat [sec.]	0	31	49	48	49
Power Consumption [W]	98.5	99.0 (+.5%)	102.9 (+4.4%)	97.1	101.2

**Table 32: Data Comparison with and without Accumulator for Compressor On-Time during Cycling at the 32°C Ambient Condition**

	With Acc., 52.8g, Test 1	Without Acc., 44.0g, Test 8	Without Acc., 48.0g, Test 2	Without Acc., 50.2g, Test 4	Without Acc., 52.0g, Test 6
Suction Pressure [kPa]	46.1	47.0 (+2.0%)	55.7 (+20.8%)	57.5	58.9
Discharge Pressure [kPa]	581.3	591.9 (+1.8%)	684.7 (+17.8%)	715.9	737.0
Condenser Outlet Pressure [kPa]	556.3	564.7 (+1.5%)	655.2 (+17.8%)	684.7	704.8
Evaporator Inlet Pressure [kPa]	57.8	57.5 (-0.5%)	65.1 (+12.6%)	66.7	68.0
Suction Temperature [°C]	32.9	32.1	11.9	6.1	4.6
Inside Compressor Temperature [°C]	65.3	45.8	47.2	47.1	47.9
Discharge Temperature [°C]	63.9	66.0	68.8	71.2	73.4
Condenser Outlet Temperature [°C]	39.0	41.3	37.5	37.3	37.8
Evaporator Inlet Temperature [°C]	- 27.2	-26.3	- 28.9	- 29.2	- 28.9
Evaporator Outlet Temperature [°C]	- 23.4	-25.3	- 23.9	- 23.4	- 23.1
Compressor Solubility [mass %]	0.2	0.5	0.6	0.6	0.6
Degrees of Superheat [K]	63.1	61.9	37.9	31.4	29.3
Time of Negative Superheat [sec.]	0	0	8	20	29
Power Consumption [W]	109.6	109.8 (+0.2%)	122.5 (+11.8%)	125.3	127.1

### 5.3.1.2 Temperature Results

Suction and inside compressor temperatures for the 5°C ambient condition are shown in Figure 92. Compared to cases with the accumulator, inside compressor temperature without the accumulator was lower, 10°C compared to 15-25°C, and experienced less fluctuation throughout the cycling period. The decrease in temperature may be due to colder liquid and vapor returning directly from the evaporator where before, cold liquid was captured in the accumulator and warmer vapor returned to the compressor. Suction temperatures during compressor off-time did not experience a significant change between charges or between conditions with or without the accumulator. A difference in this temperature is observed as the compressor is turned on, however, with a large decrease in suction temperature for cases without the accumulator.

As will be seen in later sections, less superheat is available to the system for cases without the accumulator and as the compressor is turned back on, cold liquid (and vapor) is flashed to the compressor, producing this sharp decrease in temperature.

Similar results are observed for the 32°C ambient condition, as shown in Figure 93. Again there are differences in the suction temperature with a more pronounced change for higher charges. Higher charges without the accumulator produced lower suction temperatures during on- and off-times during cycling.

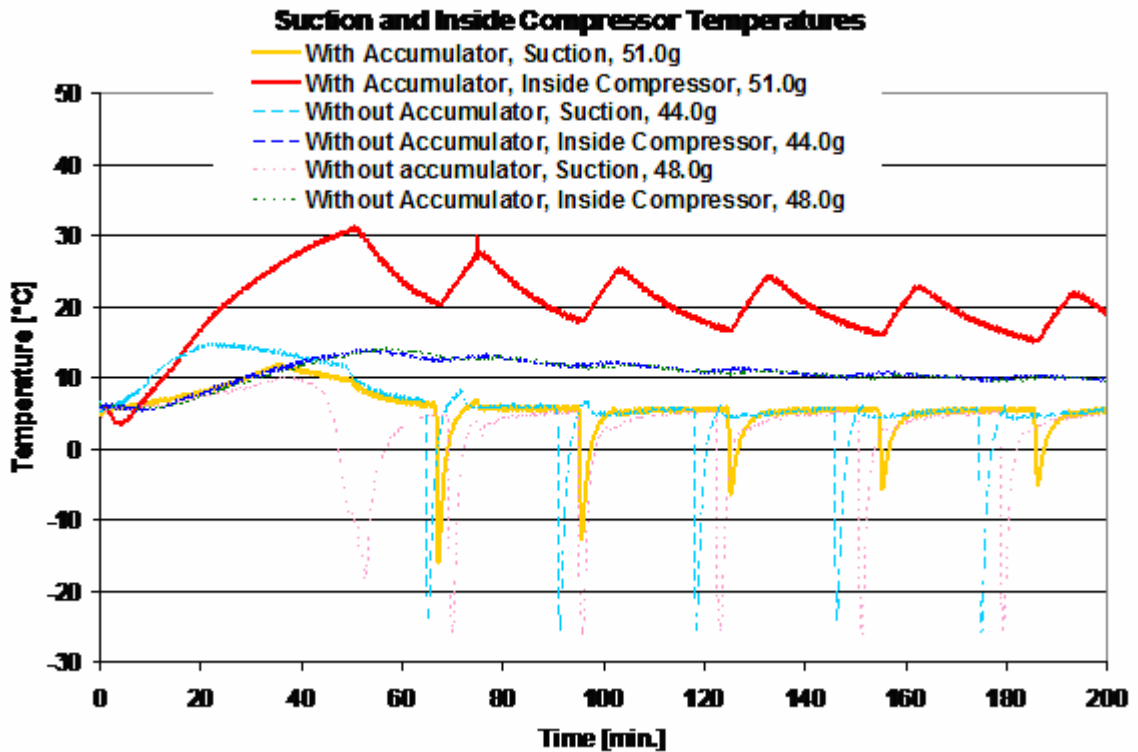


**Figure 92: Suction and Inside Compressor Temperatures for Tests with and without the Accumulator at Various Charges at the 5°C Ambient Condition**

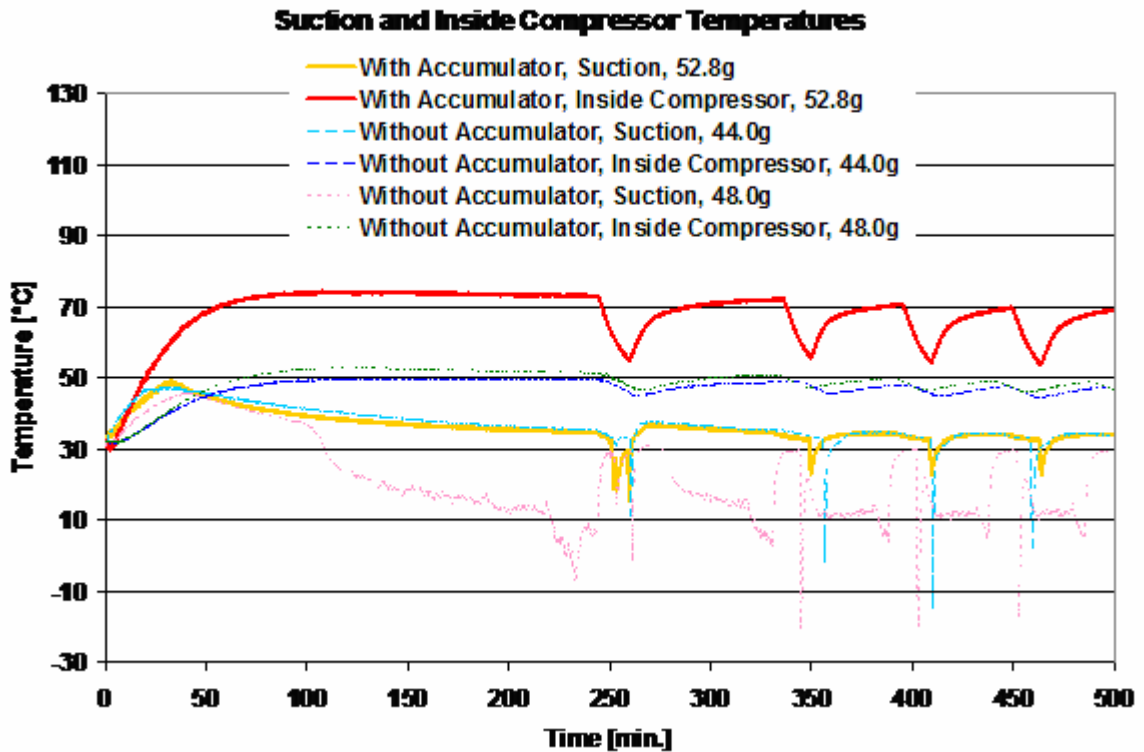


**Figure 93: Suction and Inside Compressor Temperatures for Tests with and without the Accumulator at Various Charges at the 32°C Ambient Condition**

Evaporator inlet and outlet temperatures for the 5°C and 32°C ambient conditions are given in Figure 94 and Figure 95, respectively. Little difference is observed between all tests. Evaporator inlet temperatures for all 5°C ambient tests were between -29°C and -33°C; outlet temperatures ranged between -23°C and -27°C. The difference between the inlet and outlet temperatures was generally between two and four degrees, though tests with a higher refrigerant charge saw differences between evaporator inlet and outlet temperatures by as much as ten degrees. Evaporator inlet temperatures for the 32°C condition ranged between -27°C and -29°C and evaporator outlet temperatures ranged between -23°C and -25°C. The difference between these temperatures were often low,

but were as high as six degrees for tests without the accumulator and more refrigerant charge. What is interesting to note is that for the 5°C ambient condition, the evaporator outlet temperature matches the suction temperature when the compressor is first turned on. This observation suggests that as the compressor is turned on during a cycling period, refrigerant and oil at cold temperatures are flashed to the compressor. Such trends help to support superheat and suction line visualization results outlined in sections 5.3.1.5 and 5.3.2.3, respectively.

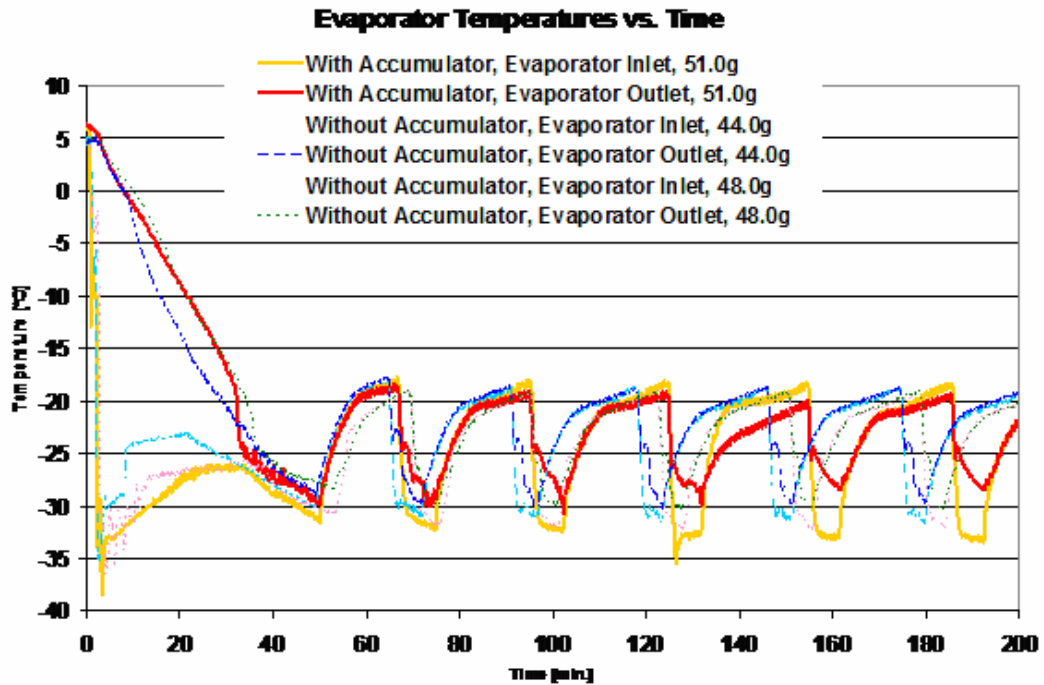


**Figure 94: Evaporator Temperatures for Tests with and without the Accumulator at Various Charges at the 5°C Ambient condition**

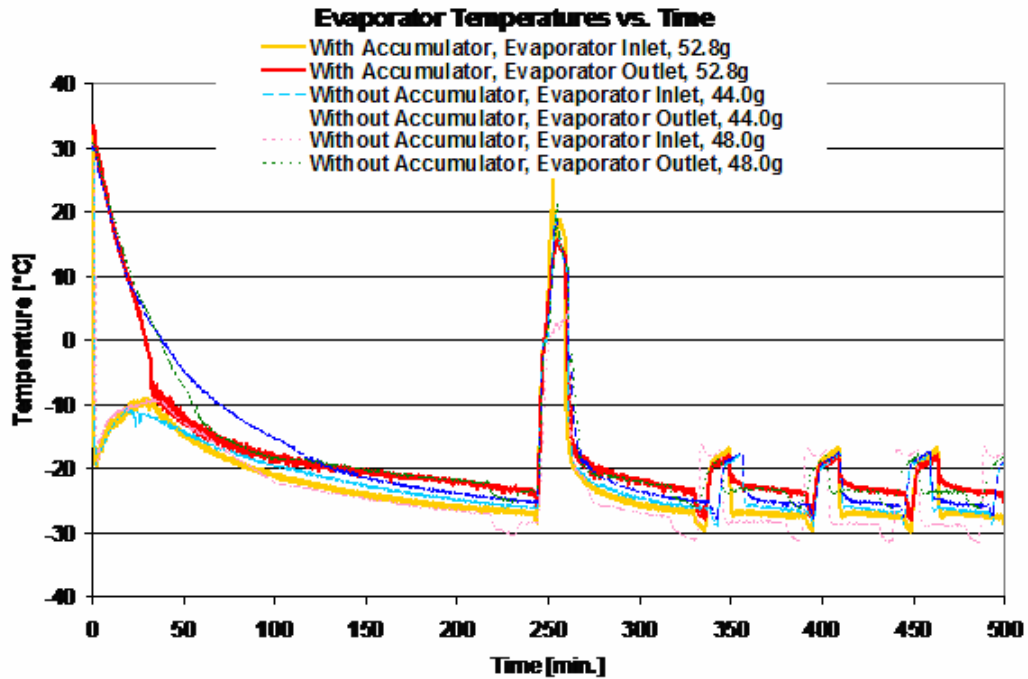


**Figure 95: Evaporator Temperatures for Tests with and without the Accumulator at Various Charges at the 32°C Ambient condition**

### 5.3.1.3 Power Results

In general, the total power measured for the system increased with increasing refrigerant charge for tests without the accumulator, as seen for both the 5°C and 32°C ambient conditions in Figure 96 and Figure 97, respectively. Testing without the accumulator at a charge of 44.0g produced a power within 0.5% of the power achieved with the accumulator for both ambient conditions. The difference in pull-down and cycling times can also be seen in these graphs. Higher charge without the accumulator produced longer pull-down times and varying cycling times. With more charge in the system, more refrigerant was available in the free volume and did not absorb with the oil prior to start-up, increasing the starting pressure and consequent power required from the motor. Similar trends in absorption patterns are true for the cycling period as well.

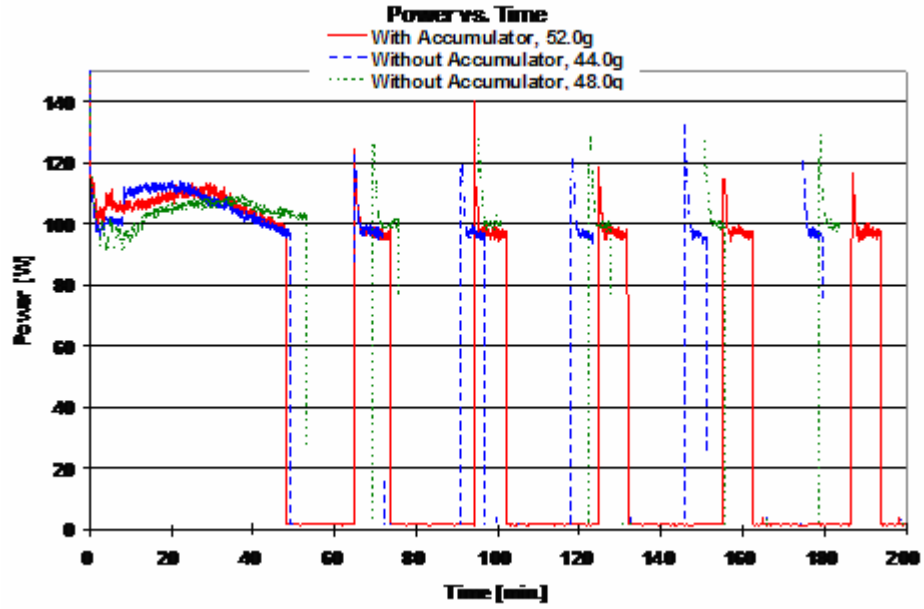


Figure 96: Power Results for Tests with and without the Accumulator at Various Charges at the 5°C Ambient Condition

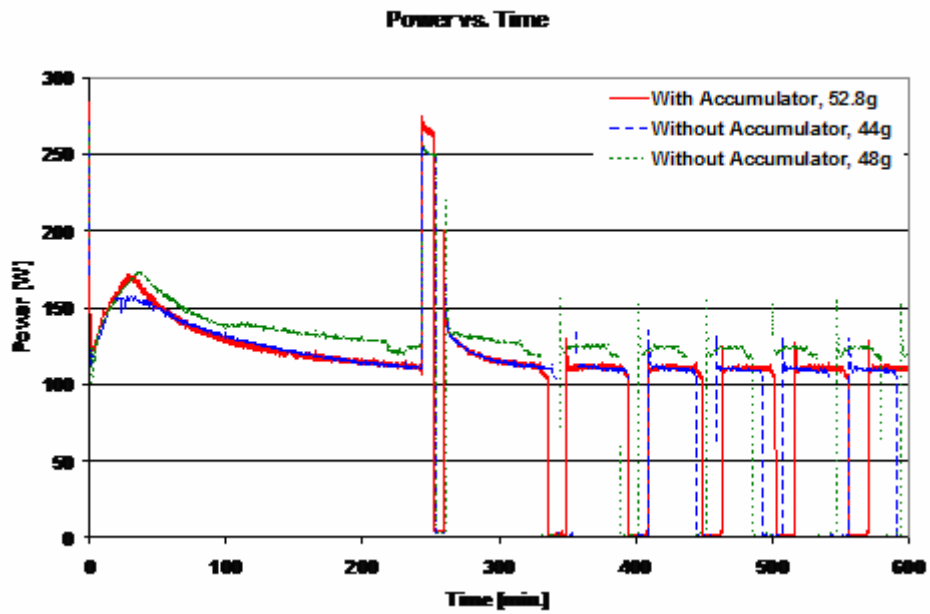


Figure 97: Power Results for Tests with and without the Accumulator at Various Charges at the 32°C Ambient Condition

#### 5.3.1.4 Specific Capacity Results

Evaporator specific capacity for the 5°C ambient condition, shown in Figure 98, did not show a considerable difference between refrigerant charges or between cases with and without the accumulator. This is due to little changes in high and low side pressures for this ambient condition. Evaporator capacity for the 32°C ambient condition, however, shown in Figure 99, shows a decrease in capacity for higher refrigerant charges without the accumulator. As shown above, higher refrigerant charges increase the high and low side pressure by as much as 20% for the 48g test, impacting the capacity available at that condition.

Like the evaporator results, condenser specific capacity at the 5°C ambient condition did not show much difference between cases with or without the accumulator, as seen in Figure 100. Slight increases in condenser capacity are noticeable for higher refrigerant charges without the accumulator. Again, these differences are due to the small changes in discharge pressure at the lower ambient condition.

Condenser capacity results for the 32°C ambient condition are shown in Figure 101. Again, little difference is observed between cases, though there is a slight increase for higher charges without the accumulator due to the increase in high side pressure.

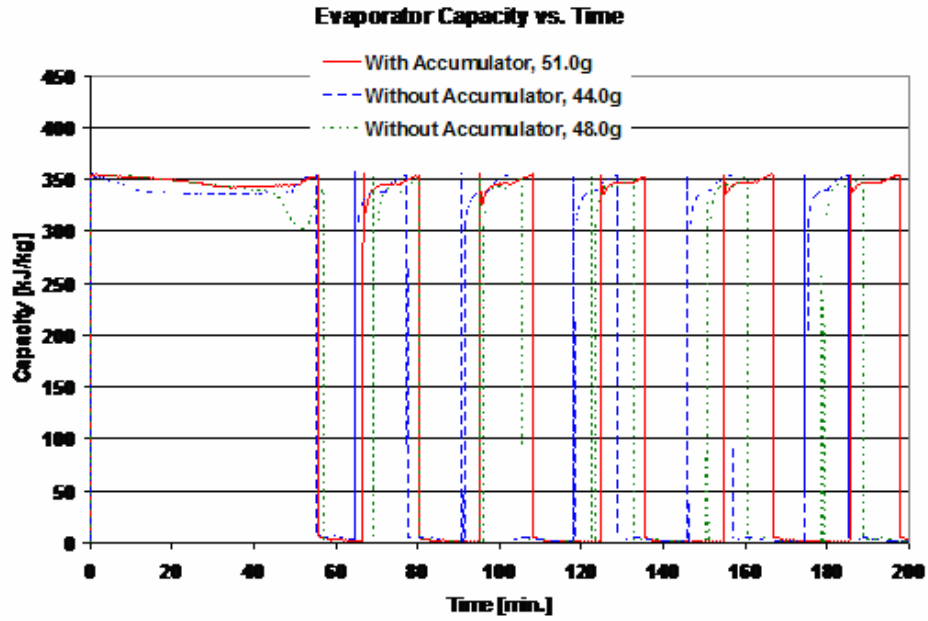


Figure 98: Evaporator Capacity for Tests with and without the Accumulator at Various Charges at the 5°C Ambient Condition

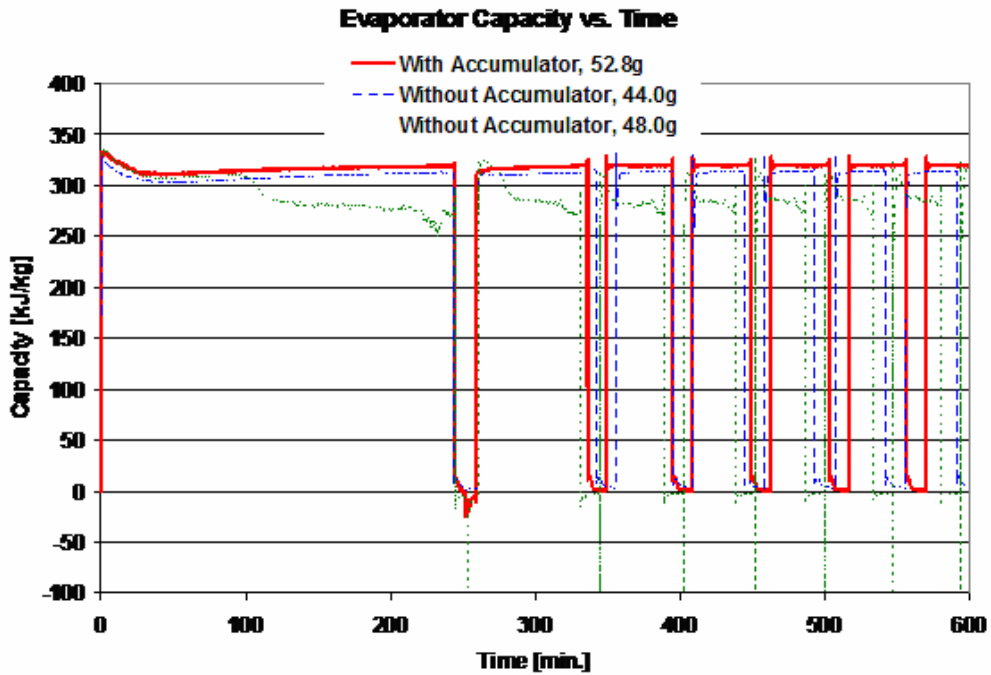


Figure 99: Evaporator Capacity for Tests with and without the Accumulator at Various Charges at the 32°C Ambient Condition

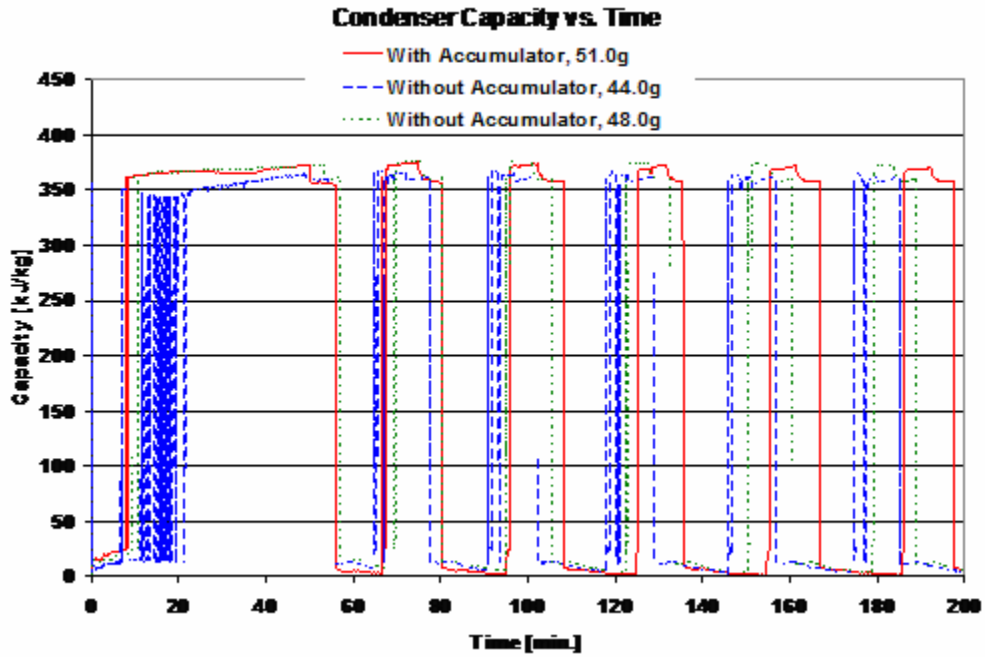


Figure 100: Condenser Capacity for Tests with and without Accumulator at Various Charges at the 5°C Ambient Condition

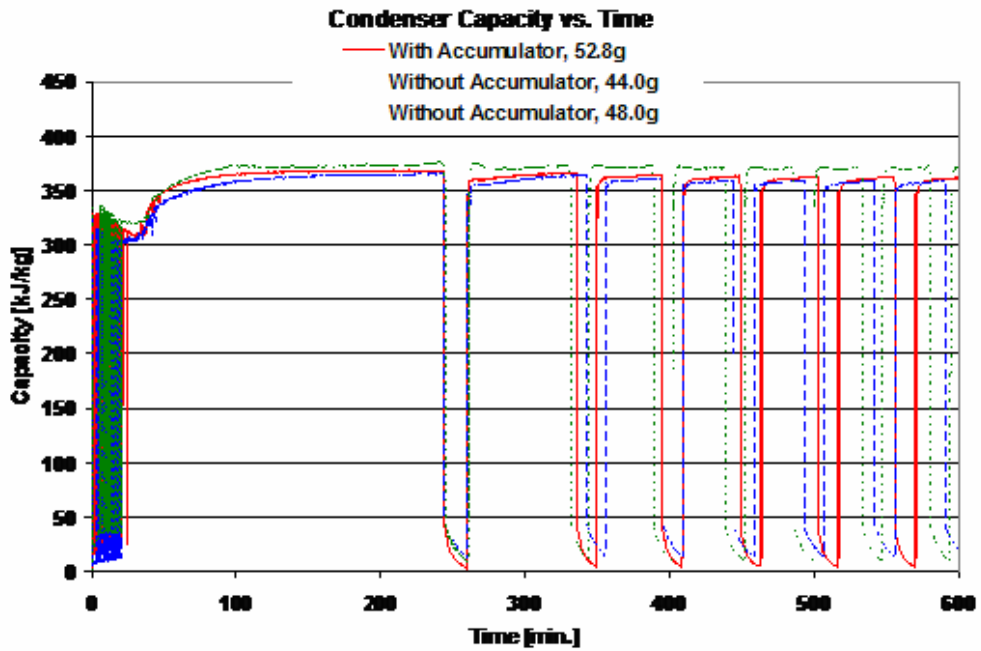


Figure 101: Condenser Capacity for Tests with and without Accumulator at Various Charges at the 32°C Ambient Condition

### 5.3.1.5 Total Superheat Results

The most important difference between results with and without the accumulator is the amount of superheat available in each condition. As can be seen in Figure 102 and Figure 103, less superheat in general is available for cases without the accumulator, especially for conditions with a larger charge. While superheat is sometimes comparable during compressor on-periods, the most drastic difference is noticed during cycling when the compressor is first turned on. In both ambient conditions, a sharp decrease in superheat is experienced at this time, allowing for possible liquid refrigerant to return to the compressor. Periods of low or negative superheat do not last more than 30 seconds or 1 minute. The duration of this lack in superheat is longer and more critical at the 5°C ambient condition as less excess heat is available at the lower ambient temperature. When the compressor is on during cycling, there are 24K of superheat available without the accumulator with a 44g charge compared to 30K of superheat available with the accumulator at the 5°C ambient condition. At the 32°C ambient condition, 62K of superheat are available without the accumulator with a 44g charge compared to 63K of superheat with the accumulator. Higher charges result in lower amounts of superheat in both ambient conditions. With a 48g charge, the degrees of superheat drop to 20K at the 5°C condition and 40K at the 32°C condition.

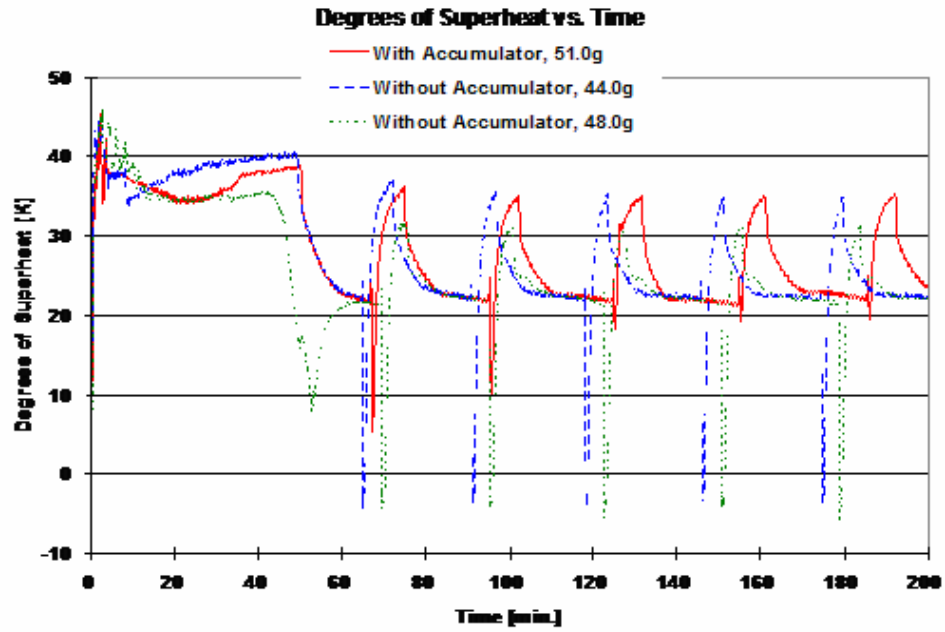


Figure 102: Superheat Results for Tests with and without the Accumulator for Various Charges at the 5°C Ambient Condition

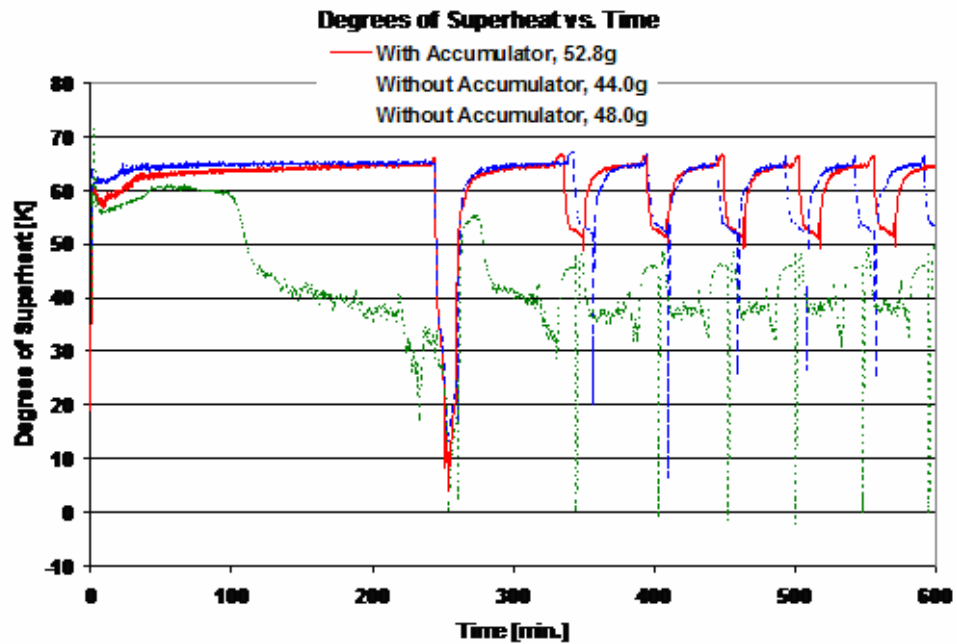
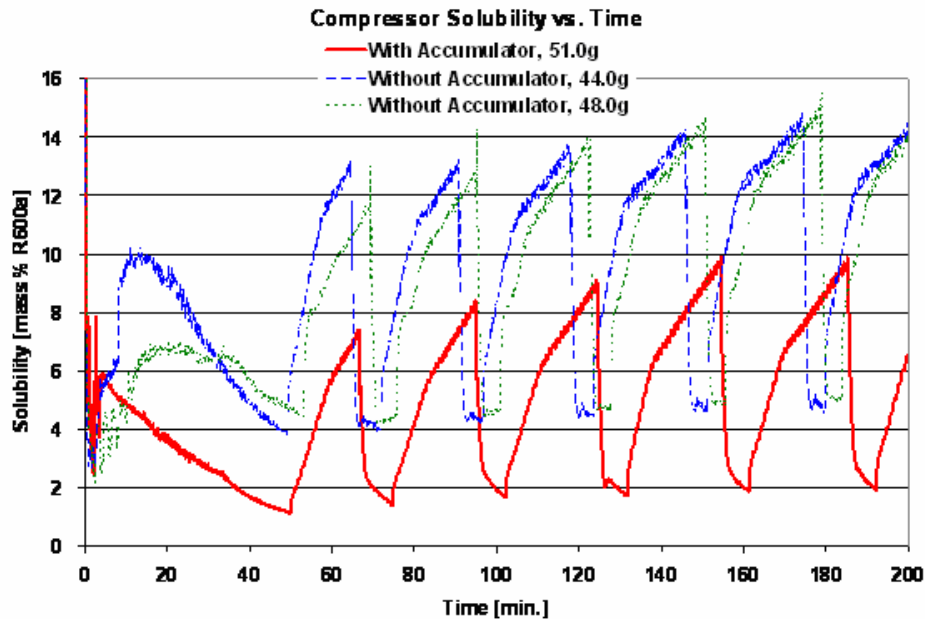


Figure 103: Superheat Results for Tests with and without the Accumulator for Various Charges at the 32°C Ambient Condition

### 5.3.1.6 Solubility Results

Regardless of charge, solubility in the compressor for tests without the accumulator is always higher than that for cases with the accumulator. While pressures are similar in both experimental set-ups, inside compressor temperatures are generally lower without the accumulator, increasing the solubility. Differences are most drastic at the 5°C ambient condition as solubility without the accumulator is twice as high as it was for cases with the accumulator; compare 2% solubility with the accumulator when the compressor is on versus 4 - 4.5% solubility without the accumulator as seen in Figure 104. Compressor solubility does not see as significant a rise without the accumulator when the compressor is on for the 32°C ambient condition, as shown in Figure 105.



**Figure 104: Compressor Solubility for Tests with and without the Accumulator for Various Charges at the 5°C Ambient Condition**

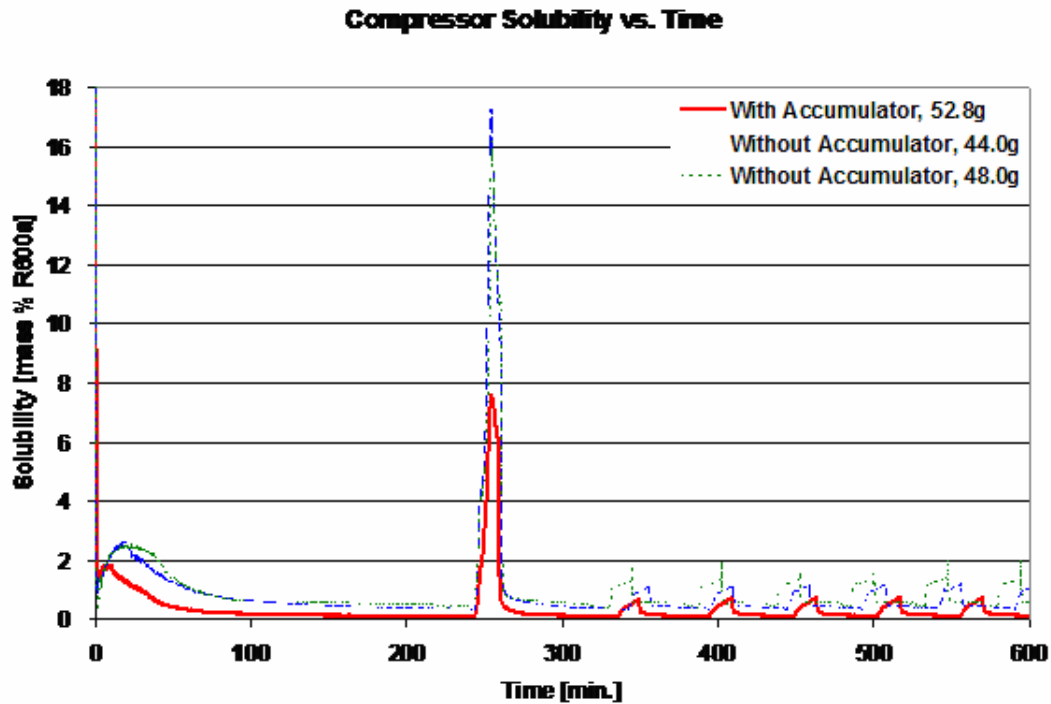


**Figure 105: Compressor Solubility for Tests with and without the Accumulator for Various Charges at the 32°C Ambient Condition**

### 5.3.2 Visualization Results and Trends without the Accumulator

As with the first set of experiments with the accumulator, video results for testing without the accumulator were recorded for appropriate points within the system including the compressor shell, the evaporator outlet, and the suction and discharge lines. Observed results are noted in the following sections.

#### 5.3.2.1 Compressor Visualization Results

##### 5.3.2.1.1 Start-up and Pull-down

Trends in the compressor were similar to those observed with the accumulator. Some bubbling and liquid fluctuation was observed at the 5°C ambient condition and a

larger amount of bubbling and foaming was observed at the 32°C ambient condition when the system was started. Starting liquid levels for both ambient conditions without the accumulator were higher (6-11% for 5°C and 6-25% for 32°C) than starting levels for tests with the accumulator. This increase in liquid volume is expected as oil and liquid refrigerant can no longer be trapped in the accumulator during off-times. More liquid thus remains within the compressor.

### ***5.3.2.1.2 Cycling***

As observed during the start-up and pull-down periods, liquid levels in the compressor for tests without the accumulator were higher than previous tests with the accumulator during the cycling periods. When the compressor was on, liquid levels fluctuated between 105-120mL at the 5°C condition compared to the previous 100mL observed before, a 5 - 15% increase from cases with the accumulator. When the compressor was off, liquid levels remained calm between 120-130mL, depending on the test, for the 5°C ambient condition. In tests with the accumulator, this rest level was generally around 115mL, making the total increase in liquid volume in the compressor without the accumulator 4 – 13% higher than the volume previously observed with the accumulator.

The 32°C condition showed slightly different trends. The liquid surface level during on-time was observed to be lower than seen in cases with the accumulator; 95-105mL as compared to previous 115-120mL. More bubbles, however, were observed on top of the liquid surface level, bringing the total level up to the 120-130mL calibration mark. This increase in bubbling may be accounted for by the increase in solubility observed in the compressor without the accumulator. With a higher solubility, more

refrigerant would be able to dissolve in the oil during off periods. When the compressor is turned back on, more bubbles are observed as more refrigerant is released from the lubricant oil. Similar bubbling, though not as severe, is observed during the initial start-up for the same reason. Liquid levels in the compressor with and without the accumulator for the 32°C ambient condition during off periods were comparable around 130mL.

#### ***5.3.2.1.3 Defrost***

Again, liquid levels in the compressor for tests without the accumulator at the 5°C ambient condition were higher than those cases with the accumulator. During defrost stages, liquid levels rose from 120-130mL to 130-145mL, depending on the specific test and/or refrigerant charge. Previous cases with the accumulator only experienced level rise to 120-130mL. At the end of the defrost period, bubbling was observed similar to the bubbling that occurs during the initial start of the system.

For the 32°C condition, liquid level for tests without the accumulator is comparable to results with the accumulator and is even a little lower during the defrost period. Again, lots of bubbling and foaming are observed when the compressor is started after defrost.

A summary of the observed liquid levels in the compressor during each period at the 5°C and 32°C ambient condition for tests without the accumulator is given in Table 33.

**Table 33: Compressor Liquid Level Results for Each Ambient Condition for Testing  
without the Accumulator**

<b>Ambient Condition</b>	<b>Start-up/Pull-down</b>	<b>Cycling</b>	<b>Maximum Level during Defrost</b>
5°C	170-200mL (start) 105mL (pull-down)	105-120mL (on) 120-130mL (off)	130-145mL
32°C	170-200mL (start) 85-105mL with bubbles up to the 130-150mL mark (pull-down)	95-105 with bubble layer up to 120- 130mL mark (on) 120-130mL (off)	130mL

### 5.3.2.2 Evaporator Outlet Visualization Results

Evaporator outlet results for tests without the accumulator are comparable to accumulator outlet results from previous tests with the accumulator. The position of this sight glass was maintained during both sets of tests. Only the name of the position was changed as the second set of testing no longer included the accumulator.

#### 5.3.2.2.1 *Start-up and Pull-down*

The same start-up and pull-down trends were observed for tests with and without the accumulator at both ambient conditions. At the 5°C ambient condition, a small amount of liquid is observed sitting in the bottom of the sight glass and some bubbling and liquid motion is observed in the sight glass as the system is started. No motion was noted in the 32°C condition at start-up. More motion and bubbling was observed in the glass for both ambient conditions as the pull-down period progressed. The amount of bubbling and motion observed towards the beginning of the pull-down is expected to depend on the starting position of the oil and refrigerant distributed throughout the

system. As tests were not always stopped at equivalent times, oil and refrigerant distribution at start-up varied among tests, affecting initial video observations.

#### ***5.3.2.2.2 Cycling***

Again, cycling trends were very similar for tests with and without the accumulator for both ambient conditions. When the compressor is on, fluctuations and fluid movement are observable in the evaporator outlet sight glass. Lots of liquid and bubbles are observed when the compressor is first turned on after an off-period as refrigerant boils out of any available oil, and following, the liquid motion settles into the usual fluctuations. Liquid bubbling and popping is periodically observed during the off-period for both ambient conditions with and without the accumulator as refrigerant evaporates with warming temperatures in the evaporator.

#### ***5.3.2.2.3 Defrost***

Poor visualization generally plagued the defrost period, though some trends were able to be observed. At the 5°C ambient condition, lots of liquid motion and violent liquid surging were observed through the evaporator outlet as the defrost period began. Visualization then prevented observation of any further trends until cycling had resumed. Similar liquid motion and surging was observed for the 32°C condition and lots of liquid was also observed after the defrost as the compressor was turned back on. These results are consistent with observations from tests with the accumulator.

### 5.3.2.3 Suction and Discharge Line Visualization Results

#### ***5.3.2.3.1 Start-up and Pull-down***

For cases with and without the accumulator at both ambient conditions, liquid is observed through both the suction and discharge sight glasses as the system is turned on. In some cases, such as tests without the accumulator at 32°C, a surge of liquid is observed in both lines which then settles into a lower level of liquid motion along the bottom of the sight glass. In all cases, liquid motion within both the suction and discharge lines is minimal and appears to be mostly oil as evidenced by the observation of the dye color in the compressor oil.

#### ***5.3.2.3.2 Cycling***

Observations at the suction and discharge sight glasses during cycling show one of the most noticeable changes from prior testing with the accumulator. Without the accumulator, surges of liquid are observed for several seconds through both lines as the compressor is started after an off-period. Some amount of liquid through both lines continues afterwards, as also observed in cases with the accumulator. No motion in either line is observed in the off-period, but condensation forms on the suction line sight glass at the 5°C ambient condition. Condensation on the suction line occurs because without the accumulator to trap cold oil and refrigerant, colder fluid and vapor enters the suction line. Results show that temperatures are colder than the ambient air, allowing for the condensation of water vapor. The suction and discharge lines are also the only locations that show a difference in trends between different refrigerant charges for cases without the accumulator. Larger charges, including 48.0g, 50.2g, and 52.0g, show more liquid

through the suction line as the compressor is turned on during cycling and for a longer period of time than is observed for the 44.0g test. This trend is most prominent at the 5°C condition and relates directly to the lack of superheat available when the compressor is first turned on.

Not as much liquid is observed through either line at the 32°C condition when the compressor starts during cycling as more superheat is available with the higher ambient temperature. As seen with the above mentioned temperature, pressure, and superheat results without the accumulator, the warmer ambient condition does not present as much of a risk for liquid flow back to the compressor.

#### ***5.3.2.3.3 Defrost***

Like the case for cycling, the liquid motion through the suction and discharge lines is also different in tests without the accumulator than was observed in tests with the accumulator. Changes are primarily notable for the 5°C ambient condition and not as much for the 32°C case for above mentioned reasons relating to superheat. For the 5°C condition, previous observations showed no motion through the discharge line during defrost and only some occasional surging of liquid through the suction line. For tests without the accumulator, surging of liquid is observed through both the suction and discharge lines, but more so in the suction line. As with cycling, motion is more pronounced with larger refrigerant charges, but the case with only 44.0g of R600a sees less motion through both glasses initially and no motion through much of the defrost period. For the 32°C, trends are very similar to those observed for tests with the accumulator. Motion initially stops in both lines and some bubbling of liquid is observed in the sight glasses throughout the defrost period. There are not as many noticeable

changes between refrigerant charges for cases without the accumulator at this ambient condition.

### **5.3.3 Refrigerant and Oil Mass Analysis Results**

Using solubility, mixture density, and visualization results, the mass of oil and refrigerant was calculated for the compressor volume for experiments without the accumulator. Accumulator masses were no longer included as the accumulator was removed from the system. Results for cases with a 44g charge without the accumulator are outlined below. Sample results for other charges are included in Appendix 7.2.

#### **5.3.3.1 Mass Balance Trends during Pull-down**

An example of values and calculated masses for oil and refrigerant within the compressor during pull-down without the accumulator with a 44g system charge are listed in Table 34 and correspond to the points in Figure 106. As seen in tests with the accumulator, total compressor mass starts high as a large amount of oil with absorbed refrigerant initially starts within the compressor. As the system is started, refrigerant boils from the lubricant and both oil and refrigerant leave the compressor to move throughout the system. Following the initial start-up, the mass of oil and refrigerant within the compressor remains relatively constant. Because of higher solubility in the compressor for tests without the accumulator, the amount of refrigerant left within the compressor is calculated to be greater than that for cases with the accumulator. In tests with the accumulator, refrigerant mass within the compressor reaches levels less than 2g, whereas in tests without the accumulator, the lowest amount of refrigerant calculated during pull-down is 3.5g, a 75% increase over the previous condition.

Table 34: Compressor Data Points for Mass Balance for Pull-down at 5°C, 44g Charge, for Testing without the Accumulator

Measurement	Point 1	Point 2	Point 3	Point 4	Point 5	Point 6
Point Description	System Start-up	10 min. after start	20 min. after start	30 min. after start	40 min. after start	End of Pull-down
Suction Pressure [kPa]	124.6	59.1	61.5	58.3	52.3	51.1
Inside Compressor Temperature [°C]	5.7	5.4	8.1	10.2	12.4	13.2
Compressor Solubility [mass %]	45.2	9.9	8.8	6.8	4.8	4.2
Liquid Level inside Compressor [mL]	170	105	105	105	105'	105'
$\rho_{mix}$ at Compressor [g/mL]	0.64	0.76	0.76	0.77	0.79	0.80
Approx. $m_{R600a}$ at Compressor [g]	49.2	7.9	7.0	5.5	4.0	3.5
Approx. $m_{oil}$ at Compressor [g]	59.6	71.9	72.8	75.4	79.0	80.5
Total Mass in the Compressor [g]	108.8	79.8	79.8	80.9	83.0	84.0

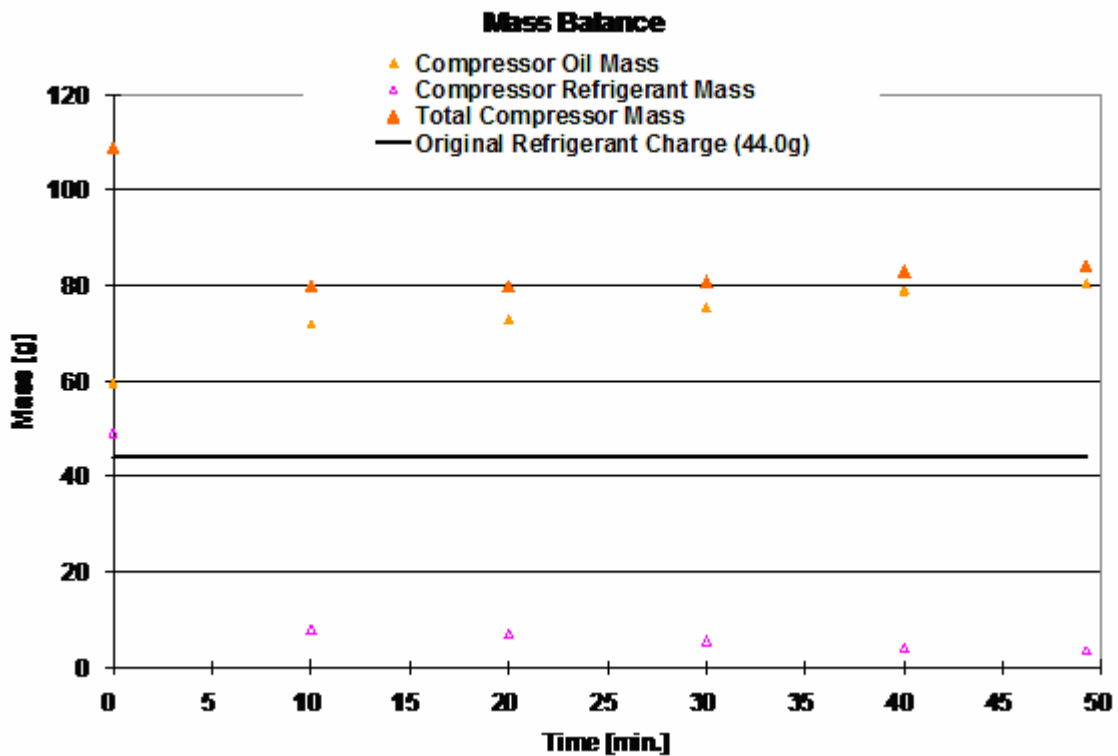
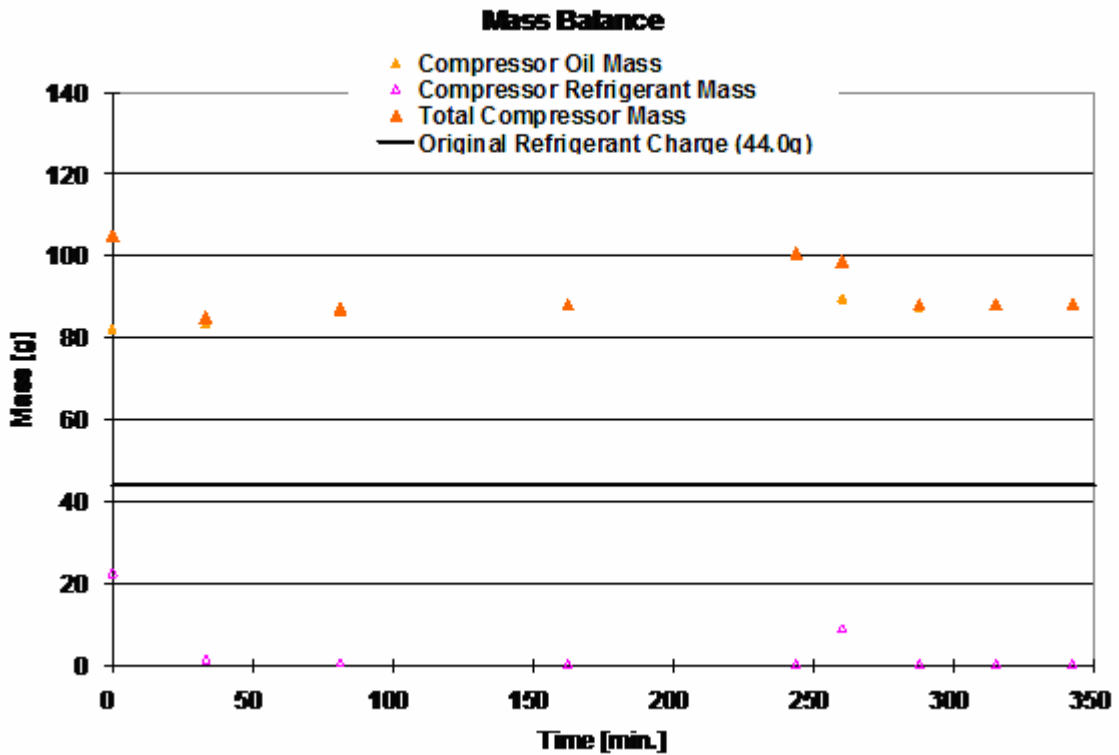


Figure 106: Mass Balance for Pull-down Period for 5°C Ambient Condition, 44g Charge, for Testing without the Accumulator

Pull-down mass balance results for the compressor at the 32°C ambient condition with a 44g charge without the accumulator are shown in Figure 107. Defrost during pull-down occurs approximately 245 minutes after the initial start of the system. As in the 5°C ambient condition, total compressor mass starts high with a large amount of refrigerant assumed to be absorbed in the oil. As the system starts, refrigerant boils out and little mass is left within the compressor. Solubility levels rise during the defrost period, accounting for the increase in refrigerant mass during and after this time. Once the system starts again, the refrigerant boils back out of the oil and moves to other parts of the system. Data for Figure 107 are included in Appendix 7.2.1.



**Figure 107: Mass Balance for Pull-down Period for 32°C Ambient Condition, 44g Charge, for Testing without the Accumulator**

### 5.3.3.2 Mass Balance Trends during Cycling

As mentioned above with the visualization results, cycling trends were similar for cases with and without the accumulator, though there were increases in the total liquid volume level and changes in flow patterns shortly after the compressor was turned on. To capture what was happening during the first minute of compressor operation, data was observed just 30 seconds after the compressor was turned on. As can be seen for the 5°C ambient condition with a 44g charge without the accumulator in Figure 108, shortly after the compressor turns on at time zero, liquid volume is flashed from the compressor, possibly accounting for the surge of liquid observed through the discharge line. In addition, more liquid refrigerant mass is calculated at this point, suggesting liquid flow from the suction line brings more liquid refrigerant into the compressor. Following the initial start of cycling, the liquid level and amount of oil and refrigerant mass in the compressor gradually decrease as the system distribution slowly equalizes. Little change is observed during the off period, indicated by points between 5 and 30 minutes in Figure 108, though more refrigerant mass is calculated at this time as it is able to absorb within the compressor oil.

Mass balance results for the compressor at the 32°C ambient condition with a 44g charge without the accumulator are shown in Figure 109. At this condition, cycling off time was shorter and is indicated by points between 0 – 14 minutes. Again, data was examined just 30 seconds following the beginning of the on-period, but as can be seen by the sharp overlay of points in the figure, little change is noted at this condition. As mentioned above, the warmer ambient was still able to provide sufficient superheat

without the accumulator and did not experience significant differences in oil and refrigerant flow trends from previous results with the accumulator.

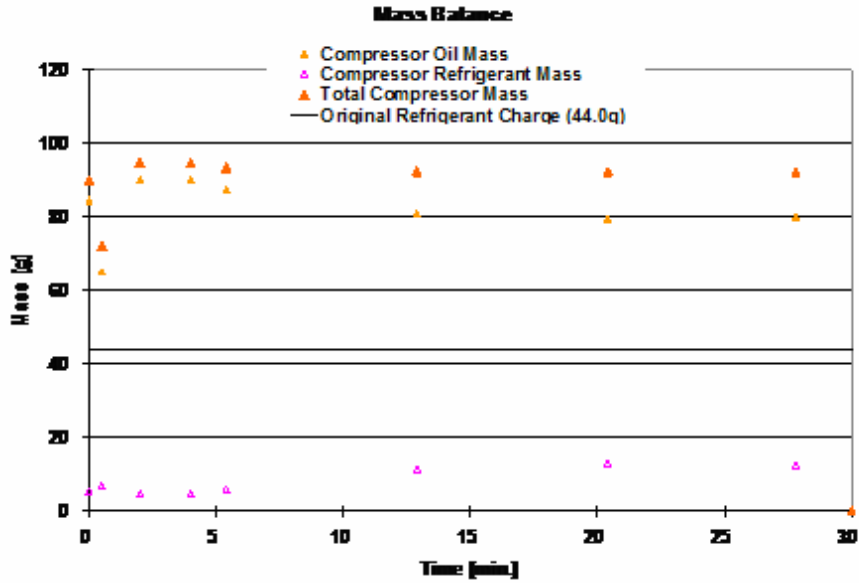


**Figure 108: Mass Balance for Cycling Period at 5°C Ambient Condition, 44g Charge, for Testing without the Accumulator**

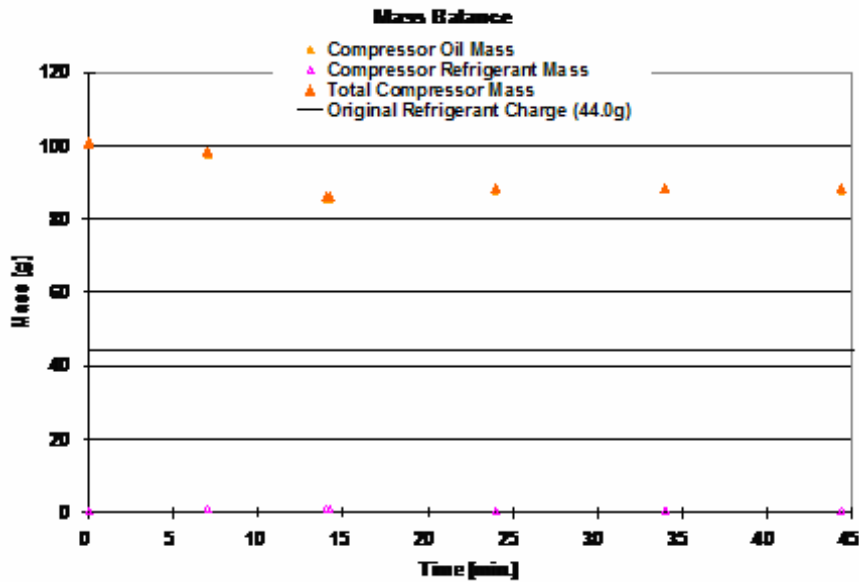


**Figure 109: Mass Balance for Cycling Period at 32°C Ambient Condition, 44g Charge, for Testing without the Accumulator**

### 5.3.3.3 Mass Balance Trends during Defrost

Results for the 5°C ambient condition during the defrost period suggested that solubility within the compressor reached levels as high as 100%, as seen in tables presented in Appendix 7.2.3. Using the given method of analysis, this would suggest that all oil leaves the compressor and any observed liquid is purely liquid refrigerant, which is virtually impossible. This analysis problem was also experienced in the accumulator in prior tests during the defrost stage; low temperatures and moderate pressures produced high solubility levels, suggesting only pure liquid refrigerant in the accumulator. Individual observations at other points of operation, including times when the system was not operating, suggested that a small amount of oil was trapped in the accumulator at all times. Such observations and measurements of solubility clearly illustrate the challenges in the current method of analysis.

The problem of high solubility in the compressor during defrost did not, however, occur during the higher 32°C ambient condition. This case allowed for a more appropriate assessment of the mass balance within the compressor during the defrost stage. Results are shown for a 44g charge without the accumulator in Figure 110. Periods of high power are represented by points between 0-10 minutes and periods of low power are represented by points between 10-17 minutes. As with the off-period in cycling, solubility increases while the compressor is off during defrost and refrigerant is able to absorb within the compressor oil. Whether the amount of oil and total mass actually decrease during the defrost period, however, is questionable.

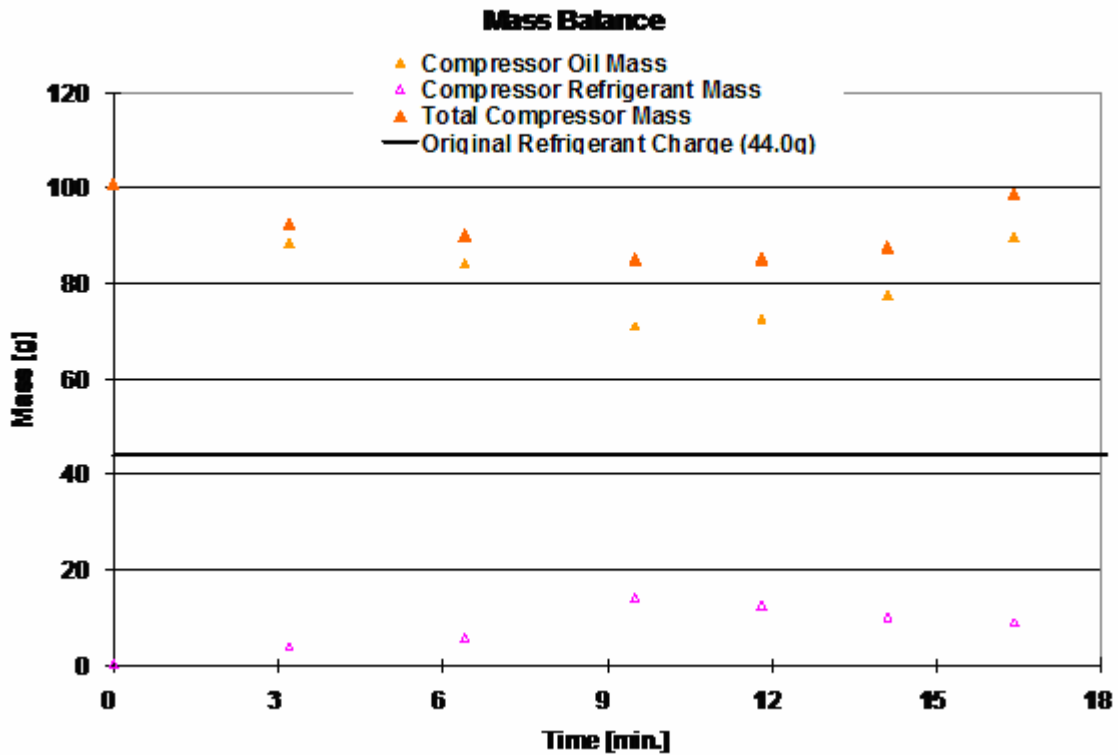


**Figure 110: Mass Balance for Defrost Period at 32°C Ambient Condition, 44g Charge, for Testing without the Accumulator**

#### 5.4 Summary of Oil and Refrigerant Flow without the Accumulator

While inaccuracies in correlations and calculation methods discourage the use of exact numerical results, the above findings do allow for general statements and observations about oil and refrigerant flow throughout a household refrigerator without an accumulator. The following section summarizes the above results, noting the major differences between systems with and without an accumulator.

General trends with and without the accumulator are quite similar in terms of oil and refrigerant flow through the system. Without the accumulator, however, oil and refrigerant cannot accumulate within this volume. Consequently, more liquid starts in the compressor and remains here as well during operation. Prior to start-up, higher volumes

of liquid rest within the compressor compared to the system with the accumulator. As the system is started, bubbling occurs within the compressor as refrigerant boils from the lubricant, as observed in cases with the accumulator. As the liquid volume decreases and fluctuates in the compressor during pull-down the overall volume continues to remain higher than what is observed for conditions with the accumulator. This is due both to the lack of accumulator volume for oil and refrigerant accumulation as well as to an increased solubility from a decrease in compressor temperature. Without the accumulator, colder liquid and vapor traverses the suction line and enters the compressor, increasing the solubility within the volume.

During cycling, again higher liquid volume levels occur in the compressor than do in cases with the accumulator. A more important difference, however, occurs during this period of operation. In cold ambient conditions, liquid enters the compressor just after the compressor is turned on after an off-period. Without the accumulator at low ambient temperatures, sufficient superheat is not available during the initial start of the compressor during cycling. For periods of 30 seconds to 1 minute, liquid flows through the suction line and enters the compressor, most likely containing liquid refrigerant as well as oil. Following this time, the suction line is able to warm as the system re-approaches operating conditions, and superheat is available to ensure that only vapor returns to the compressor. This phenomenon is more prevalent with larger refrigerant charges to the system and is not observed at all at the higher ambient conditions.

Liquid levels during the defrost period rise in the compressor as solubility increases and refrigerant is able to absorb within the compressor oil. At low ambient temperatures, as in during cycling periods, an insufficient amount of superheat is

available to ensure that only refrigerant vapor returns to the compressor. Liquid periodically surges and bubbles in the suction line at this time and larger amounts of liquid flow through both the suction and discharge line when the compressor is re-started following the defrost stage. This problem was also observed for cases with the accumulator, but not to the degree it was seen for tests without the accumulator. Again, the warmer ambient temperatures provide sufficient superheat and the threat of refrigerant liquid flow to the compressor is less of a concern.

## **5.5 Advantages and Disadvantages of Removing the Accumulator**

As indicated by the above results, the removal of the accumulator, while there are periods of insufficient superheat, does not appear to cause significant damage to the compressor for short time periods. The following section outlines some of the advantages and disadvantages of removing the accumulator in existing and future household refrigerator models.

Advantages of removing the accumulator come in many forms. For one, removing any portion of a system safely helps to eliminate material cost, manufacturing challenges, and labor time. Removing the accumulator also allows for more space within the freezer cabinet for evaporator piping and installation. As suggested by several researchers, removing the accumulator also allows for any liquid refrigerant in or near the evaporator to flow back to the evaporator during off-periods, making it easier and quicker to bring the evaporator back to appropriate temperatures when the compressor is re-started. Accumulator removal also ensures that the maximum amount of oil will remain within the compressor as a separate volume is no longer available to trap needed lubricant for the compressor. Finally, as seen through the charge tests conducted without the

accumulator, less refrigerant for a system without an accumulator is needed to obtain similar results for a system with an accumulator. Less refrigerant allows for lower system cost as well as the conservation of refrigerant liquids.

While removing the accumulator may provide several benefits, there are also several disadvantages, some with potentially hazardous consequences. To begin, while removing the accumulator allows for a lower refrigerant charge, it also makes the entire system much more sensitive to any change in refrigerant charge. More extensive testing would be necessary to determine the appropriate refrigerant charge and the system would also become much more sensitive and reactive to system leaks. Removing the accumulator also causes major concern for the amount of superheat available to the system. Especially at lower temperatures, liquid is observed to flow back to the compressor as it turns on during cycling. While this liquid flow may not always contain significant amounts of liquid refrigerant and while it only lasts for a matter of seconds, the long term effects of continued periodic liquid flow back to the compressor are unknown and potentially damaging.

## **5.6 Conclusions**

Experimentation without the accumulator was successfully conducted at the 5°C and 32°C ambient conditions. Testing at the 43°C ambient condition without the accumulator was not conducted as cycling was not observed at this ambient temperature in prior tests with the accumulator. Data and visualization results were collected and compared to results obtained in experiments with the accumulator. In order to find results that were similar to those for tests with the accumulator, various refrigerant charges were explored in the system without the accumulator. A charge of 44g in the system without

the accumulator was found to have the best agreement with results from tests with the accumulator for both the 5°C and 32°C condition. Original charge to the system with the accumulator was 52g R600a.

Variations in data temperatures and pressures were noted, primarily lower temperatures in the suction line and compressor shell as colder liquid and vapor was returned to the compressor in tests without the accumulator. Major differences included the lack of superheat available at the lower ambient condition during the cycling period when the compressor was turned back on. During this period of operation, liquid was observed flowing back to the compressor and data suggested a lack of superheat for several seconds. This trend was not observed at the warmer ambient condition and it is believed that the removal of the accumulator at higher ambient temperatures has little negative effect on the system. Variations in pull-down and cycling times were again observed and depended on ambient temperature as well as on the individual test.

In total, the accumulator was successfully removed from the system and did not cause compressor damage or system failure. Liquid was observed to flow back to the compressor during cycling at the lower ambient condition, but this liquid flow only lasted a short time and did not appear to cause stress to the compressor. Effects of this liquid flow over a longer life of the system, however, are unknown.

## 6 Recommendations and Future Work

In order to better understand the role of the accumulator and the effect of its removal on the compressor and other components of a household refrigeration system and the relationship between Freol S-10 mineral oil and R600a, more research and experimentation are recommended. Due to the limitations in this study, accurate real-time measurements of oil and refrigerant solubility and mixture density were not achieved and instead, analysis methods depended on set correlations based on equilibrium measurements, ultimately leading to inaccuracies in transient mass balance calculations. To provide more accurate results and a better representation of the amount of oil and refrigerant in the compressor and accumulator during operation, future work should include the real-time measurement of oil and refrigerant liquid volume, solubility, and mixture density.

While results show that the removal of the accumulator does not pose a threat to the life of the compressor at higher ambient temperatures, there is a lack of superheat available to the system and liquid flow back to the compressor is observed during cycling and defrost periods at cold ambient conditions. Future experimentation should evaluate the long term effects this periodic flow back to the compressor may cause. If damage to the compressor is minimal and does not cause premature failure of the system, the removal of the accumulator may be a viable option without much consequence. If, however, periodic pulses of liquid refrigerant to the compressor cause the system to fail sooner than experienced in normal operation, it will be necessary to keep the accumulator or some other storage device in the system.

In addition to a better understanding of accumulator removal, future work should contain the investigation of alternative components that could replace or relocate the accumulator. As suggested by Coulter and Bullard [3], testing should be performed with the accumulator outside of the freezer cabinet closer to the compressor, allowing for the ambient temperature to aid in the boiling of refrigerant from any trapped oil. Larger piping in the suction line should also be explored. Providing longer and larger diameter piping in a system without an accumulator may provide oil and liquid refrigerant flowing back to the compressor more time to warm up to ensure that any liquid refrigerant evaporates prior to entering the compressor. Using straight piping as opposed to an accumulator volume outside of the freezer cabinet also helps to solve the problem of trapping needed lubricant from the compressor. Additional large piping for the suction line outside of the unit could also be enhanced by installing it close to or winding it around the compressor. Orientating the suction line in this way would provide additional heat from the compressor to aid in the evaporation of any liquid refrigerant coming back through the suction line. Finally, other investigations should include the use of solenoid valves in the system to discourage refrigerant migration. While this method may not directly aid in providing sufficient superheat in critical areas, solenoid valves would prevent refrigerant migration back to the evaporator during off-periods, making it easier to re-start the compressor and possibly preventing large liquid surges from the evaporator to the compressor during this time.

In total, more information is necessary to suggest whether or not the accumulator can be safely removed from the household refrigerator. Relationships between the oil and

refrigerant are still not perfectly understood and long-term effects of accumulator removal are unknown. These issues should be explored in future work.

## 7 Appendices

### 7.1 Mass Balance Data for Results with the Accumulator

The superscript “1” noted for some liquid level measurements indicates that the liquid level was not actually observed at that time period. Estimates were used based on system trends and results from similar tests.

#### 7.1.1 Pull-down Data

**Table 35: Compressor Mass Balance Data for Pull-down for 32°C, I**

Measurement	Point 1	Point 2	Point 3	Point 4	Point 5
Point Description	System Start-up	Peak Power Point	2 hours after Start	3 hours after Start	Start of Defrost
Suction Pressure [kPa]	190.9	94.8	55.2	48.8	49.0
Inside Compressor Temperature [°C]	32.1	59.3	76.2	76.0	75.4
Compressor Solubility [mass %]	17.9	0.9	0.2	0.1	0.1
Liquid Level inside Compressor [mL]	160 <sup>1</sup>	115	115 <sup>1</sup>	115	115 <sup>1</sup>
$\rho_{\text{mix}}$ at Compressor [g/mL]	0.71	0.82	0.83	0.83	0.83
Approx. $m_{\text{R600a}}$ at Compressor [g]	20.3	0.8	0.2	0.1	0.1
Approx. $m_{\text{oil}}$ at Compressor [g]	93.3	93.5	95.3	95.4	95.4
Total Mass in the Compressor [g]	113.6	94.3	95.5	95.5	95.5

**Table 36: Compressor Mass Balance Data for Pull-down for 32°C, II**

Measurement	Point 6	Point 7	Point 8	Point 9
Point Description	End of Defrost	25 min after Defrost end	50 min after Defrost end	Compressor turns off
Suction Pressure [kPa]	169.3	51.3	46.8	45.5
Inside Compressor Temperature [°C]	58.0	71.6	73.7	74.6
Compressor Solubility [mass %]	3.4	0.2	0.1	0.1
Liquid Level inside Compressor [mL]	135 <sup>1</sup>	115 <sup>1</sup>	115 <sup>1</sup>	115 <sup>1</sup>
$\rho_{\text{mix}}$ at Compressor [g/mL]	0.77	0.83	0.83	0.83
Approx. $m_{\text{R600a}}$ at Compressor [g]	3.5	0.2	0.1	0.1
Approx. $m_{\text{oil}}$ at Compressor [g]	100.4	95.3	95.4	95.4
Total Mass in the Compressor [g]	104.0	95.5	95.5	95.5

**Table 37: Accumulator Mass Balance Data for Pull-down for 32°C, I**

Measurement	Point 1	Point 2	Point 3	Point 4	Point 5
Point Description	System Start-up	Peak Power Point	2 hours after Start	3 hours after Start	Start of Defrost
Suction Pressure [kPa]	190.9	94.8	55.2	48.8	49.0
Ave. Accumulator Temperature [°C]	32.4	-0.5	-17.7	-21.1	-23.2
Accumulator Solubility [mass %]	17.7	40.7	51.7	52.8	62.9
Liquid Level inside Accumulator [mL]	30	35	40 <sup>1</sup>	45	50
$\rho_{\text{mix}}$ at Accumulator [g/mL]	0.71	0.66	0.63	0.63	0.59
Approx. $m_{\text{R600a}}$ at Accumulator [g]	3.8	9.4	13.0	15.0	18.6
Approx. $m_{\text{oil}}$ at Accumulator [g]	17.5	13.7	12.2	13.4	10.9
Total Mass in the Accumulator [g]	21.3	23.1	25.2	28.4	29.5
Total Mass in both Acc. And Comp. [g]	134.9	117.4	120.7	123.8	125.0

**Table 38: Accumulator Mass Balance Data for Pull-down for 32°C, II**

Measurement	Point 6	Point 7	Point 8	Point 9
Point Description	End of Defrost	25 min after Defrost end	50 min after Defrost end	Compressor turns off
Suction Pressure [kPa]	169.3	51.3	46.8	45.5
Ave. Accumulator Temperature [°C]	11.0	-20.4	-22.6	-26.5
Accumulator Solubility [mass %]	58.2	55.2	54.6	70.5
Liquid Level inside Accumulator [mL]	50 <sup>1</sup>	50	50 <sup>1</sup>	50 <sup>1</sup>
$\rho_{\text{mix}}$ at Accumulator [g/mL]	0.59	0.62	0.62	0.57
Approx. $m_{\text{R600a}}$ at Accumulator [g]	17.2	17.1	16.9	20.1
Approx. $m_{\text{oil}}$ at Accumulator [g]	12.3	13.9	14.1	8.4
Total Mass in the Accumulator [g]	29.5	31.0	31.0	28.5
Total Mass in both Acc. And Comp. [g]	133.5	126.5	126.5	124.0

**Table 39: Compressor Mass Balance Data for Pull-down for 43°C, I**

Measurement	Point 1	Point 2	Point 3	Point 4
Point Description	System turned on	15 min after system on	Peak Power Point	69 min after system on
Suction Pressure [kPa]	273.6	90.9	112.5	76.9
Inside Compressor Temperature [°C]	43.0	61.4	77.2	91.1
Compressor Solubility [mass %]	20.1	0.8	0.7	0.2
Liquid Level inside Compressor [mL]	160	115	115	115 <sup>1</sup>
$\rho_{mix}$ at Compressor [g/mL]	0.70	0.82	0.81	0.82
Approx. $m_{R600a}$ at Compressor [g]	22.5	0.8	0.7	0.2
Approx. $m_{oil}$ at Compressor [g]	89.5	93.5	92.5	94.1
Total Mass in the Compressor [g]	112.0	94.3	93.2	94.3

**Table 40: Compressor Mass Balance Data for Pull-down for 43°C, II**

Measurement	Point 5	Point 6	Point 7	Point 8
Point Description	109 min after system on	149 min after system on	189 min after system on	Defrost period starts
Suction Pressure [kPa]	64.5	57.6	54.0	59.5
Inside Compressor Temperature [°C]	92.0	93.1	89.6	90.7
Compressor Solubility [mass %]	0.1	0.1	0.1	0.1
Liquid Level inside Compressor [mL]	115 <sup>1</sup>	115 <sup>1</sup>	115	115 <sup>1</sup>
$\rho_{mix}$ at Compressor [g/mL]	0.82	0.82	0.82	0.82
Approx. $m_{R600a}$ at Compressor [g]	0.1	0.1	0.1	0.1
Approx. $m_{oil}$ at Compressor [g]	94.2	94.2	94.2	94.2
Total Mass in the Compressor [g]	94.3	94.3	94.3	94.3

**Table 41: Accumulator Mass Balance Data for Pull-down for 43°C, I**

Measurement	Point 1	Point 2	Point 3	Point 4
Point Description	System turned on	15 min after system on	Peak Power Point	69 min after system on
Suction Pressure [kPa]	273.6	90.9	112.5	76.9
Ave. Accumulator Temperature [°C]	44.4	25.0	9.5	-4.3
Accumulator Solubility [mass %]	18.5	6.0	27.6	35.5
Liquid Level inside Accumulator [mL]	20	30	35	40 <sup>1</sup>
$\rho_{mix}$ at Accumulator [g/mL]	0.70	0.77	0.70	0.68
Approx. $m_{R600a}$ at Accumulator [g]	2.6	1.4	6.8	9.7
Approx. $m_{oil}$ at Accumulator [g]	11.4	21.7	17.7	17.5
Total Mass in the Accumulator [g]	14.0	23.1	24.5	27.2
Total Mass in both Acc. And Comp. [g]	126.0	117.4	117.7	121.5

**Table 42: Accumulator Mass Balance Data for Pull-down for 43°C, II**

Measurement	Point 5	Point 6	Point 7	Point 8
Point Description	109 min after system on	149 min after system on	189 min after system on	Defrost period starts
Suction Pressure [kPa]	64.5	57.6	54.0	59.5
Ave. Accumulator Temperature [°C]	-8.8	-14.6	-15.6	-18.1
Accumulator Solubility [mass %]	35.1	44.1	41.8	62.1
Liquid Level inside Accumulator [mL]	40 <sup>1</sup>	40 <sup>1</sup>	50	50
$\rho_{mix}$ at Accumulator [g/mL]	0.68	0.66	0.67	0.59
Approx. $m_{R600a}$ at Accumulator [g]	9.5	11.6	14.0	18.3
Approx. $m_{oil}$ at Accumulator [g]	17.7	14.8	19.5	11.2
Total Mass in the Accumulator [g]	27.2	26.4	33.5	29.5
Total Mass in both Acc. And Comp. [g]	121.5	120.7	127.8	123.8

### 7.1.2 Cycling Data

**Table 43: Compressor Mass Balance Data for Cycling for 5°C, I**

Measurement	Point 1	Point 2	Point 3	Point 4
Point Description	Compressor turns on	2 min after comp. on	4 min after comp. on	Compressor turns off
Suction Pressure [kPa]	71.6	43.0	43.9	50.1
Inside Compressor Temperature [°C]	16.1	12.8	17.9	25.6
Compressor Solubility [mass %]	6.8	3.1	2.2	1.7
Liquid Level inside Compressor [mL]	102	102	102	115
$\rho_{mix}$ at Compressor [g/mL]	0.77	0.81	0.82	0.82
Approx. $m_{R600a}$ at Compressor [g]	5.3	2.6	1.8	1.6
Approx. $m_{oil}$ at Compressor [g]	73.2	80.1	81.8	92.7
Total mass in Compressor [g]	78.5	82.7	83.6	94.3

**Table 44: Compressor Mass Balance Data for Cycling for 5°C, II**

Measurement	Point 5	Point 6	Point 7	Point 8
Point Description	6 min after comp. off	12 min after comp. off	18 min after comp. off	Compressor turns back on
Suction Pressure [kPa]	75.3	79.9	81.5	72.4
Inside Compressor Temperature [°C]	13.7	16.7	18.3	15.2
Compressor Solubility [mass %]	8.8	8.1	7.5	7.3
Liquid Level inside Compressor [mL]	115	115	115	102
$\rho_{mix}$ at Compressor [g/mL]	0.76	0.76	0.76	0.77
Approx. $m_{R600a}$ at Compressor [g]	7.7	7.1	6.6	5.7
Approx. $m_{oil}$ at Compressor [g]	79.7	80.3	80.8	72.8
Total mass in Compressor [g]	87.4	87.4	87.4	78.5

**Table 45: Accumulator Mass Balance Data for Cycling for 5°C, I**

Measurement	Point 1	Point 2	Point 3	Point 4
Point Description	Compressor turns on	2 min after comp. on	4 min after comp. on	Compressor turns off
Suction Pressure [kPa]	71.6	43.0	43.9	50.1
Ave. Accumulator Temperature [°C]	-19.0	-25.8	-29.4	-29.4
Accumulator Solubility [mass %]	97.1	59.4	81.8	100
Liquid Level inside Accumulator [mL]	50	40	40	40
$\rho_{mix}$ at Accumulator [g/mL]	0.48	0.61	0.54	0.48
Approx. $m_{R600a}$ at Accumulator [g]	23.3	14.5	17.7	19.2
Approx. $m_{oil}$ at Accumulator [g]	0.7	9.9	3.9	0.0
Total mass in Accumulator [g]	24.0	24.4	21.6	19.2
Total mass in Acc. And Comp. [g]	102.5	107.1	105.2	113.5

**Table 46: Accumulator Mass Balance Data for Cycling for 5°C, II**

Measurement	Point 5	Point 6	Point 7	Point 8
Point Description	6 min after comp. off	12 min after comp. off	18 min after comp. off	Compressor turns back on
Suction Pressure [kPa]	75.3	79.9	81.5	72.4
Ave. Accumulator Temperature [°C]	-20.5	-23.8	-18.2	-19.5
Accumulator Solubility [mass %]	100	100	100	100
Liquid Level inside Accumulator [mL]	40	40	40	50
$\rho_{mix}$ at Accumulator [g/mL]	0.48	0.48	0.47	0.48
Approx. $m_{R600a}$ at Accumulator [g]	19.2	19.2	18.8	24.0
Approx. $m_{oil}$ at Accumulator [g]	0.0	0.0	0.0	0.0
Total mass in Accumulator	19.2	19.2	18.8	24.0
Total mass in Acc. And Comp. [g]	106.6	106.6	106.2	102.5

**Table 47: Compressor Mass Balance Data for Cycling for 32°C, I**

Measurement	Point 1	Point 2	Point 3	Point 4
Point Description	Compressor turns on	11 min after comp. on	22 min after comp. on	33 min after comp. on
Suction Pressure [kPa]	64.4	45.8	45.2	44.4
Inside Compressor Temperature [°C]	57.6	68.2	70.7	71.9
Compressor Solubility [mass %]	0.5	0.1	0.1	0.1
Liquid Level inside Compressor [mL]	115 <sup>1</sup>	115	115	115
$\rho_{mix}$ at Compressor [g/mL]	0.83	0.83	0.83	0.83
Approx. $m_{R600a}$ at Compressor [g]	0.5	0.1	0.1	0.1
Approx. $m_{oil}$ at Compressor [g]	95.0	95.4	95.4	95.4
Total mass in Compressor [g]	95.5	95.5	95.5	95.5

**Table 48: Compressor Mass Balance Data for Cycling for 32°C, II**

Measurement	Point 5	Point 6	Point 7	Point 8
Point Description	Compressor turns off	5 min after comp. off	10 min after comp. off	Compressor turns back on
Suction Pressure [kPa]	46.3	72.0	73.1	65.3
Inside Compressor Temperature [°C]	73.0	66.3	60.1	56.1
Compressor Solubility [mass %]	0.1	0.4	0.5	0.5
Liquid Level inside Compressor [mL]	125	125	125	115
$\rho_{mix}$ at Compressor [g/mL]	0.83	0.83	0.83	0.83
Approx. $m_{R600a}$ at Compressor [g]	0.1	0.4	0.5	0.5
Approx. $m_{oil}$ at Compressor [g]	103.6	103.3	103.2	95.0
Total mass in Compressor [g]	103.8	103.8	103.8	95.5

**Table 49: Accumulator Mass Balance Data for Cycling for 32°C, I**

Measurement	Point 1	Point 2	Point 3	Point 4
Point Description	Compressor turns on	11 min after comp. on	22 min after comp. on	33 min after comp. on
Suction Pressure [kPa]	64.4	45.8	45.2	44.4
Ave. Accumulator Temperature [°C]	-17.4	-22.8	-23.2	-23.7
Accumulator Solubility [mass %]	68.7	52.9	53.3	53.8
Liquid Level inside Accumulator [mL]	50 <sup>1</sup>	50	50	50
$\rho_{mix}$ at Accumulator [g/mL]	0.57	0.63	0.63	0.63
Approx. $m_{R600a}$ at Accumulator [g]	19.6	16.7	16.8	16.9
Approx. $m_{oil}$ at Accumulator [g]	8.9	14.8	14.7	14.6
Total mass in Accumulator [g]	28.5	31.5	31.5	31.5
Total mass in Acc. And Comp. [g]	124.0	127.0	127.0	127.0

**Table 50: Accumulator Mass Balance Data for Cycling for 32°C, II**

Measurement	Point 5	Point 6	Point 7	Point 8
Point Description	Compressor turns off	5 min after comp. off	10 min after comp. off	Compressor turns back on
Suction Pressure [kPa]	46.3	72.0	73.1	65.3
Ave. Accumulator Temperature [°C]	-26.3	-19.5	-18.4	-17.1
Accumulator Solubility [mass %]	71.2	100.0	96.4	69.1
Liquid Level inside Accumulator [mL]	50	50	50	50
$\rho_{mix}$ at Accumulator [g/mL]	0.57	0.48	0.49	0.57
Approx. $m_{R600a}$ at Accumulator [g]	20.3	24.0	23.6	19.7
Approx. $m_{oil}$ at Accumulator [g]	8.2	0.0	0.9	8.8
Total mass in Accumulator	28.5	24.0	24.5	28.5
Total mass in Acc. And Comp. [g]	132.3	127.8	128.3	124.0

### 7.1.3 Defrost Data

**Table 51: Compressor Mass Balance Data for Defrost for 5°C, I**

Measurement	Point 1	Point 2	Point 3	Point 4
Point Description	Defrost period starts	4 min after defrost start (max power)	8 min after defrost start	Minimum power begins
Suction Pressure [kPa]	39.3	120.1	168.2	201.2
Inside Compressor Temperature [°C]	39.7	37.4	28.9	21.0
Compressor Solubility [mass %]	0.4	4.9	16.8	41.6
Liquid Level inside Compressor [mL]	102	102	102	102
$\rho_{\text{mix}}$ at Compressor [g/mL]	0.84	0.77	0.72	0.64
Approx. $m_{\text{R600a}}$ at Compressor [g]	0.3	3.8	12.3	27.2
Approx. $m_{\text{oil}}$ at Compressor [g]	85.3	74.7	61.1	36.1
Total mass in Compressor [g]	85.6	78.5	73.4	65.3

**Table 52: Compressor Mass Balance Data for Defrost for 5°C, II**

Measurement	Point 5	Point 6	Point 7
Point Description	2 min after min. begins	4 min after min. begins	Defrost over
Suction Pressure [kPa]	204.8	200.0	146.9
Inside Compressor Temperature [°C]	26.5	26.8	21.7
Compressor Solubility [mass %]	29.8	27.9	20.4
Liquid Level inside Compressor [mL]	102	102	102
$\rho_{\text{mix}}$ at Compressor [g/mL]	0.68	0.68	0.71
Approx. $m_{\text{R600a}}$ at Compressor [g]	20.7	19.4	14.8
Approx. $m_{\text{oil}}$ at Compressor [g]	48.7	50.0	57.6
Total mass in Compressor [g]	69.4	69.4	72.4

**Table 53: Accumulator Mass Balance Data for Defrost for 5°C, I**

Measurement	Point 1	Point 2	Point 3	Point 4
Point Description	Defrost period starts	4 min after defrost start (max power)	8 min after defrost start	Minimum power begins
Suction Pressure [kPa]	39.3	120.1	168.2	201.2
Ave. Accumulator Temperature [°C]	-38.6	-12.2	0.7	12.2
Accumulator Solubility [mass %]	100	100	100	77.2
Liquid Level inside Accumulator [mL]	40	50	55	60
$\rho_{mix}$ at Accumulator [g/mL]	0.49	0.47	0.46	0.53
Approx. $m_{R600a}$ at Accumulator [g]	19.6	23.5	25.3	24.5
Approx. $m_{oil}$ at Accumulator [g]	0.0	0.0	0.0	7.3
Total mass in Accumulator [g]	19.6	23.5	25.3	31.8
Total mass in Acc. And Comp. [g]	105.3	102.0	98.7	97.1

**Table 54: Accumulator Mass Balance Data for Defrost for 5°C, II**

Measurement	Point 5	Point 6	Point 7
Point Description	2 min after min. begins	4 min after min. begins	Defrost over
Suction Pressure [kPa]	204.8	200.0	146.9
Ave. Accumulator Temperature [°C]	13.3	7.9	6.3
Accumulator Solubility [mass %]	73.7	100	61.1
Liquid Level inside Accumulator [mL]	-	-	-
$\rho_{mix}$ at Accumulator [g/mL]	0.54	0.46	0.58
Approx. $m_{R600a}$ at Accumulator [g]	-	-	-
Approx. $m_{oil}$ at Accumulator [g]	-	-	-
Total mass in Accumulator	-	-	-
Total mass in Acc. And Comp. [g]	-	-	-

Video could not be captured during the last three points due to poor visualization. These points were estimated when calculating the final mass balance.

Table 55: Compressor Mass Balance Data for Defrost for 32°C, I

Measurement	Point 1	Point 2	Point 3	Point 4
Point Description	Defrost period starts	3 min. after defrost starts	6 min. after defrost starts	Start minimum power
Suction Pressure [kPa]	51.1	141.5	164.6	224.8
Inside Compressor Temperature [°C]	75.6	71.5	66.9	63.2
Compressor Solubility [mass %]	0.1	1.3	2.1	4.8
Liquid Level inside Compressor [mL]	115	115	115	115
$\rho_{\text{mix}}$ at Compressor [g/mL]	0.83	0.80	0.79	0.75
Approx. $m_{\text{R600a}}$ at Compressor [g]	0.1	1.2	1.9	4.1
Approx. $m_{\text{oil}}$ at Compressor [g]	95.4	90.8	88.9	82.1
Total mass in Compressor [g]	95.5	92.0	90.9	86.3

Table 56: Compressor Mass Balance Data for Defrost for 32°C, II

Measurement	Point 5	Point 6	Point 7
Point Description	2.3 min. after minimum power starts	4.6 min. after minimum power starts	Defrost period over
Suction Pressure [kPa]	227.2	209.8	165.6
Inside Compressor Temperature [°C]	60.9	58.9	57.3
Compressor Solubility [mass %]	5.4	5.1	3.3
Liquid Level inside Compressor [mL]	115	115	100
$\rho_{\text{mix}}$ at Compressor [g/mL]	0.75	0.75	0.77
Approx. $m_{\text{R600a}}$ at Compressor [g]	4.7	4.4	2.5
Approx. $m_{\text{oil}}$ at Compressor [g]	81.6	81.9	74.5
Total mass in Compressor [g]	86.3	86.3	77.0

Table 57: Accumulator Mass Balance Data for Defrost for 32°C, I

Measurement	Point 1	Point 2	Point 3	Point 4
Point Description	Defrost period starts	3 min. after defrost starts	6 min. after defrost starts	Start minimum power
Suction Pressure [kPa]	51.1	141.5	164.6	224.8
Ave. Accumulator Temperature [°C]	-23.3	-4.1	2.0	10.0
Accumulator Solubility [mass %]	68.6	100.0	100.0	100.0
Liquid Level inside Accumulator [mL]	50	50	55	55
$\rho_{\text{mix}}$ at Accumulator [g/mL]	0.58	0.46	0.46	0.45
Approx. $m_{\text{R600a}}$ at Accumulator [g]	19.9	23.0	25.3	24.8
Approx. $m_{\text{oil}}$ at Accumulator [g]	9.1	0.0	0.0	0.0
Total mass in Accumulator [g]	29.0	23.0	25.3	24.8
Total mass in Acc. And Comp. [g]	124.5	115.0	116.2	111.0

**Table 58: Accumulator Mass Balance Data for Defrost for 32°C, II**

Measurement	Point 5	Point 6	Point 7
Point Description	2.3 min. after minimum power starts	4.6 min. after minimum power starts	Defrost period over
Suction Pressure [kPa]	227.2	209.8	165.6
Ave. Accumulator Temperature [°C]	12.7	11.5	9.7
Accumulator Solubility [mass %]	95.9	88.2	61.2
Liquid Level inside Accumulator [mL]	60	55	50
$\rho_{mix}$ at Accumulator [g/mL]	0.47	0.49	0.58
Approx. $m_{R600a}$ at Accumulator [g]	27.0	23.8	17.7
Approx. $m_{oil}$ at Accumulator [g]	1.2	3.2	11.3
Total mass in Accumulator	28.2	27.0	29.0
Total mass in Acc. And Comp. [g]	114.5	113.2	106.0

**Table 59: Compressor Mass Balance Data for Defrost for 43°C, I**

Measurement	Point 1	Point 2	Point 3	Point 4
Point Description	Defrost period starts	2.4 min after defrost begins	4.8 min after defrost begins	Minimum power period begins
Suction Pressure [kPa]	59.5	148.1	168.3	221.9
Inside Compressor Temperature [°C]	90.7	86.0	77.0	77.8
Compressor Solubility [mass %]	0.1	0.9	1.5	2.6
Liquid Level inside Compressor [mL]	115	115	115	115
$\rho_{mix}$ at Compressor [g/mL]	0.82	0.80	0.79	0.77
Approx. $m_{R600a}$ at Compressor [g]	0.1	0.8	1.4	2.3
Approx. $m_{oil}$ at Compressor [g]	94.2	91.2	89.5	86.2
Total Mass in the Compressor [g]	94.3	92.0	90.9	88.6

**Table 60: Compressor Mass Balance Data for Defrost for 43°C, II**

Measurement	Point 5	Point 6	Point 7
Point Description	2.3 min. after minimum power begins	4.6 min after minimum power begins	Defrost period ends
Suction Pressure [kPa]	231.6	218.8	171.4
Inside Compressor Temperature [°C]	76.2	71.1	70.2
Compressor Solubility [mass %]	3.1	3.3	2.0
Liquid Level inside Compressor [mL]	115	115	115
$\rho_{mix}$ at Compressor [g/mL]	0.76	0.76	0.78
Approx. $m_{R600a}$ at Compressor [g]	2.7	2.9	1.8
Approx. $m_{oil}$ at Compressor [g]	84.7	84.5	87.9
Total Mass in the Compressor [g]	87.4	87.4	89.7

**Table 61: Accumulator Mass Balance Data for Defrost for 43°C, I**

Measurement	Point 1	Point 2	Point 3	Point 4
Point Description	Defrost period starts	2.4 min after defrost begins	4.8 min after defrost begins	Minimum power period begins
Suction Pressure [kPa]	59.5	148.1	168.3	221.9
Ave. Accumulator Temperature [°C]	-18.1	-2.3	3.9	11.6
Accumulator Solubility [mass %]	62.1	100.0	97.1	98.8
Liquid Level inside Accumulator [mL]	50	55	55	55
$\rho_{mix}$ at Accumulator [g/mL]	0.59	0.46	0.47	0.46
Approx. $m_{R600a}$ at Accumulator [g]	18.3	25.3	25.1	25.0
Approx. $m_{oil}$ at Accumulator [g]	11.2	0.0	0.7	0.3
Total Mass in the Accumulator [g]	29.5	25.3	25.9	25.3
Total Mass in both Acc. And Comp. [g]	123.8	117.3	116.7	113.9

**Table 62: Accumulator Mass Balance Data for Defrost for 43°C, II**

Measurement	Point 5	Point 6	Point 7
Point Description	2.3 min. after minimum power begins	4.6 min after minimum power begins	Defrost period ends
Suction Pressure [kPa]	231.6	218.8	171.4
Ave. Accumulator Temperature [°C]	13.7	10.8	12.5
Accumulator Solubility [mass %]	93.0	100.0	53.5
Liquid Level inside Accumulator [mL]	60	55	50
$\rho_{mix}$ at Accumulator [g/mL]	0.48	0.45	0.60
Approx. $m_{R600a}$ at Accumulator [g]	26.8	24.8	16.1
Approx. $m_{oil}$ at Accumulator [g]	2.0	0.0	14.0
Total Mass in the Accumulator [g]	28.8	24.8	30.0
Total Mass in both Acc. And Comp. [g]	116.2	112.2	119.7

## 7.2 Mass Balance Data for Results without the Accumulator

### 7.2.1 Pull-down Data

**Table 63: Compressor Mass Balance Data for Pull-down for 32°C, 44g Charge, I**

Measurement	Point 1	Point 2	Point 3	Point 4	Point 5
Point Description	System Start-up	Peak Power Point	81.2 min. after start	162.4 min. after start	Defrost period begins
Suction Pressure [kPa]	209.7	81.4	66.1	53.0	48.0
Inside Compressor Temperature [°C]	32.3	40.4	48.7	49.7	49.4
Compressor Solubility [mass %]	21.6	1.8	0.8	0.4	0.4
Liquid Level inside Compressor [mL]	150	105	105 <sup>1</sup>	105 <sup>1</sup>	120
$\rho_{\text{mix}}$ at Compressor [g/mL]	0.70	0.81	0.83	0.84	0.84
Approx. $m_{\text{R600a}}$ at Compressor [g]	22.7	1.5	0.7	0.4	0.4
Approx. $m_{\text{oil}}$ at Compressor [g]	82.3	83.5	86.5	87.8	100.4
Total Mass in the Compressor [g]	105.0	85.1	87.2	88.2	100.8

**Table 64: Compressor Mass Balance Data for Pull-down for 32°C, 44g Charge, II**

Measurement	Point 6	Point 7	Point 8	Point 9
Point Description	Defrost period ends	27.4 min. after defrost	54.8 min. after defrost	End of Pull-down
Suction Pressure [kPa]	202.2	51.9	48.2	47.5
Inside Compressor Temperature [°C]	45.7	47.5	48.5	48.9
Compressor Solubility [mass %]	9.1	0.5	0.4	0.4
Liquid Level inside Compressor [mL]	105	105	105 <sup>1</sup>	105 <sup>1</sup>
$\rho_{\text{mix}}$ at Compressor [g/mL]	0.94	0.84	0.84	0.84
Approx. $m_{\text{R600a}}$ at Compressor [g]	9.0	0.4	0.4	0.4
Approx. $m_{\text{oil}}$ at Compressor [g]	89.7	87.8	87.8	87.8
Total Mass in the Compressor [g]	98.7	88.2	88.2	88.2

**Table 65: Compressor Mass Balance Data for Pull-down for 32°C, 48g Charge, I**

Measurement	Point 1	Point 2	Point 3	Point 4
Point Description	System Start-up	Peak Power Point	108 min. after start	3 hrs. after start
Suction Pressure [kPa]	266.0	94.8	66.2	62.3
Inside Compressor Temperature [°C]	32.2	42.8	52.6	52.2
Compressor Solubility [mass %]	36.0	2.2	0.6	0.6
Liquid Level inside Compressor [mL]	185	85	85 <sup>1</sup>	105 <sup>1</sup>
$\rho_{\text{mix}}$ at Compressor [g/mL]	0.65	0.80	0.83	0.83
Approx. $m_{\text{R600a}}$ at Compressor [g]	43.3	1.5	0.4	0.5
Approx. $m_{\text{oil}}$ at Compressor [g]	77.0	66.5	70.1	86.6
Total Mass in the Compressor [g]	120.3	68.0	70.6	87.2

**Table 66: Compressor Mass Balance Data for Pull-down for 32°C, 48g Charge, II**

Measurement	Point 5	Point 6	Point 7	Point 8	Point 9
Point Description	Defrost period begins	Defrost period ends	23 min. after defrost end	46 min. after defrost end	End of Pull-down
Suction Pressure [kPa]	58.7	168.0	61.6	59.2	61.4
Inside Compressor Temperature [°C]	51.2	47.2	48.6	50.2	50.8
Compressor Solubility [mass %]	0.5	5.7	0.7	0.6	0.6
Liquid Level inside Compressor [mL]	130	105	105	105 <sup>1</sup>	105 <sup>1</sup>
$\rho_{\text{mix}}$ at Compressor [g/mL]	0.83	0.76	0.83	0.83	0.83
Approx. $m_{\text{R600a}}$ at Compressor [g]	0.5	4.5	0.6	0.5	0.5
Approx. $m_{\text{oil}}$ at Compressor [g]	107.4	75.3	86.5	86.6	86.6
Total Mass in the Compressor [g]	107.9	79.8	87.2	87.2	87.2

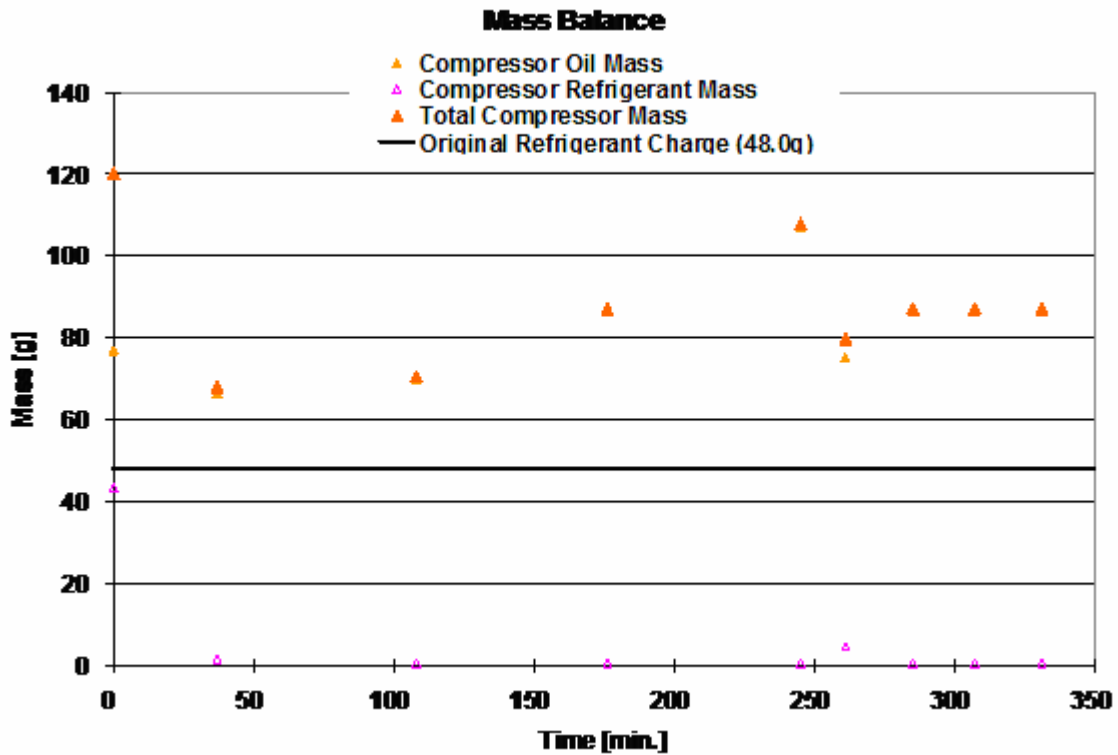


Figure 111: Mass Balance for Pull-down Period at 32°C Ambient Condition, 48g Charge, for Testing without the Accumulator

## 7.2.2 Cycling Data

Table 67: Compressor Mass Balance Data for Cycling for 5°C, 44g Charge, I

Measurement	Point 1	Point 2	Point 3	Point 4
Point Description	Compressor Turns On	30 sec. after Comp. On	2 min. after Comp. On	4 min. Comp. On
Suction Pressure [kPa]	74.3	67.2	48.2	48.5
Inside Compressor Temperature [°C]	9.1	9.2	9.5	9.6
Compressor Solubility [mass %]	6.0	9.7	4.9	4.9
Liquid Level inside Compressor [mL]	120	95	120	120
$\rho_{\text{mix}}$ at Compressor [g/mL]	0.75	0.76	0.79	0.79
Approx. $m_{\text{R600a}}$ at Compressor [g]	5.4	7.0	4.6	4.6
Approx. $m_{\text{oil}}$ at Compressor [g]	84.6	65.2	90.2	90.2
Total Mass in the Compressor [g]	90.0	72.2	94.8	94.8

**Table 68: Compressor Mass Balance Data for Cycling for 5°C, 44g Charge, II**

Measurement	Point 5	Point 6	Point 7	Point 8
Point Description	Compressor Turns Off	7.5 min. after Comp. Off	15 min. after Comp. Off	Compressor Turns Back On
Suction Pressure [kPa]	55.5	78.4	81.0	79.5
Inside Compressor Temperature [°C]	9.6	10.1	9.4	9.4
Compressor Solubility [mass %]	6.4	12.5	14.1	13.5
Liquid Level inside Compressor [mL]	120	125	125 <sup>1</sup>	125 <sup>1</sup>
$\rho_{\text{mix}}$ at Compressor [g/mL]	0.78	0.74	0.74	0.74
Approx. $m_{\text{R600a}}$ at Compressor [g]	6.0	11.6	13.0	12.5
Approx. $m_{\text{oil}}$ at Compressor [g]	87.6	80.9	79.5	80.0
Total Mass in the Compressor [g]	93.6	92.5	92.5	92.5

**Table 69: Compressor Mass Balance Data for Cycling for 5°C, 48g Charge, I**

Measurement	Point 1	Point 2	Point 3	Point 4
Point Description	Compressor Turns On	30 sec. after Comp. On	1.5 min. after Comp. On	3.5 min. Comp. On
Suction Pressure [kPa]	73.5	72.5	50.9	49.8
Inside Compressor Temperature [°C]	8.7	8.9	8.6	8.9
Compressor Solubility [mass %]	12.1	11.6	5.6	5.4
Liquid Level inside Compressor [mL]	120	105	105	105
$\rho_{\text{mix}}$ at Compressor [g/mL]	0.75	0.75	0.78	0.79
prox. $m_{\text{R600a}}$ at Compressor [g]	10.9	9.1	4.6	4.5
Approx. $m_{\text{oil}}$ at Compressor [g]	79.1	69.7	77.3	78.5
Total Mass in the Compressor [g]	90.0	78.8	81.9	83.0

**Table 70: Compressor Mass Balance Data for Cycling for 5°C, 48g Charge, II**

Measurement	Point 5	Point 6	Point 7	Point 8
Point Description	Compressor Turns Off	8 min. after Comp. Off	16 min. after Comp. Off	Compressor Turns Back On
Suction Pressure [kPa]	56.9	78.5	81.4	73.9
Inside Compressor Temperature [°C]	8.9	9.3	8.9	8.6
Compressor Solubility [mass %]	7.1	13.2	14.7	12.3
Liquid Level inside Compressor [mL]	105	130	130 <sup>1</sup>	130 <sup>1</sup>
$\rho_{\text{mix}}$ at Compressor [g/mL]	0.77	0.74	0.74	0.75
Approx. $m_{\text{R600a}}$ at Compressor [g]	5.7	12.7	14.1	12.0
Approx. $m_{\text{oil}}$ at Compressor [g]	75.2	83.5	82.1	85.5
Total Mass in the Compressor [g]	80.9	96.2	96.2	97.5

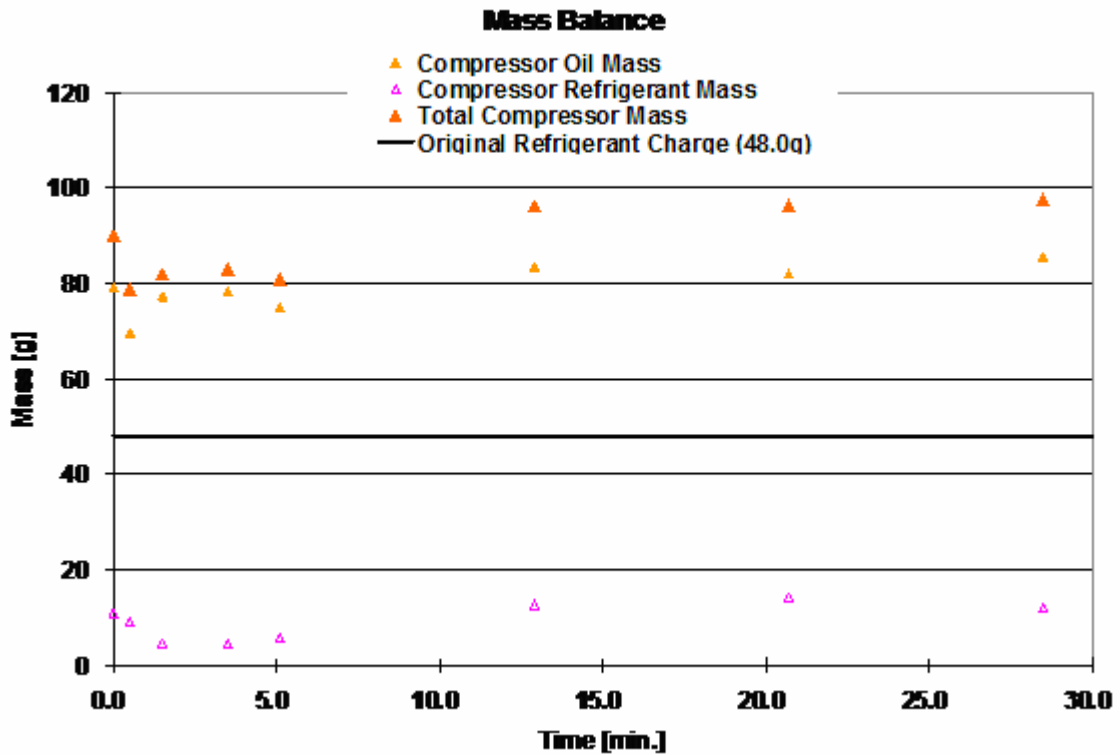


Figure 112: Mass Balance for Cycling Period at 5°C Ambient Condition, 48g Charge, for Testing without the Accumulator

Table 71: Compressor Mass Balance Data for Cycling for 5°C, 52g Charge, I

Measurement	Point 1	Point 2	Point 3	Point 4
Point Description	Compressor Turns On	30 sec. after Comp. On	2.3 min. after Comp. On	4.6 min. after Comp. On
Suction Pressure [kPa]	88.9	83.0	43.8	42.6
Inside Compressor Temperature [°C]	10.4	10.0	9.9	10.0
Compressor Solubility [mass %]	15.8	14.2	3.9	3.7
Liquid Level inside Compressor [mL]	130	105	120	120
$\rho_{\text{mix}}$ at Compressor [g/mL]	0.73	0.74	0.80	0.80
Approx. $m_{\text{R600a}}$ at Compressor [g]	15.0	11.0	3.7	3.6
Approx. $m_{\text{oil}}$ at Compressor [g]	79.9	66.7	92.3	92.4
Total Mass in the Compressor [g]	94.9	77.7	96.0	96.0

Table 72: Compressor Mass Balance Data for Cycling for 5°C, 52g Charge, II

Measurement	Point 5	Point 6	Point 7	Point 8
Point Description	Compressor Turns Off	7.3 min. after Comp. Off	14.6 min. after Comp. Off	Compressor Turns On
Suction Pressure [kPa]	42.5	90.1	92.0	82.2
Inside Compressor Temperature [°C]	9.9	10.7	10.0	9.8
Compressor Solubility [mass %]	3.7	15.9	17.5	14.0
Liquid Level inside Compressor [mL]	120	120	130	130
$\rho_{\text{mix}}$ at Compressor [g/mL]	0.80	0.73	0.73	0.74
Approx. $m_{\text{R600a}}$ at Compressor [g]	3.6	13.9	16.6	13.5
Approx. $m_{\text{oil}}$ at Compressor [g]	92.4	73.7	78.3	82.7
Total Mass in the Compressor [g]	96.0	87.6	94.9	96.2

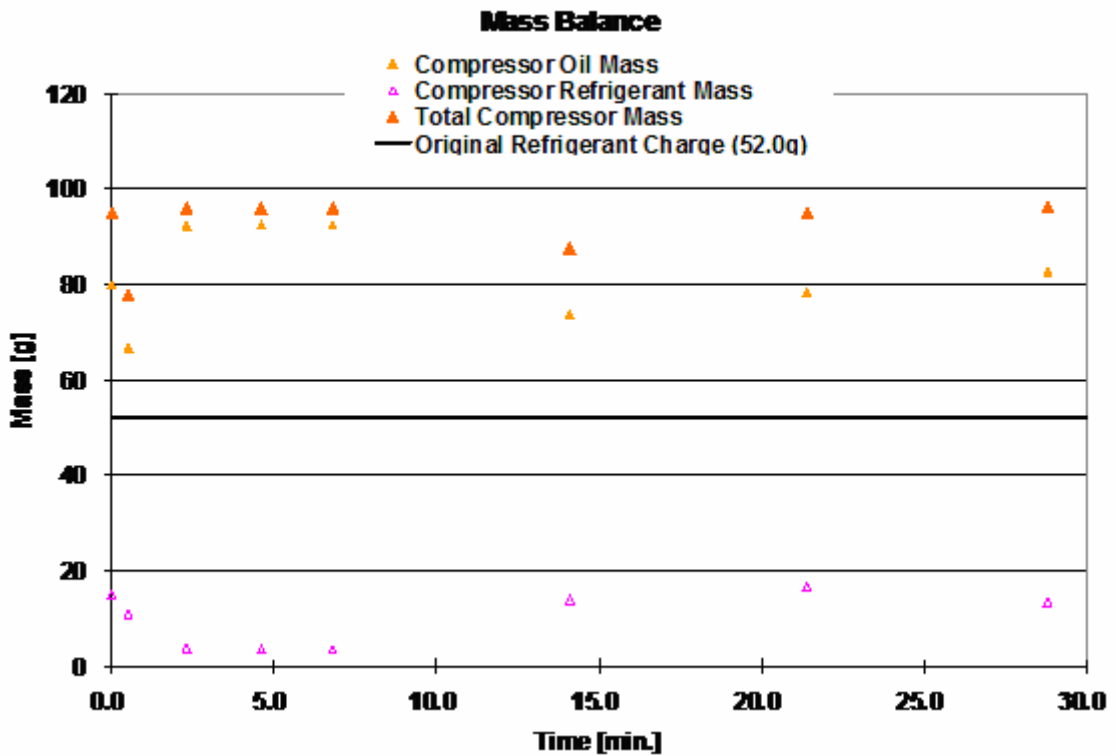


Figure 113: Mass Balance for Cycling Period at 5°C Ambient Condition, 52g Charge, for Testing without the Accumulator

**Table 73: Compressor Mass Balance Data for Cycling for 32°C, 44g Charge, I**

Measurement	Point 1	Point 2	Point 3	Point 4
Point Description	Compressor Turns Off	7 min. after Comp. Off	Compressor Turns On	10 sec. after Comp. On
Suction Pressure [kPa]	47.7	70.8	72.3	70.9
Inside Compressor Temperature [°C]	47.2	46.7	45.2	45.1
Compressor Solubility [mass %]	0.4	1.0	1.1	1.1
Liquid Level inside Compressor [mL]	120	120	105	105
$\rho_{\text{mix}}$ at Compressor [g/mL]	0.84	0.82	0.82	0.82
Approx. $m_{\text{R600a}}$ at Compressor [g]	0.4	1.0	0.9	0.9
Approx. $m_{\text{oil}}$ at Compressor [g]	100.4	97.4	85.2	85.2
Total Mass in the Compressor [g]	100.8	98.4	86.1	86.1

**Table 74: Compressor Mass Balance Data for Cycling for 32°C, 44g Charge, II**

Measurement	Point 5	Point 6	Point 7
Point Description	10 min. after Comp. On	20 min. after Comp. On	System Turns Off
Suction Pressure [kPa]	47.0	45.5	52.8
Inside Compressor Temperature [°C]	45.0	46.3	47.2
Compressor Solubility [mass %]	0.5	0.4	0.5
Liquid Level inside Compressor [mL]	105	105	105
$\rho_{\text{mix}}$ at Compressor [g/mL]	0.84	0.84	0.84
Approx. $m_{\text{R600a}}$ at Compressor [g]	0.4	0.4	0.4
Approx. $m_{\text{oil}}$ at Compressor [g]	87.8	87.8	87.8
Total Mass in the Compressor [g]	88.2	88.2	88.2

**Table 75: Compressor Mass Balance Data for Cycling for 32°C, 50g Charge, I**

Measurement	Point 1	Point 2	Point 3	Point 4
Point Description	Compressor Turns Off	7 min. after Comp. Off	Compressor Turns On	10 sec. after Comp. On
Suction Pressure [kPa]	55.9	88.8	78.4	107.3
Inside Compressor Temperature [°C]	48.5	47.8	46.1	46.0
Compressor Solubility [mass %]	0.5	1.5	1.2	2.4
Liquid Level inside Compressor [mL]	120 <sup>1</sup>	130	105	105
$\rho_{\text{mix}}$ at Compressor [g/mL]	0.83	0.81	0.82	0.80
Approx. $m_{\text{R600a}}$ at Compressor [g]	0.5	1.6	1.0	2.0
Approx. $m_{\text{oil}}$ at Compressor [g]	99.1	103.7	85.1	82.0
Total Mass in the Compressor [g]	99.6	105.3	86.1	84.0

Table 76: Compressor Mass Balance Data for Cycling for 32°C, 50g Charge, II

Measurement	Point 5	Point 6	Point 7
Point Description	13.3 min. after Comp. On	26.6 min. after Comp. On	Compressor Turns Off
Suction Pressure [kPa]	58.5	59.3	54.4
Inside Compressor Temperature [°C]	46.5	47.5	48.4
Compressor Solubility [mass %]	0.7	0.6	0.5
Liquid Level inside Compressor [mL]	105	105	120
$\rho_{\text{mix}}$ at Compressor [g/mL]	0.83	0.83	0.84
Approx. $m_{\text{R600a}}$ at Compressor [g]	0.6	0.5	0.5
Approx. $m_{\text{oil}}$ at Compressor [g]	86.5	86.6	100.3
Total Mass in the Compressor [g]	87.2	87.2	100.8

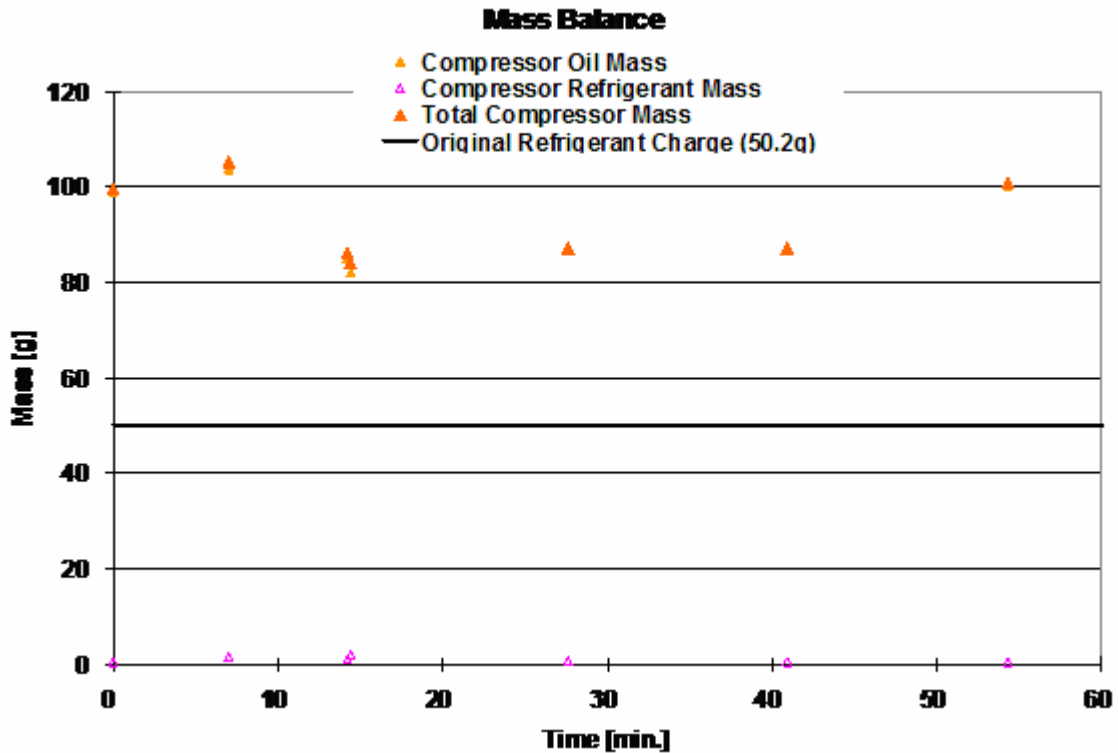


Figure 114: Mass Balance for Cycling Period at 32°C Ambient Condition, 50g Charge, for Testing without the Accumulator

### 7.2.3 Defrost Data

Table 77: Compressor Mass Balance Data for Defrost for 5°C, 44g Charge, I

Measurement	Point 1	Point 2	Point 3	Point 4
Point Description	Defrost Period Begins	5 min. after defrost start	10 min. after defrost start	Minimum Power Period Begins
Suction Pressure [kPa]	73.4	165.7	195.4	205.1
Inside Compressor Temperature [°C]	9.4	10.2	9.7	9.2
Compressor Solubility [mass %]	11.5	58.9	86.5	99.4
Liquid Level inside Compressor [mL]	120	120	120	130
$\rho_{\text{mix}}$ at Compressor [g/mL]	0.75	0.58	0.50	0.46
prox. $m_{\text{R600a}}$ at Compressor [g]	10.4	41.0	51.9	59.4
Approx. $m_{\text{oil}}$ at Compressor [g]	79.7	28.6	8.1	0.4
Total Mass in the Compressor [g]	90.0	69.6	60.0	59.8

Table 78: Compressor Mass Balance Data for Defrost for 5°C, 44g Charge, II

Measurement	Point 5	Point 6	Point 7
Point Description	2.3 min. after Min. power period begins	4.6 min. after min. power period begins	Defrost Period Ends
Suction Pressure [kPa]	203.4	198.2	173.0
Inside Compressor Temperature [°C]	9.3	8.8	8.8
Compressor Solubility [mass %]	97.3	95.6	71.8
Liquid Level inside Compressor [mL]	130	130	130
$\rho_{\text{mix}}$ at Compressor [g/mL]	0.46	0.47	0.54
Approx. $m_{\text{R600a}}$ at Compressor [g]	58.2	58.4	50.4
Approx. $m_{\text{oil}}$ at Compressor [g]	1.6	2.7	19.8
Total Mass in the Compressor [g]	59.8	61.1	70.2

**Table 79: Compressor Mass Balance Data for Defrost for 32°C, 44g Charge, I**

Measurement	Point 1	Point 2	Point 3	Point 4
Point Description	Defrost period begins	3.2 min. after defrost start	6.4 min. after defrost start	Minimum Power Period Begins
Suction Pressure [kPa]	48.0	153.6	184.3	282.6
Inside Compressor Temperature [°C]	49.4	49.0	48.6	47.6
Compressor Solubility [mass %]	0.4	4.3	6.4	16.6
Liquid Level inside Compressor [mL]	120	120	120	120
$\rho_{mix}$ at Compressor [g/mL]	0.84	0.77	0.75	0.71
Approx. $m_{R600a}$ at Compressor [g]	0.4	4.0	5.8	14.1
Approx. $m_{oil}$ at Compressor [g]	100.4	88.4	84.2	71.1
Total Mass in the Compressor [g]	100.8	92.4	90.0	85.2

**Table 80: Compressor Mass Balance Data for Defrost for 32°C, 44g Charge, II**

Measurement	Point 5	Point 6	Point 7
Point Description	2.3 min. after min. power begins	4.6 min. after min. power begins	Defrost period ends
Suction Pressure [kPa]	262.5	229.5	202.2
Inside Compressor Temperature [°C]	47.0	46.4	45.7
Compressor Solubility [mass %]	14.7	11.5	9.1
Liquid Level inside Compressor [mL]	120	120	105
$\rho_{mix}$ at Compressor [g/mL]	0.71	0.73	0.94
Approx. $m_{R600a}$ at Compressor [g]	12.5	10.1	9.0
Approx. $m_{oil}$ at Compressor [g]	72.7	77.5	89.7
Total Mass in the Compressor [g]	85.2	87.6	98.7

**Table 81: Compressor Mass Balance Data for Defrost for 32°C, 48g Charge, I**

Measurement	Point 1	Point 2	Point 3	Point 4
Point Description	Defrost Period begins	3 min. after defrost start	6 min. after defrost start	Minimum Power Period Begins
Suction Pressure [kPa]	58.7	154.8	172.3	279.6
Inside Compressor Temperature [°C]	51.2	51.3	50.7	49.2
Compressor Solubility [mass %]	0.5	3.9	5.0	15.0
Liquid Level inside Compressor [mL]	130	130	130	130
$\rho_{mix}$ at Compressor [g/mL]	0.83	0.77	0.76	0.71
Approx. $m_{R600a}$ at Compressor [g]	0.5	3.9	4.9	13.8
Approx. $m_{oil}$ at Compressor [g]	107.4	96.2	93.9	78.5
Total Mass in the Compressor [g]	107.9	100.1	98.8	92.3

Table 82: Compressor Mass Balance Data for Defrost for 32°C, 48g Charge, II

Measurement	Point 5	Point 6	Point 7
Point Description	2 min. after min. power begins	4 min. after min. power begins	Defrost period ends
Suction Pressure [kPa]	269.5	245.1	168.0
Inside Compressor Temperature [°C]	49.1	48.0	47.2
Compressor Solubility [mass %]	13.9	12.1	5.7
Liquid Level inside Compressor [mL]	130	130	105
$\rho_{mix}$ at Compressor [g/mL]	0.71	0.72	0.76
Approx. $m_{R600a}$ at Compressor [g]	12.8	11.3	4.5
Approx. $m_{oil}$ at Compressor [g]	79.5	82.3	75.3
Total Mass in the Compressor [g]	92.3	93.6	79.8

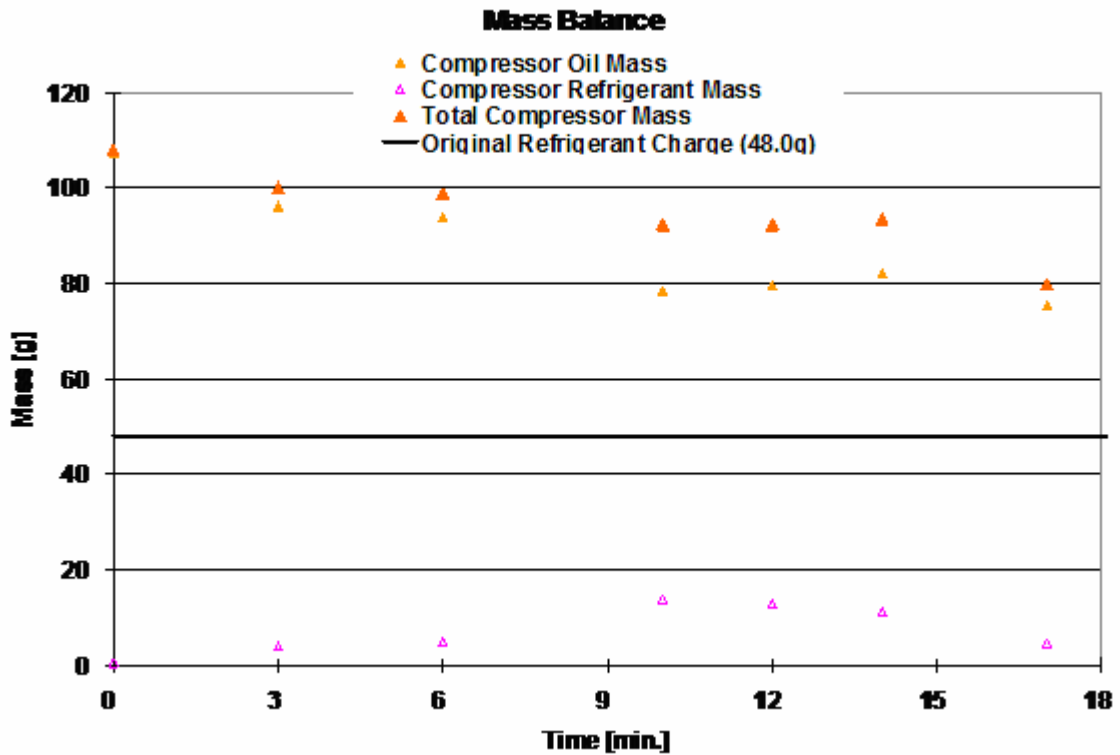


Figure 115: Mass Balance for Defrost Period at 32°C Ambient Condition, 48g Charge, for Testing without the Accumulator

## 8 References

- [1] Cengel, Y.A. and Boles, M.A. Thermodynamics: An Engineering Approach. 4<sup>th</sup> ed. 2002. New York: McGraw Hill.
- [2] Wikipedia, “Refrigerator”, available at <http://en.wikipedia.org/wiki/Refrigerator>.
- [3] Coulter, W. and Bullard, C., An Experimental Analysis of Cycling Losses in Domestic Refrigerator-Freezers, *ASHRAE Trans: Symposia (PH-97-6-1)* (1997) 587-596.
- [4] Manwell, S. and Bergles, A., Gas-liquid Flow Patterns in Refrigerant-Oil Mixtures, *ASHRAE Trans: SL-90-1-4* (1989) 456-464.
- [5] Asano, H., et al., Application of neutron radiography to a diagnosis of refrigerator, *Nuclear Instruments and Methods in Physics Research A* (1996) 170-173.
- [6] Inan, C., Gonul, T. and Tanes, M., X-ray Investigation of a domestic refrigerator. Observations at 25°C ambient temperature, *Int J Refrigeration* 26 (2003) 205-213.
- [7] Prasad, B.G. S., Effect of liquid on a reciprocating compressor, *J Energy Res Technology* 124 (2002) 187- 190.
- [8] Lebreton, J. et al., Real-time measurement of the oil concentration in liquid refrigerant flowing inside a refrigeration machine, *Fifteenth International Compressor Engineering Conference at Purdue University*, July 2000, pg. 319-326.
- [9] Fukuta, M. et al., Real-time measurement of mixing ratio of refrigerant/refrigeration oil mixture, *Int J Refrigeration* 29 (2006) 1058-1065.
- [10] Fukuta, M., Yanagisawa, T., Omura, M., Ogi, Y., Mixing and separation characteristics of isobutane with refrigeration oil, *Int J Refrigeration* 28 (2005) 997-1005.

- [11] Elvassore, N., Bertuccio, A. and Wahlstrom, A., A cubic equation of state with group contributions for the calculation of vapor-liquid equilibria of mixtures of hydrofluorocarbons and lubricant oils, *Ind. Eng. Chem. Res.* 38 (1999) 2110-2118.
- [12] Zhelezny, P. et al., An experimental investigation and modeling of the thermodynamic properties of isobutane-compressor oil solutions: some aspects of experimental methodology, *Int J Refrigeration* 30 (2007) 433-445.
- [13] ASHRAE, 2002 Refrigeration Handbook: Chapter 7: Lubricants in Refrigerant Systems.
- [14] Bjork, E. and Palm, B., Performance of a domestic refrigerator under influence of varied expansion device capacity, refrigerant charge and ambient temperature, *Int J Refrigeration* 29 (2006) 789-798.
- [15] Lee, S. et al., Quantitative analysis of flow inside the accumulator of a rotary compressor, *Int J Refrigeration* 26 (2003) 321-327.
- [16] Samsung. "Owners Manual." Model DA68-01281L. More information available at <http://www.samsung.com>.
- [18] Japan Energy Corporation. Freol S Series: Refrigeration Oil for Hydrocarbon Refrigerant. More information available at: <http://www.j-energy.co.jp/english/>.
- [18] UView Ultraviolet Systems. "Material Data Safety Sheet: Universal A/C Dye"
- [19] Setra. Pressure Measurement Division. Model 280E/C280E. Available at [http://www.setra.com/tra/pro/p\\_hv\\_280.htm](http://www.setra.com/tra/pro/p_hv_280.htm)
- [20] Omega Engineering, Inc. GG-T, TG-T, TT-T FF-T, PR-T Series. Available at [http://www.omega.com/pptst/GG\\_T\\_TC\\_WIRE.html](http://www.omega.com/pptst/GG_T_TC_WIRE.html)

[21] Ohio Semitronics. More information available at:

<https://www.ohiosemitronics.com/default.asp>

[22] Vaisala. Humidity Transmitters for Fixed Installations. More information available

at: <http://www.vaisala.com/instruments/products/humidity/fixed>.

[23] Advanced Gas Technologies Inc., “Material Safety Data Sheet: Refrigerant R600a – Isobutane,” 09/04, Available at

[http://www.advgas.com/images/products/R600a%20\\_Isobutane\\_%20MSDS.pdf](http://www.advgas.com/images/products/R600a%20_Isobutane_%20MSDS.pdf)

[24] Airgas, Isobutane: Chemically Pure Product Information. Available at:

<http://www.airgas.com/browse/product.aspx?Msg=RecID&recIds=257770>

[25] National Institute of Standards and Technology, Reference Fluid Thermodynamic and Transport Properties Database (REFPROP) Version 7.0, more information available

at: [www.nist.gov](http://www.nist.gov).

[26] Systat, TableCurve® 3D, Version 4.0 for Windows, more information available at:

[www.systat.com](http://www.systat.com).

[27] Ohaus® Balances and Scales. Ohaus® Explorer® Pro Precision Top Loading Balances. More information available at :

<http://www.ohaus.com/products/view/overview.asp?HKEY=001001001002002&Source>

=.